UNCLASSIFIED

AD NUMBER

ADB219006

NEW LIMITATION CHANGE

TO

Approved for public release, distribution unlimited

FROM

Distribution authorized to U.S. Gov't. agencies only; Proprietary Info.; Sep 96. Other requests shall be referred to U.S. Army Medical Research and Materiel Command, Attn: MCMR-RMI-S, Fort Detrick, Frederick, MD 21702-5012

AUTHORITY

USAMRMC ltr. 14 Oct 99

THIS PAGE IS UNCLASSIFIED

AD_____

GRANT NUMBER DAMD17-94-J-4314

TITLE: Molecular Analysis of Motility in Metastatic Mammary
Adenocarcinoma Cells

PRINCIPAL INVESTIGATOR: Jeffrey E. Segall, Ph.D.

CONTRACTING ORGANIZATION: Albert Einstein College of Medicine
of Yeshiva University

REPORT DATE: September 1996

TYPE OF REPORT: Annual

PREPARED FOR: Commander
U.S. Army Medical Research and Materiel Command
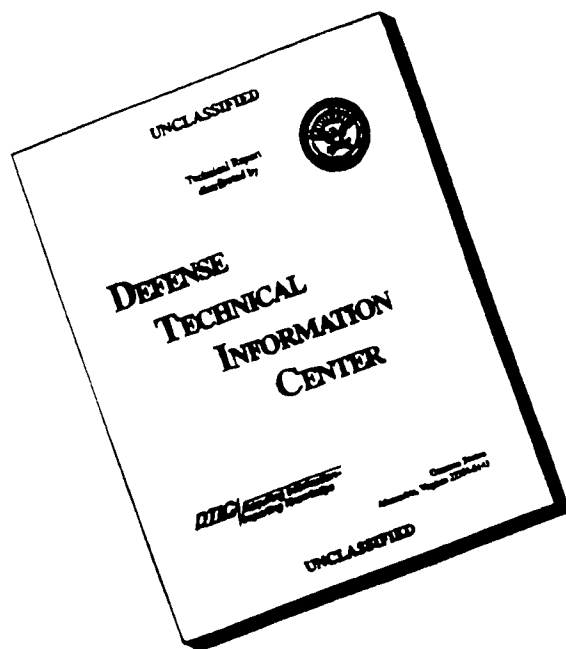Fort Detrick, Frederick, Maryland 21702-5012

The views, opinions and/or findings contained in this report are
those of the author(s) and should not be construed as an official
Department of the Army position, policy or decision unless so
designated by other documentation.

19970117 093

DTIC QUALITY INSPECTED 1

DISCLAIMER NOTICE

UNCLASSIFIED

Technical Report
distributed by

DEFENSE
TECHNICAL
INFORMATION
CENTER

DTIC

UNCLASSIFIED

THIS DOCUMENT IS BEST
QUALITY AVAILABLE. THE
COPY FURNISHED TO DTIC
CONTAINED A SIGNIFICANT
NUMBER OF PAGES WHICH DO
NOT REPRODUCE LEGIBLY.

REPORT DOCUMENTATION PAGE

1. AGENCY USE ONLY *(Leave blank)*	2. REPORT DATE September 1996	3. REPORT TYPE AND DATES COVERED Annual (26 Aug 95 - 25 Aug 96)

4. TITLE AND SUBTITLE
Molecular Analysis of Motility in Metastatic Mammary Adenocarcinoma Cells

5. FUNDING NUMBERS
DAMD17-94-J-4314

6. AUTHOR(S)
Jeffrey E. Segall, Ph.D.

7. PERFORMING ORGANIZATION NAME(S) AND ADDRESS(ES)
Albert Einstein College of Medicine
  of Yeshiva University
Bronx, New York 10461

8. PERFORMING ORGANIZATION REPORT NUMBER

9. SPONSORING/MONITORING AGENCY NAME(S) AND ADDRESS(ES)
U.S. Army Medical Research and Materiel Command
Fort Detrick, Frederick, Maryland 21702-5012

10. SPONSORING/MONITORING AGENCY REPORT NUMBER

11. SUPPLEMENTARY NOTES

12a. DISTRIBUTION / AVAILABILITY STATEMENT
Distribution authorized to U.S. Government agencies only;
Proprietary Information, Sep 96. Other requests for this
document shall be referred to Commander, U.S. Army
Medical Research and Materiel Command, ATTN: MCMR-RMI-S,
Fort Detrick, Frederick, MD 21702-5012

12b. DISTRIBUTION CODE

13. ABSTRACT *(Maximum 200*

Chemotaxis of metastatic MTLn3 cells towards EGF involves the rapid extension of lamellipods. We have characterized extending lamellipods in terms of the location and possible composition of the growth zones. Stimulation of MTLn3 cells with EGF causes a transient increase in actin nucleation activity resulting from the appearance of free barbed ends very close to the leading edge of extending lamellipods. Both actin polymerization and depolymerization are stimulated by EGF. The timing and location of EGF-induced actin nucleation activity in MTLn3 cells can account for the observed accumulation of F-actin at the leading edge and demonstrates that this F-actin rich zone is the primary actin polymerization zone after stimulation. Talin is present in the sites of actin nucleation with appropriate kinetics. Extension of lamellipods does not directly require adhesion to the substratum, but stabilization of lamellipods and focal contacts does depend on adhesion. EF1-alpha is also present in lamellipods, but is not localized to nucleation sites. These results identify a key area involved in metastatic cell motility and a potential regulatory molecule for that site - talin.

14. SUBJECT TERMS Breast Cancer

15. NUMBER OF PAGES
85

16. PRICE CODE

17. SECURITY CLASSIFICATION OF REPORT	18. SECURITY CLASSIFICATION OF THIS PAGE	19. SECURITY CLASSIFICATION OF ABSTRACT	20. LIMITATION OF ABSTRACT
Unclassified	Unclassified	Unclassified	Limited

FOREWORD

Opinions, interpretations, conclusions and recommendations are those of the author and are not necessarily endorsed by the US Army.

_____ Where copyrighted material is quoted, permission has been obtained to use such material.
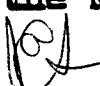
_____ Where material from documents designated for limited distribution is quoted, permission has been obtained to use the material.

_____ Citations of commercial organizations and trade names in this report do not constitute an official Department of Army endorsement or approval of the products or services of these organizations.

_____ In conducting research using animals, the investigator(s) adhered to the "Guide for the Care and Use of Laboratory Animals," prepared by the Committee on Care and Use of Laboratory Animals of the Institute of Laboratory Resources, National Research Council (NIH Publication No. 86-23, Revised 1985).

_____ For the protection of human subjects, the investigator(s) adhered to policies of applicable Federal Law 45 CFR 46.

_____ In conducting research utilizing recombinant DNA technology, the investigator(s) adhered to current guidelines promulgated by the National Institutes of Health.

_____ In the conduct of research utilizing recombinant DNA, the investigator(s) adhered to the NIH Guidelines for Research Involving Recombinant DNA Molecules.

_____ In the conduct of research involving hazardous organisms, the investigator(s) adhered to the CDC-NIH Guide for Biosafety in Microbiological and Biomedical Laboratories.

_____   9/24/96
PI - Signature   Date

TABLE OF CONTENTS

Introduction

Chemotaxis plays an important role in many basic biological processes including embryogenesis, neurite growth, wound healing, inflammation and cancer metastasis. Studies with highly motile cells such as *Dictyostelium* (Condeelis, 1993), neutrophils (Zigmond, 1996) and platelets (Hartwig et al., 1995) in particular have shown that stimulation of cells with chemoattractant generates a transient increase in actin nucleation activity in the actin cytoskeleton. It is unclear how stimulation of cell surface receptors is linked to actin polymerization. Actin polymerization could be stimulated by severing or uncapping of pre-existing actin filaments, increasing availability of polymerization competent monomeric actin, or by de novo assembly of new filaments (Condeelis (1993), Zigmond (1996)).

EGF is a chemoattractant for MTLn3, a metastatic cell line derived from the 13762 NF rat mammary adenocarcinoma (Neri et al., 1982). MTLn3 cells rapidly extend F-actin filled lamellipods in response to stimulation with EGF(Segall et al., 1996). Lamellipod extension begins within 1 minute after addition of EGF and becomes maximal by 3 minutes after stimulation. Optimum lamellipod extension occurs at about 5 nM EGF, near the Kd of the binding of EGF to its receptor. Microchemotaxis chamber measurements also demonstrate that the chemotactic and chemokinetic responses of MTLN3 cells are greatest at 5 nM EGF(Segall et al., 1996). Actin polymerization is necessary for these EGF-stimulated responses because cytochalasin D inhibits the EGF-stimulated lamellipod extension, increases in F-actin in lamellipods, and chemotaxis in response to the addition of EGF. There is no significant change in the total F-actin content after a 3 minute stimulation with EGF compared to control cells, suggesting that either new actin polymerization was terminated by 3 minutes, that actin polymerization is exactly balanced by actin depolymerization or that actin polymerization was not involved in the EGF-stimulated redistribution of F-actin (Segall et al., 1996).

Well characterized chemoattractants for amoeboid phagocytes such as cAMP, fMLP and autocrine motility factor act through G-protein coupled receptors (Devreotes and Zigmond (1988), Silletti and Raz (1993), Stracke et al., (1993)). However, chemoattractants for cells derived from mesenchymal and epithelial tissues, such as EGF, act through receptors that are receptor tyrosine kinases(Hoelting et al. (1994), Pedersen et al. (1994), Wang et al (1994) Royce and Baum(1991), Grotendorst et al (1989), and Blay and Brown (1985)). Most studies on EGF-stimulated signal transduction have been done on A431 cells (Boonstra et al. (1995), Peppelenbosch et al (1993) and Dadabay et al (1991)). Previous studies on EGF-induced reorganization of the actin cytoskeleton in A431 cells demonstrate the massive accumulation of F-actin and EGF-R in ruffles and under the plasma membrane at the free cell edge in colonies of A431 cells. F-actin content continues to increase with time after EGF addition in A431 cells (Rijken et al. (1991), Rijken et al (1995)). Lipoxygenase and cycloxygenase products (Peppelenbosch et al, 1993) but not phosphoinositide turnover (Dadabay et al, 1991) are involved in EGF-induced remodeling of the actin cytoskeleton in A431 cells. These results are consistent with the observation that the EGF-R is an actin binding protein den Hartigh et al, 1992) and that an EGF-R F- actin association may facilitate formation of a signaling complex containing other kinases and PLC γ in A431 cells (Diakonova et al. (1995), van Delft et al. (1995)).

Although A431 cells are useful for studies of signal transduction, A431 cells are neither highly metastatic nor motile and express abnormally high levels of EGF-R (Price et al, 1988). MTLn3 cells on the other hand have high metastatic potential (Welch et al, 1983), are

chemotactic to EGF (Segall et al., 1996) and the cell surface receptor for EGF is expressed at normal levels (Kaufmann et al. (1990), Lichtner et al. (1992). In addition, the motile and chemotactic responses of MTLn3 cells have similarities to those seen in well-characterized cells such as *Dictyostelium* and neutrophils (Segall et al., 1996). Thus MTLn3 cells provide a powerful model system for the study of EGF involvement in cell motility, metastasis and tumor cell chemotaxis.

The relationship between EGF-induced signal transduction and cortical actin reorganization in MTLn3 cells is presently unclear. For example, does the EGF-stimulated accumulation of actin filaments at the tip of the lamellipod (Segall et al., 1996) result from new actin polymerization? If so, when and where does this polymerization occur?

The research funded by grant DAMD17-94-J-4314 is focussed on identifying key proteins involved in regulation of cell motility and chemotaxis. The Technical Objectives are:

1) Determine the time course and dose response range of changes in cell motility and morphology after stimulation with EGF using time-lapse video microscopy. This determines the appropriate time scale and stimulus concentrations for performing the experiments described in Technical Objectives 2 - 3.

2) Determine the role of actin capping proteins by: a) studying the kinetics of actin nucleation and capping activity following stimulation of cells, and b) measuring the kinetics of aginactin and gelsolin association with the cytoskeleton.

3) Measure actin crosslinking activity and compare with the association of ABP-280, EF-1alpha, and alpha-actinin with the cytoskeleton.

4) Based on the results in Technical Objectives 1 - 3, rank the proteins tested in terms of potential importance in mediating changes in cell motility or morphology after stimulation, and identify or acquire clones for the rat gene for the most important proten.

5) Using clones for the protein chosen in Technical Objective 4, alter xpression of the protein and determine the effects on motility and metastatic capability.

The first Technical Objective was achieved in the first year of the grant. That work demonstrated that regulation of actin polymerization was critical for the motility of MTLn3 cells. During the second year of the grant, work has focussed on Technical Objectives 2 and 3. Our first studies described below demonstrate an EGF-induced actin nucleation activity in MTLn3 cells, and localize that activity to the leading edge of the lamella. This provides the basis for studies related to Technical Objective 2. However, other work performed in our labs and by others has indicated that aginactin is not involved in actin nucleation in other systems. Similarly, studies using mice lacking gelsolin (Witke et al., 1995) have demonstrated that gelsolin is not absolutely necessary for cell motility and actin nucleation. Thus we have shifted focus to two other proteins that currently seem the best candidates for regulating actin polymerization at the leading edge - talin and cofilin. The work on talin is further along and is covered in this report. Studies on cofilin are still in the initial stages, and will be discussed in the next report. With respect to Technical Objective 3, our initial results have focussed on EF-1alpha. In that work we have determined that there is relatively little actin cross-linking occurring in MTLn3 cells upon EGF stimulation. EF-1alpha does associate with actin filaments, but its role in cell motility is less likely. Preliminary work with available antibodies for ABP280 has indicated that more work is necessary to develop them for our particular uses,

and we will explore them further during the coming year. Studies with alpha-actinin will be initiated in the coming year.

PLEASE NOTE: DUE TO A WORD PROCESSOR INCOMPATIBILITY, EF1ALPHA IS REFERRED TO AS "EF1" IN MOST OF THE TEXT OF THIS DOCUMENT.

MATERIALS AND METHODS

All reagents were purchased from Sigma unless otherwise noted.

Cell Culture

MTLn3 cells were clonally derived from a lung metastasis of the 13762NF rat mammary adenocarcinoma (Neri et al., 1982) (kindly provided by Dr. G. Nicolson, MD Anderson Cancer Center, Houston, Texas). MTLn3 cells were grown to 60-80% confluence in minimal essential media (Gibco MEM 12560) supplemented with 5 % bovine serum as described in detail elsewhere (Segall et al., 1996).

Preparation of cell lysates

Cells were harvested with 10 mM EDTA in MEM, centrifuged for 5 minutes at 1000g and 4° C, and resuspended to a concentration of 1.75- 2.0 million cells /ml in serum -free MEM supplemented with 12 mM Hepes at pH 7.4 and 0.35% bovine serum albumin (buffer).

The cell suspension was brought to 37°C in a water bath with occasional mixing of the tube by hand. Within 30 minutes of their removal from the substratum, control cells were treated with buffer, and experimental cells with a final concentration of 5 nM EGF(Life Technologies). The stock of EGF was prepared in filtered Dulbeco's PBS. At various times after treatment of cells with EGF or buffer, one part cell suspension was lysed directly in a spectrofluorometer cuvette held at 22°C and containing four parts lysis buffer (88 mM KCl, 5 mM DTT, 20 mM PIPES, 1mM ATP, 10 mg/ml BSA, 1ug/ml chymostatin, leupeptin, and pepstatin, 5 mM EGTA, 0.2 mM MgCl2, and 0.5% Triton X-100). A 10uM stock of cytochalasin D was prepared in DMSO. In experiments involving use of cytochalasin D, the drug or DMSO was added to each cuvette subsequent to cell lysis. Cytochalasin D was added to a final concentration of 100 nM and allowed to react for five minutes before addition of pyrene actin.

Preparation of Pyrene-labeled Actin and Fluorescence Measurements

Pyrene-labeled actin was prepared by reacting rabbit muscle actin with N (1-pyrenyl) iodoacetamide as described by Cooper et al. (1983) except that the reagent was dissolved in DMSO. Pyrene -labeled and unlabeled G-actin were chromatographed on Sephadex G150 (Pharamcia Fine Chemicals, Piscataway, NJ) before use. Both pyrene-labeled and unlabeled G-actin were stored by dialysis against buffer A (2 mM Tris-Cl, 0.2 mM ATP, 0.5 mM DTT, 0.2 mM CaCl2) at an approximate concentration of 20 uM and used as a mixture of 10 % pyrene-labeled and 90% unlabeled G-actin. Actin was added to cell lysates at a final concentration of 2-3 uM. Fluorescence was measured in a spectrofluorometer (F2000, Hitachi Corp.) at 22 ° C with an excitation wavelength of 365 nm (slit width 10 nm) and an emission wavelength of 407 nm (slit width 10 nm). Samples were exposed to the excitation beam intermittently and through a neutral density filter to avoid photobleaching. Cell lysates had no measurable autofluorescence at these wavelengths. The increase in fluorescence intensity was linear for the duration of the measurement. Data (change in fluorescence intensity over time) for the calculation of barbed ends and relative rate was taken from the initial rate of increase of pyrene-actin fluorescence. The contribution of barbed ends to this rate and therefore the number of barbed ends was determined by subtracting the rate in the presence of 0.1 uM cytochalasin D from the total rate. The number of barbed ends was calculated by converting

the change in fluorescence of pyrene-actin to concentration of F-actin using a standard curve and dividing the rate of change in concentration of F-actin by $(K_+ C - K_-)$ where $C=3$ uM, K_+ $=11.6$/uM sec and $K_- = 1.4$ /sec (Pollard, 1986).

F-actin content was measured using the NBD-phallicidin binding assay as described previously (Segall et al., 1996).

Preparation of Rodamine-Labeled Actin

Rodamine-labeled actin was prepared by reacting rabbit muscle actin with 5-(and) 6-carboxytetramethylrhodamine, succinimidy ester (NHSR, Molecular Probes c-1171). Two cycles of actin assembly-disassembly were performed to characterize the rhodamine-labeled actin. Thirty nine mgs of Spudich and Watt actin (Spudich and Watt, 1971) was dialyzed against two changes of 250 ml of 5mM Tris pH 8, 0.2 mM $CaCl_2$ and 0.2 mM ATP for 24 hours. G-actin was then clarified and diluted to 3 mg/ml with 50 mM K pipes pH 6.8, 50 mM KCl, 0.2 mM $CaCl_2$, and 0.2 mM ATP. G-actin was polymerized by dialyzing it against 1000 ml of the above solution for 3 hours. F-actin was then dounced on ice to break up aggregates, ATP was added to 0.5 mM and NHSR was added to a concentration of 0.625mg/ml. The reaction mixture was polymerized at room temperature in the dark for 1 hour and F-actin was pelleted by spinning for 2 hours at 48K rev/min at 4°C. The pellet was resuspended and dounced on ice with 2 ml of 20 mM Tris pH 8.1, 5 mM DTT, 5 mM K glutamate, 0.2 mM $CaCl_2$ and 1 mM ATP and 1 ml of buffer A, 2mM Tris-Cl, 0.2 mM ATP, 0.5 mM DTT, 0.2 mM $CaCl_2$ and 0.02% sodium azide. Actin filaments were dialyzed against buffer A for 48 hours to depolymerize the filaments. G-actin was clarified in a TL100 at 95 K rpm for 15 minutes at 4 °C and chromatographed over a G-150 column that was previously equilibrated with buffer A. The G-actin from the protein pool was polymerized with 10mM PIPES, pH 7, 2mM $MgCl_2$ and 50 mM KCl at room temperature for 1 hour. F-actin was pelleted with Ti 70 at 48 Krpm at 4°C for 2 hours, resuspended in 5 ml of buffer A and dialyzed for 2 days on ice against buffer A. Another cycle of actin assembly and disassembly was carried out as described to characterize the rhodamine-labeled actin and demonstrate that the dye : protein ratio remained constant. The dye to protein ratio was determined by absorption spectrophotometry using extinction coefficients of $\varepsilon_{280} = 48,988$ /M cm for actin and $\varepsilon_{560} = 50,000$ / M cm for tetramethyl Rhodamine (Molecular Probes). The final G-actin was dialyzed against 1M sucrose in buffer A for 6 hours and stored frozen in liquid nitrogen. The frozen rhodamine-labeled actin stock was stored at a concentration of 237 uM with a dye to protein ratio of approximately 1 to 1.

Saponin Permeabilization of MTLn3 cells

MTLn3 cells were plated on collagen I coated MATTEK tissue culture dishes for 24 hours. Cells were plated at a density of 5000 cells/sq cm and incubated overnight in complete growth medium including 5 % FCS as described above. On the day of the experiment, the complete growth medium was replaced with a serum free medium and cells were incubated for 3 hours at 37 °C, 5% CO_2. Stock rhodamine-labeled actin was rapidly thawed from liquid nitrogen and diluted to 12 uM with 1 mM Hepes pH 7.5, 0.2 mM $MgCl_2$, and 0.2 mM ATP , sonicated and clarified in a airfuge for 20 minutes. Control cells were treated with buffer, and experimental cells with a final concentration of 5nM EGF in buffer for various times at 37 °C. Further steps were done at room temperature. The stimulation medium was aspirated and cells

were permeabilized with permeabilization buffer (PB)(20 mM Hepes, pH 7.5, 138 mM KCl, 4 mM MgCl2, 3 mM EGTA, 0.2mg/ml of saponin, 1mM ATP) containing 0.45 uM rhodamine-actin that was added just before application to cells.   At various times after incubation with PB containing rhodamine-labeled actin, cells were fixed for 5 minutes with 3.7 % formaldehyde in PBS (145mM NaCl, 4 mM NaH2PO4, 6 mM Na2 HPO4. 7 H2O and 0.02 % NaN3). This was then replaced with 0.1 M glycine in PBS for 10 minutes.   After washing the cells 5 X with PBS, the cells were stained with 1µM fluorescein phalloidin for 20 minutes in a humidified chamber.   Unbound stain was then washed off with PBS 5X and a coverslip was mounted on the MATTEK dish with 0.1 M. N-propyl gallate,0.2 % NaN3 in 50 % glycerol in PBS, pH 7.0.

Capping protein from *Dictyostelium* (Eddy, et al., 1996) kindly provided by Jing Hua Hang, was kept at a stock concentration of 2uM in mono Q buffer (20mM TRIS pH 7.5, 35 mM NaCl, 0.5 mM DTT and 1 mM EGTA). Cytochalasin D was obtained from Sigma, and stored at a 2 uM stock in DMSO.

Fluorescence Microscopy

Fluorescent imaging and data collection was done using a SIT camera (Hamamatsu), 60X objective, with a N.A. 1.4, on a Nikon Diaphot with fluorescence optics. Images of single optical sections 0.5 um from the substratum were collected using a N.A. 1.4 60x objective on BioRad MRC-600 confocal microscope. Identical settings were used to collect images from cells at each of the experimental conditions being tested in the linear range of either detector's response and at a sensitivity such that none of the pixels in the image were saturated. To quantitat the fluorescence as a function of distance from the edge of the lamellipod, data was collected for equal numbers of cells from each experimental condition tested. Images from the SIT camera or the confocal were collected and stored on a Macintosh computer using NIH Image. Analysis of the images from the SIT camera and the confocal microscope was done by a macro program described previously that measures the fluorescence as function of distance from the tip of the lamellipod (Segall et al., 1996).

The cytoskeletal distribution of EF1 was imaged by reducing the amount of soluble intracellular material with mild detergent extraction prior to fixation. For these experiments cells were plated on Mattek dishes, starved and stimulated as above. After aspiration of the bathing medium, 100 µl Buffer E (20 mM Pipes , pH 6.5 with 30 mM KOH; 4 mM MgCl2; 10 mM EGTA pH 6.5 with 20 mM KOH; 5 µM phallacidin; 0.025% saponin) was added to the culture well. After 15 seconds of extraction the dish was flooded with Fix Buffer containing 3.7% formaldehyde. The specimens were then processed for immunofluorescence microscopy as described above.

Measurement of rhodamine-actin intensity in different cell regions

Rhodamine-actin intensity at the cell periphery was first measured as function of distance from the tip of lamellipod as described previously (Segall et al., 1996).   The average pixel intensity of this peak of rhodamine-actin fluorescence was used to calculate the rate of incorporation of rhodamine-actin after permeabilization with saponin. Rhodamine-actin intensity at the cell center was measured as the average pixel intensity of the traced centroid as indicated in Figure 4 B.

The generation of tumors

MTLn3 and MTC cell cultures were grown to 60-80% confluence, harvested and then were resuspended at a density of 6.7×10^6 cells / ml and placed on ice. For tumor production, female Fisher 344 rats (Charles River) were injected with either MTLn3 or MTC cells. In all cases, 1×10^6 cells were injected subcutaneously into the fat pad located between the 3rd and 4th nipples. The growth of tumors was allowed to progress for 3 - 5 weeks.

For the purification of EF1 and histopathology analysis, tumors were harvested by excision of the primary tumor following CO_2 euthanasia. To determine the metastatic activity of each cell line, the lungs and ipsilateral and contralateral axillary lymph nodes were removed and fixed in Dubellco's PBS (Gibco) containing 3.7% formaldehyde (Fluka). Representative sections of the fixed tissues were submitted for routine histologic examination.

The purification of EF1 from MTLn3-generated tumors

The purification of EF1 from vertebrate tissues was modified from Edmonds et al. (1995). All procedures were performed at 4° C. Excised tumors were weighed, then minced and diluted 5-fold (w/v) with Buffer L (5 mM PIPES pH 7.0, 1 mM DTT, 1 mM EGTA) containing the protease inhibitors: chymostatin, leupeptin, and pepstatin (10 μg / ml each). The tumor was homogenized 3 x 10 sec (Polytron) and then further homogenized in a Teflon / glass homogenizer for 30 passes. The homogenate was spun at 100,000 g • hours in a Beckman Ti70 rotor. The supernatant was brought to 15% glycerol (v/v) and then was loaded onto a 5 x 20 cm DE52 (Whatman) anion exchange column equilibrated with Buffer 52 (20 mM PIPES pH 7.0, 1 mM DTT, 0.1 mM EDTA, 15% glycerol (v/v)). EF1 , as detected by SDS-PAGE and western blot analysis (see below), eluted in the flow-through fractions and was immediately loaded onto a 1.6 x 10 cm Poros II HS (PerSeptive Biosystems, Cambridge MA) cation exchange column equilibrated with Buffer 52. EF1 was eluted using a 200 ml 0 - 1 M NaCl gradient. The EF1 -containing fractions were determined by SDS-PAGE / western blot, pooled, diluted to a NaCl concentration of 100 - 200 mM, and then loaded onto a 1 x 10 cm ceramic hydroxylapatite column (BioRad) equilibrated in Buffer HTP (10 mM Pipes pH 6.8, 10 mM KPO_4, 1 mM DTT, 15% glycerol). EF1 was eluted with a 100 ml 0 - 1 M NaCl gradient. To rapidly concentrate the sample, the EF1 -containing fractions were again pooled, diluted to a 100 - 200 mM NaCl concentration, and then loaded onto a 0.46 x 10 cm Poros II HS column equilibrated in Buffer HTP. The EF1 sample was eluted with a 1 M NaCl pulse and then vacuum concentrated / dialyzed into Buffer S (10 mM Pipes pH 7.0, 1 mM DTT, 0.1 mM EDTA, 20% glycerol, 0.02% NaN_3) containing 0.5 M NaCl. The final EF1 sample was dialyzed against Buffer S lacking NaCl and stored under liquid nitrogen. The typical yield from a 8 g tumor was 0.5 mg EF1 with >90% purity as assessed by scanning densitometry of SDS-PAGE gels (Figure 23B).

Purification of EF1 from normal rat liver

The livers from female Fisher 344 rats were excised, weighed, minced, diluted 5-fold (w / v) with Buffer L and then were homogenized in a Teflon / glass homogenizer for 30 passes. The remainder of the purification was as described above for tumor EF1 .

Poly (U)-directed polyphenylalanine synthesis

The procedure for the in vitro synthesis of polyphenylalanine was as described (Carvalho et al., 1984). The purified reagents for the assay: ribosomes, EF-2 and (^{14}C)Phe-tRNA (850 cpm/pmol) from rabbit reticulocytes, and EF1 from yeast, were kindly provided by Dr. William Merrick (Case Western Reserve University, Cleveland OH).

Assessment of the specificity of an anti-EF1 antibody

An anti-EF1 antibody was produced in chicken against a synthetic peptide, AGAGKVTKSAQKAQKAK, corresponding to the carboxyl terminus of mouse EF1 which is highly conserved between all EF1 s. The peptide was coupled to poly-L-lysine (MW 15,000 - 30,000) via an N-terminal cysteine residue at a molar ratio of peptide:poly-L-lysine of ~5. Total immunoglobulin Y was isolated from egg yolk by polyethylene glycol precipitation as described elsewhere (Carroll and Stollar 1983), and was further purified by affinity chromatography against the same peptide immobilized on epoxy-activated Sepharose. Monospecific antibodies were eluted with 0.1 M glycine HCl (pH 2.2), neutralized immediately with 1 M Tris-HCl (pH 9.0), concentrated with a Centricon-30 (Amicon) and stored at -20°C in 50% glycerol.

The specificity for EF1 was assessed by western blot analysis. Samples were transferred to nitrocellulose membranes from SDS-PAGE gels using a semi-dry blotter (BioRad) and the immunoreactive polypeptides were visualized with an ECL chemiluminescence kit (Amersham). As shown in Figure 23, the antibody recognizes a single polypeptide of 50 kDa apparent M_r in homogenates from both whole tumors derived from MTLn3 cells (lanes a, b) and normal rat liver (lanes c, d). In addition, the antibody recognizes a single 50 kDa band in whole cell homogenates of MTC cells, Dictyostelium, and EF1 purified from Dictyostelium (data not shown).

To determine the specificity of the anti-EF1 peptide antibody for immunofluorescence the antibody was preabsorbed against purified rat liver EF1 transferred to nitrocellulose (Olmsted 1981). As a parallel control, the anti-EF1 peptide antibody also was preabsorbed against nitrocellulose alone. As shown for MTLn3 cells, following preabsorption against EF1 (Figure 25G), but not nitrocellulose (data not shown), the fluorescence intensity is greatly reduced (compare to Figure 25B), while the rhodamine-phalloidin staining of F-actin is unaffected (Figure 25H). Taken together the above data affirm the monospecificity of this antibody for EF1 .

The determination of the expression levels of EF1

Rat MTLn3 tumor, MTC tumor and normal liver tissues were excised and processed as described above. MTLn3 and MTC cultured cells were placed directly into SDS-PAGE sample buffer. Duplicate samples were separated by SDS-PAGE, and then either stained with Coomassie Blue, or processed for western blotting. For quantitation of EF1 by densitometry a standard curve of purified liver EF1 concentrations was included on all western blots. Western transfer and membrane processing were performed as above except ^{125}I-Protein A was used to detect the primary antibody. Densitometry analysis of Coomassie Blue-stained SDS-PAGE gels for actin and corresponding ^{125}I autoradiograms for EF1 was performed with a laser scanning densitometer equipped with ImageQuant software, (Molecular Dynamics). To determine the total cellular protein per MTLn3 and MTC cell, a BCA protein assay (Pierce) was performed. Cultured cells were lysed as above except 0.5% Triton X-100 was used.

The evaluation of F-actin binding by EF1

F-actin binding to purified MTLn3 tumor and rat liver EF1 was assessed by differential co-sedimentation analysis (Edmonds et al., 1995). EF1 (1 μM) was co-polymerized with rabbit skeletal muscle actin (3 μM; Condeelis et al., 1982) in Sedimentation Buffer (20 mM Pipes pH 6.0-8.0 with 30-35 mM KOH, 1 mM MgOAc, 0.2 mM DTT, 1 mM ATP, 25% glycerol) overnight at 4 °C. To distinguish between crosslinked versus single actin filaments, the EF1 -F-actin mixtures were centrifuged differentially in an Airfuge (Beckman). Crosslinked filaments were pelleted preferentially at 50,000 x g for 4 minutes (Low Speed Pellets). Then the resultant low speed supernatants were spun at 130,000 x g for 45 minutes to pellet single actin filaments (High Speed Pellets). In some experiments co-sedimentation assays were performed in a buffer designed to mimic the intracellular ionic composition of mammalian cells (Alberts et al., 1994): 30 mM Pipes, pH 7.5; 130 mM K$^+$ gluconate; 1 mM DTT; 10 mM NaCl; 1 mM MgOAc; 1 mM ATP; 70 mg/ml polyethylene glycol 8000. To determine the percentage of EF1 in each sample, SDS-PAGE, western blotting and laser scanning densitometry were performed as described above.

Cell fractionation following stimulation with EGF

Cells were harvested, resuspended to a density of 5 x 10^6 cells / ml in MEMH, and allowed to re-equilibrate to 37° C for 10 min. For cell lysis, 200 μl of the cell suspension was removed and mixed with 800 μl of ice cold Lysis Buffer (20 mM Pipes pH 6.5, 88 mM KCl, 5 mM EGTA, 0.2 mM MgCl$_2$, 5 mM DTT, 1 mM ATP, 10 μg / ml each of chymostatin, leupeptin and pepstatin, 0.5 % Triton X-100). Cell aliquots were obtained both before and after the addition of EGF (5 nM) in MEMH. As a control, instead of stimulation with EGF, an equal volume of MEMH was added and pre- and post-addition time points were collected. Triton-insoluble cytoskeletons were pelleted at 400,000 g for 20 min at 4° C to obtain high speed pellet (HSP) and supernatant (HSS) fractions.

SDS-PAGE gels and corresponding ^{125}I-protein A western blots were prepared for all time points for LSP, HSP and HSS fractions. The amount of EF1 per time point was determined by densitometry analysis of autoradiograms and the amount of actin per time point was determined by densitometry analysis of Coomassie Blue-stained SDS-PAGE gels as described above. The amount of total protein in each lane was also determined by densitometry analysis of the Coomassie Blue-stained SDS-Page gels, and the ratios for EF1 :total protein and actin: total protein were determined for each time point.

To determine if the EGF-mediated redistribution of EF1 is dependent on the integrity of the actin cytoskeleton, cells were prepared as above, then cytochalasin D (100 nM), or an equal volume of MEMH containing DMSO was added five minutes before stimulation with EGF. Stocks of cytochalasin D were prepared in DMSO and then diluted into MEMH. The final concentration of DMSO was 0.1%.

RESULTS

Part 1: Temporal and Spatial Analysis of Actin Nucleation

In this section, we examine in detail the temporal and spatial distribution of actin polymerization in EGF-stimulated MTLn3 cells. We used a pyrene- labeled actin nucleation assay to determine the kinetics of the nucleation activity in EGF-stimulated MTLn3 cells and an *in situ* rhodamine- actin polymerization assay to determine the location of these nucleation sites.

Actin Nucleation Activity in Lysates Varies with Time After Stimulation

Our previous studies have demonstrated that addition of EGF to MTLN3 cells stimulates extension of lamellipods that contain increased amounts of F-actin at their tips (Segall et al., 1996). To determine if there is a transient burst of actin polymerization after EGF stimulation that can account for this redistribution of F-actin, pyrene-labeled actin was used to measure the timing of actin nucleation after EGF stimulation of MTLN3 cells. Cells were lysed with Triton X-100 at various times after stimulation with EGF. The amount of nucleation activity present in the lysate at each time point was measured as an increase in fluorescence and expressed either as the number of free barbed ends, Figure 1A (calculated as described in Materials and Methods) or as a ratio of the initial rate of polymerization in the stimulated state relative to that in the unstimulated state (Figure1A, inset). This ratio is referred to as the relative rate. The unstimulated samples used for calculating relative rate were obtained by lysing cells prior to addition of EGF to the cell suspension.

The initial rate of actin polymerization in lysates from stimulated cells varies with time after stimulation, as shown in Figure1A. The number of barbed ends associated with this increase in rate peaks at one minute and decreases steadily until 2.5 minutes, after which levels remain roughly constant and slightly above baseline. The number of barbed ends increases by approximately 6000 by 1 minute after EGF stimulation. Addition of buffer rather than EGF clearly does not stimulate a significant increase in nucleation activity. Actin polymerization occurring in cell lysates from stimulated cells is effectively inhibited by 100 nM cytochalasin D, suggesting that the nucleation activity results in filaments that grow at the preferred, i.e., barbed end (Figure1A, inset).

Figure 1B shows the relative F-actin content of MTLn3 cells after stimulation with EGF as measured using the NBD-phallicidin binding assay on cells spread on a collagen coated substratum. F-actin content increases transiently, returning to prestimulation levels by 1.5-2 minutes. This initial transient in F-actin content roughly correlates with the transient increase in barbed ends measured in cell lysates (Figure 1A) suggesting that the increase in barbed ends stimulated by EGF causes the increase in F-actin content.

Rhodamine-G-actin is incorporated preferentially at the tips of lamellipods induced by EGF stimulation

While the pyrene-actin and NBD-phallicidin assays provided useful information on the time course of actin nucleation, they did not address the spatial organization of the EGF-stimulated nucleation sites in the cells. To determine the location of nucleation sites, exogenous rhodamine-actin was added to saponin-permeabilized MTLn3 cells, in a experiment

designed after Simons and Mitchison (1991). Exogenous rhodamine-actin incorporates into the exposed nucleation sites inside the cell marking their location. In Figures 2 and 3, MTLn3 cells were treated with either buffer or 5nM EGF for 1 minute, the peak of EGF-stimulated nucleation activity, permeabilized in the presence of rhodamine-actin monomers which were allowed to polymerize from the saponin-exposed nucleation sites and then fixed and counter stained with fluorescein-phalloidin to visualize all actin filaments. Almost all cells stimulated with EGF extend around their entire periphery a flat, hyaline, ruffle-free lamellipod that is seen only occasionally in control cells (Figure2A,B). FITC-phalloidin staining demonstrates that F-actin accumulates at the tips of these lamellipods in EGF-stimulated cells without significant changes in the rest of the cytoskeleton (Figure 2 C,D). In control cells, rhodamine-actin incorporates primarily at the leading edge, and at the ends of stress fibers(Figure 2 E, Figure 3 A). However, in EGF-stimulated cells (Figure 2 F, Figure 3 B) rhodamine-actin shows dramatic incorporation in the entire lamellipod tip whereas incorporation in stress fibers is like that seen in control cells. Thus, control cells and EGF-stimulated cells not only have a clear morphological difference but differ also in the degree of rhodamine -actin incorporation.

To determine whether the pattern of rhodamine-actin incorporation observed in EGF-stimulated MTLn3 cells is dependent on diffusion, the rhodamine fluorescence intensity at the tips of the lamellipods was compared to that in the cell center as a function of the rhodamine-actin incubation time. Since the thickness of the cell differs between the center and the lamellipod tip, the time required for actin to diffuse throughout may be different for these two compartments. If rhodamine-actin incorporation is diffusion limited, polymerization of rhodamine-actin at the tip of the lamellipod would reach steady state earlier than incorporation at the cell center. As shown in Figure 4A, actin incorporation at the tip of the lamellipod is completed by about 3 minutes of incubation time. As shown in Figure 4B, rhodamine -actin incorporation is also completed by 3 minutes in the cell center. At 5 minutes, the incubation time used for all the experiments, rhodamine-actin is incorporated to steady state both at the cell periphery and at the cell center. Therefore, the pattern of rhodamine-actin incorporation observed in EGF-stimulated MTLn3 cells is dependent on the availability of nucleation sites and not dependent on differences in cell thickness. This is also supported by Figure 5, which shows that the same pattern of rhodamine-labeled actin incorporation is observed whether cells are incubated for 1 minute or 5 minutes with rhodamine-actin.

As shown in Table 1, 70% of EGF-stimulated cells have an F-actin rich lamellipod, compared to only 14 % of control cells. 95 % of EGF-stimulated cells have continuous intense rhodamine fluorescence in the entire tip of the lamellipod compared to only 12% of control cells. When quantified as a function of distance from the edge of the cell, hyaline regions of the cell periphery show more rhodamine-actin staining near the plasma membrane in EGF-stimulated cells (Figure 6), as compared to control cells. As shown in Figure 3, comparison of the distribution of F-actin (green) and rhodamine-actin (red) in 2 channel overlays, demonstrates that the rhodamine-actin is narrower and closer to the plasma membrane than the F-actin zone at the tip of the lamellipod. The distribution of stain indicates that the nucleation sites are more proximal to the plasma membrane side of the F-actin rich cortex.

Actin Nucleation in permeabilized MTLN3 cells is Barbed End Dependent

To determine whether the EGF-stimulated incorporation of rhodamine-labeled actin into the saponin cytoskeleton is depended on pointed or barbed end subunit addition, we

measured the effect of capping protein that specifically caps the barbed ends of actin filaments. Cells were stimulated with 5 nM EGF for 1 minute, permeabilized in the presence or absence of 20 nM capping protein and subsequently incubated for 5 minutes with 0.45 uM rhodamine-actin in permeabilization buffer, fixed and stained with fluorescein-phalloidin as before. As shown in Figure 7, 20 nM capping protein inhibits the incorporation of rhodamine labeled actin at the tips of the lamellipods and at the ends of the stress fibers. Interestingly, capping protein caused a significant decrease in the incorporation of rhodamine-actin in EGF-stimulated cells compared to control cells as quantitated in Figure 6. Similar results were obtained with cytochalasin D (data not shown). These results suggest that both polymerization and depolymerization are stimulated by EGF and that the depolymerization can be detected when polymerization is blocked by capping the barbed ends of filaments (see Discussion).

To confirm that the actin nucleation activity in EGF-stimulated cells is barbed end dependent and that there is no cross-channel fluorescence in our imaging system, the above experiment was repeated with cytochalasin D without the addition of fluorescein-phalloidin. Cytochalasin D inhibits the rhodamine-actin incorporation into the EGF-stimulated saponin permeabilized cells (Figure 8) as observed in the presence of capping protein. In addition, Figures 7 and 8 demonstrate that the fluorescence channels were free from cross over. Therefore, the location of F-actin and sites of actin polymerization were detected as independent images. Figure 8 also supports the previous observation that the rhodamine signal seen at the end of the stress fibers in EGF-stimulated cells are sites of rhodamine - actin incorporation.

Part 2: The role of talin and adhesion in cell motility

In this section, we analyze talin as a possible protein involved in regulating lamellipod extension. Talin was selected because it has been reported to nucleate actin assembly, and has been seen at the leading edges of lamellipods in randomly locomoting cells. However, talin also has been identified as a protein involved in cell-substratum adhesion through interaction with integrins. Thus our goals were to 1) determine if talin is localized at the leading edges of lamellipods stimulated by EGF (the sites at which the studies in part 1 indicate actin nucleation is occurring),, and 2) whether cell - substratum adhesion (including focal contacts) is an important component for regulating lamellipod extension.

Metastatic cells display ameboid chemotaxis

We demonstrated previously that metastatic MTLn3 cells displayed chemotaxis towards EGF as measured in the modified Boyden chamber assay (Segall et al, 1996). An assay was developed, based on the classical pipette experiment used to analyze the chemotactic activity of *Dictyostelium discoidum*, to determine if individual MTLn3 cells would display comparable ameboid movements in response to a gradient of EGF. The gradient of EGF was generated by placing a pipette filled with a concentrated solution of EGF (1 μM) next to individual MTLn3 cells starved for 3 hours in serum-free medium in regular tissue culture dishes. Figure 9A shows a typical video sequence of one MTLn3 cell crawling towards the pipette. The cell moves at an average rate of 1.5 um/mn in the direction of the pipette, and undergoes a dramatic change in direction to follow the pipette when it is moved to another place (Figure 9A, sequence 16:31:04).

Digital analysis of the movement showed that the cell maintains a rather linear motion towards the pipette (Figure 9B insert and direction arrows). It rapidly changes direction to follow the pipette (within 2 or 3 minutes), and resume linear motion in the new direction. Analysis of the difference movie shows that the cell undergoes cycles of protrusion at the front (visualized in green) and retraction at the rear (visualized in red, Figure 9B). Protrusion mainly occurs by the extension of a flat broad lamellipodia in the direction of the pipette (Figure 9 A, sequence 16:18:17). Complete reversal of polarity was also seen when the gradient of EGF was applied next to the rear of randomly polarized cells (data not shown).

Upshift in EGF as a model to study chemotaxis

Chemotaxis has been widely studied in ameboid organism such as Dictyostelium or neutrophils (Devreotes and Zigmond, 1977). However, the molecular mechanisms underlying chemotaxis in malignant cells remain unclear. From the data on Dictyostelium or neutrophils, as well as studies on random motility in fibroblasts (Refs in Rinnerthaler et al, 1988), it was generally assumed that chemotaxis in cancer cells would mainly encompass three essential steps, i.e. protrusion, assembly of new contacts with the substrate at the front and disassembly of preexisting contacts at the rear (Lauffenburger and Horwitz, 1995). We previously showed that stimulation of MTLn3 metastatic cells with a homogeneous concentration of EGF resulted in an actin-dependent extension of a lamellipod. We attempted to use this assay as a convenient model to study the main steps of chemotaxis in metastatic tumor cells. Lamellipod extension following stimulation with a homogeneous concentration of EGF (5 nM) was analyzed in MTLn3 cells using interference reflection microscopy (IRM) coupled to time-lapse imaging. IRM was used to visualized any modification of the contacts with the substrate after EGF stimulation. Figure 10 presents a representative IRM sequence for one MTLn3 cell. EGF stimulation triggers a rapid and drastic protrusive activity, which occurs in the form of the extension of a flat broad lamellipodia. This extension is maximum around 3-4 minutes and accompanied by the simultaneous establishment of close contacts in the newly extended area. After 5 minutes, new focal contacts are forming, which are then increasing in size over the course of 20 minutes. In the mean time, many of the previously existing large focal contacts are remodeled: some of them are diffusing and are no longer visible after 20 minutes, while those located at the rear are dragged for a while by the cell and then disassembled, at least partly, as the cell rips the tail. We investigated more precisely the kinetics of the phase of EGF-stimulated protrusive activity, i.e. lamellipod extension, in the upshift assay. Lamellipod extension was followed using phase contrast microscopy coupled to time lapse video recording, and quantitated as an increase in the total cell area after digital analysis of the images. The extension starts within 1 minute after EGF stimulation (see corresponding image in Figure 10) and is maximum around 3-4 minutes after stimulation, resulting in an average increase in cell area of 45 % (Figure 11). The increase in cell area subsequent to EGF stimulation could reach up to 100% in some experiments (data not shown). The cell area then tends to plateau at or near the maximum area for at least 15 minutes after stimulation. Unstimulated cells or cells stimulated with control medium without EGF displayed no major modification in cell area over the course of 20 minutes.

Correlated with extension of the lamellipod is the presence of talin at the leading edge of the lamellipod as identified using immunofluorescent localization (Figure 12). The band of talin at the

leading edge is maximal about 3 min after EGF stimulation (Figure 12, left). Subsequently, talin is present in newly assembling focal contacts as detailed below.

EGF stimulation triggers the assembly of new focal contacts.

New focal contacts appear around 5 minutes after EGF stimulation (Figure 13). The kinetics of new focal adhesion appearance were measured using immunofluorescence confocal microscopy on fixed cells. The cells were stimulated with EGF for different amounts of time, and then fixed and stained with anti-talin antibodies, which localize in focal contacts as confirmed by IRM on the same cells. Focal contacts were then counted and their lengths were measured in a representative number of cells. The mean number of focal contacts per cell increases significantly 3 minutes after stimulation and peaks at 5 minutes (Figure 14). It then plateaus for a few minutes and slightly goes down to a steady level which is approximately twice that found in cells before stimulation. In the mean time, the mean length of the focal contacts undergoes a significant decrease 5 minutes after stimulation and then increases back to the mean size measured in non stimulated cells over the 20 minute course of the experiment (Figure 14). This reflects the appearance of numerous new small focal contacts at 5 minutes after stimulation, and their progressive growth to mature full size by 20 minutes (Figure 13). These new focal contacts are not restricted to the margin of the lamellipodia but also develop in the cytoplasm beneath the cell cortex. It should be noted they appear unumbiguously after the lamellipod had reached maximal extension.

Phosphotyrosine staining disappears from large preexisting focal contacts after EGF stimulation.

IRM studies showed that remodeling of preexisting mature focal contacts happens after 5 minutes of EGF stimulation. Some of them are diffusing and finally disappear while others may be dragged by the cell for a while before they get remodeled or vanished. Immunofluorescence studies coupled to IRM did not able us to demonstrate any obvious alteration in the pattern of talin staining in mature focal contacts (as defined by a large size) after EGF stimulation (data not shown). On the other hand, it is known that stable focal contacts display high levels of phosphotyrosine labeling using immunofluorescence light microscopy. We thus investigate whether the level of phosphotyrosine would be altered in mature focal contacts after EGF stimulation, as opposed to the level of talin staining which appeared to remain unaffected. Representative images of cells double-labeled for talin and phosphotyrosine showed that as expected, non stimulated cells display almost exactly the same distribution for talin and phosphotyrosine, i.e. mainly in focal contacts (Figure 15, top row). Comparable results were obtained within the first 3-4 minutes after EGF stimulation (data not shown). However, 5 minutes after EGF stimulation, some of the large preexisting mature focal contacts are no longer visible using phosphotyrosine staining, or at least display a much weaker staining, while they still show a very strong signal for talin (Figure 15, bottom row). The respective fluorescence intensities in each focal contacts in a representative number of cells were then quantitated on single optical sections generated using the confocal microscope as described in material and methods. The results show that in non stimulated cells the mean ratio of talin and phosphotyrosine fluorescences remain as a constant independently of the size of the focal contacts (Figure 16A). However, 5 minutes after EGF stimulation, while this ratio has not changed in the small focal contacts, it is increasing linearly as a function of the size of the focal contacts. This change appeared highly significant ($p<0.00001$, Figure 16B). Comparison of the values of mean fluorescence intensities

per area in individual focal contacts for talin and phosphotyrosine before and 5 minutes after EGF stimulation shows that the values for talin remain constant (mean integrated density per pixel in individual focal contacts 105.6±1.7 before stimulation, versus 105.6±1.1 five minutes after stimulation). However, there was a significant decrease in the mean fluorescence values for phosphotyrosine staining in focal contacts when non stimulated cells were compared to cells 5 minutes after stimulation (mean integrated density per pixel in individual focal contacts 92.2±1.8, versus 83.1±0.9 five minutes after stimulation, $P < 1.3 \times 10^{-10}$). Thus the increase in the ratio of the talin and phosphotyrosine fluorescences in the larger (and thus older) focal contacts at 5 minutes after EGF stimulation is due to a specific decrease in the phosphotyrosine fluorescence in those focal contacts when compared to the small ones (presumably the more recent ones).

EGF stimulates protrusive activity in suspension.

Since the new focal contacts form unambiguously after the lamellipod had reached maximal extension after EGF stimulation, it appeared that the extension process *per se* does not require the establishment of focal contacts. However, IRM studies show that the lamellipod does not extend completely off the substrate but rather is accompanied by the concomitant establishment of large areas of close contacts (Figure 13). We thus wondered if the cells would still be able to express EGF-stimulated protrusive activity in suspension, i.e. independently of any contact with a substrate. DIC images show that unstimulated cells in suspension appear round with a rather smooth surface (Figure 17A). Two minutes after EGF stimulation, those cells display a high number of protrusions which appear to be enriched in F-actin. By five minutes after stimulation, the number, as well as the size of the protrusions on the cell surface has decreased. Figure 18 shows that the number of cells displaying protrusive activity, as recorded with DIC, peaks at 2 minutes after EGF stimulation. The intensity of the protrusive activity (as evaluated by the number of protrusions and the size of the protrusions) follows the same kinetics.

EGF stimulates transient dorsal protrusive activity in adherent cells.

We showed that the main EGF-stimulated protrusive activity in adherent MTLn3 cells was the extension of a broad lamellipodia over the surface of the substrate. We investigated whether stimulated adherent cells might display other kind of protrusive activity, not related to any contact with the substrate. For this purpose we used confocal microscopy and 3-dimensional reconstruction of the cells at different time after stimulation to identify any protrusive activity over the cell surface that was not in contact with the substrate (i.e. on the dorsal surface). Representative images are shown in Figure 19A. The number of adherent cells displaying actin-rich protrusions over their dorsal surface was evaluated using fluorescence light microscopy on cells fixed and stained for F-actin with rhodamine-labeled phalloidin (Figure 19C). The majority of unstimulated adherent cells display rather few protrusions over their dorsal surface. However, after EGF stimulation, the number of cells displaying consistent protrusive activity over their dorsal surface increases up to a maximum of 50% at 2 minutes. This number further undergoes a rapid decrease, and by 3 minutes after stimulation 85% of the cells display a smooth dorsal surface devoid of any protrusive activity. This fraction is still much less than what is found in unstimulated cells, where approximately 30% of the cells express a constitutive level of protrusive activity on their dorsal surface. Interestingly, the cells undergo recovery of their dorsal protrusive

activity and the number of cells displaying protrusions over their dorsal surface goes back to the level of unstimulated cells (around 30%) by 20 minutes after EGF stimulation (data not shown).

Substrate-free extension of a lamellipod in EGF stimulated adherent cells.

Stimulation of cells in suspension showed that MTLn3 metastatic cells display consistent protrusive activity after EGF stimulation in the absence of any contacts with the substrate. We next attempted to study lamellipod extension in conditions where adherent cells can only extend a lamellipod free off the substrate. MTLn3 cells were plated on vitronectin for 2 hours, and the cells were stimulated with EGF in presence of 1.5 mM of active GRGDSP peptide or control GRADSP peptide (Figure 20). GRGDSP peptide completely inhibits MTLn3 cells' attachment and spreading on vitronectin, while control GRADSP has no effect (data not shown). Lamellipod extension was slightly decreased in presence of the GRGDSP peptide (approximately 70-80% of the response measured in the controls), but the kinetics of extension remained the same, with a maximum around 3-4 minutes after stimulation. However, after lamellipod had reached maximal extension, it retracted by levels until the area of the cell was back to where it was before stimulation. The retraction of the lamellipod (as measured by the decrease in area) takes place over the course of 5 to 6 minutes. Since complete inhibition of all vitronectin receptors by the GRGDSP peptide might be questionable, cells were plated in parallel on gold-coated glass coverslips which were patterned with hexadecanethiol and EG6-thiol in 10 μm lane patterns. The coverslips were designed so that only the 10 μm-width lanes would support extra-cellular matrix adsorption and cell attachment, and any protrusion that the cells would extend outside the lanes would be off any substrate, over a non adhesive surface. The cells plated on those lanes have an elongated shape with a maximal width of 12 μm, most probably due to the fact that the cell body is too large to perfectly fit in the lane and thus it runs off the lane. However, a consistent bright halo is observed in this position using phase contrast microscopy, suggesting that the small fraction of the cell body which might run off the lane only lies over the non adhesive substrate and is actually not spread and attached (Figure 21 A). When such cells are stimulated with EGF, they extend a lamellipod so that their total area increases with the same kinetics and maximum extend as that of cells on a regular substrate (data not shown). However, it appears that lamellipod extension occurs mainly in two opposite directions along the lane of adhesive substrate (Figure 21A). Digital analysis of the modification of the cells' bodies showed that they undergo a dramatic extension in length which parallels exactly the increase in total cell area, by being maximum around 3-4 minutes after EGF stimulation and plateauing further (Figure 21 A and B). Analysis of the modifications of the central width of the cells shows that the cells do not undergo any enlargement of the central part of their body after EGF stimulation but rather become thinner as they stretch in opposite directions over their length. On the contrary, closer analysis of the modifications of the maximal width of the cells demonstrate that the cells are able to extend off the adhesive lane (with a total surface of 5 μm off the 10 μm lane; Figure 21 A and B). This extension is maximum around 3-4 minutes after EGF stimulation and then the maximal width decreases slightly back to its value before stimulation. This decrease occurs by levels over the course of 5 to 6 minutes, similar to what was observed for cells stimulated on vitronectin in presence of the GRGDSP peptide (compare insert in Figure 21 B and Figure 20). The ability of the cells to extend laterally over the non adhesive substrate was further confirmed by fluorescence light microscopy using rhodamine-labeled phalloidin to stain the F-actin containing cell bodies, and anti-vitronectin antibodies to stain the lanes of adhesive substrate (Figure 22).

Part 3: Analysis of the role of EF-1alpha in cell motility

As outlined in task 3, one of the crosslinking proteins that we wished to analyze for a possible role in regulating lamellipod extension was EF-1alpha. Together with this analysis, we also explored a second cell line with reduced metastatic capability as a possible control cell line for studying nonmetastatic cells.

The experiments described in the present study employed two rat mammary adenocarcinoma cell lines, MTLn3 and MTC, that previously were shown to have different metastatic potentials and differing levels of certain mRNAs (Welch et al., 1983; Taniguchi et al., 1991; Pencil et al., 1993). Prior to our detailed analysis of one of these mRNAs, it was necessary to confirm the metastatic potentials of the specific clones used in this study. As summarized in Table 2, injection of MTLn3 cells produced tumors within four weeks in all axillary lymph nodes and the lungs; however, injection of MTC cells only produced tumors in the ipsilateral lymph nodes after five weeks. Thus, in agreement with previous work, we characterize the MTLn3 cell line as highly metastatic while the MTC cell line has low metastatic potential (Neri et al., 1982). This difference in metastatic phenotype is stable with passage under our culturing conditions. It is interesting to note that the in vitro doubling time for these two cell lines is identical (14 hours); whereas, injected MTLn3 cells produce primary tumors 1-2 weeks sooner than injected MTC cells.

EF1 expression levels in tissues of differing metastatic potential

A correlation has been drawn between the metastatic potential of breast adenocarcinoma and an increased level of expression of EF1 mRNA (Taniguchi et al., 1991; Pencil et al., 1993). However, it was unclear if this increase in mRNA expression results in increased levels of EF1 protein expression. To determine the concentrations of EF1 protein within cell lines and whole tumors, homogenates were western blotted and probed with a monospecific antibody to EF1 (See Materials and Methods and Figure 23). As summarized in Table 3 (sections I -II), in the highly metastatic MTLn3 cells, EF1 comprises ~3% of total cell protein (57 μM); whereas, in the weakly metastatic MTC cells the EF1 concentration is reduced by ~35% to 37 μM. Furthermore, the amount of EF1 protein in whole primary tumors derived from MTLn3 cells is almost twice that of normal rat liver tissue or of primary tumors derived from weakly metastatic MTC cells (Table 3, section III). These increases in the amount of EF1 protein from MTLn3 cell and MTLn3-derived tumors correlate well with the relative level of EF1 mRNA found in the MTLn3 cell line (Pencil et al., 1993). Therefore, we demonstrate that the increased amount of EF1 mRNA associated with highly metastatic tumors results in an increased level of EF1 protein and suggests a relationship between EF1 and metastasis.

Interestingly, the amounts of actin in these two cell lines also are different. As shown in Table 3, the amounts of both total cellular actin (65 μM) and F-actin in the cytoskeletons (31 μM) of MTC cells are reduced by ~ 60% compared to MTLn3 cells (153 μM total actin, 76 μM F-actin). However, due to the decrease in EF1 and F-actin in MTC relative to MTLn3 cells, there is actually a ~ 30% increase in the molar ratio of EF1 : F-actin in MTC cytoskeletons compared to MTLn3 cytoskeletons (0.68 versus 0.46). This relative increase in

the EF1 :F-actin ratio in the cytoskeletons of MTC cells suggests that the apparent binding affinity (K_d^{app}) of MTC EF1 for the cytoskeleton is increased by 3.5-fold compared to MTLn3 EF1 (7 μM versus 26 μM; for calculation see Table 3).

The above results suggest a relationship between metastatic potential and the organization of the actin cytoskeleton. The principal question is what significance might an altered level of EF1 expression have on the metastatic potential of a tumor cell? One answer may be related to the binding of EF1 to the actin cytoskeleton.

The binding of EF1 to F-actin

To characterize the binding of vertebrate EF1 to F-actin and to compare these properties for EF1 from metastatic tumor with EF1 from normal tissues, EF1 was purified from MTLn3-derived tumors and normal rat liver. The purification strategy was adapted from the scheme used to purify EF1 from the cellular slime mold, Dictyostelium *discoideum* (Edmonds et al., 1995), and yielded a preparation that is >90% pure as assessed by scanning densitometry of SDS-PAGE gels (Figure 23B). The identity of the purified proteins as bona fide EF1 was confirmed (i) by immunoreactivity with the monospecific antibody directed against EF1 (Figure 24A) and (ii) by the ability of the purified proteins to support the in vitro synthesis of polyphenylalanine (Figure 23C). The difference in specific activity of MTLn3 compared to rat liver EF1 in the in vitro translation assay falls within the variability of this assay and is not significant.

EF1 s from many species bind actin (see Introduction). For example, EF1 from Dictyostelium, when mixed with purified F-actin, not only binds to but also crosslinks actin filaments into unique bundles (Demma et al., 1990; Owen et al., 1992). As shown in Figure 24A (lanes f-j), EF1 purified from MTLn3-derived tumors also displays a robust F-actin crosslinking activity as assessed by a differential centrifugation co-sedimentation assay. In this assay a low g-force spin pellets actin filaments crosslinked by EF1 (LSP). The resulting supernatant is then spun at high g-force to pellet single actin filaments and associated EF1 (HSP). Unbound EF1 remains in the high speed supernatant (HSS). The protein which co-sediments with F-actin in Figure 24A (lanes f-j) was confirmed to be EF1 by western blot analysis utilizing the anti-EF1 peptide antibody (Figure 24A, lanes f'-j') thereby discounting the possibility that the observed actin crosslinking activity is due to a contaminating protein which co-purifies with EF1 . The majority of tumor EF1 is distributed between the two fractions containing F-actin: the low speed pellet which contains crosslinked actin filaments (lanes h, h') and the high speed pellet which contains single filaments (lanes j, j').

The binding of EF1 from Dictyostelium to F-actin is sensitive to pH, a possible intracellular signal which may mediate the cytoskeletal redistribution observed after hormone stimulation of Dictyostelium (Edmonds et al., 1995) and other cell types (Liu et al., 1996). Often, changes in intracellular pH are associated with stimulation in many cell types and may serve as a stimulus for proliferation involving changes in the rate of protein synthesis (for reviews see Winkler 1988; Grinstein et al., 1989).

To determine if the binding of MTLn3-derived tumor EF1 to F-actin also is pH-sensitive, co-sedimentation assays were performed at five pH that span the physiological range. Similar to EF1 from Dictyostelium, the binding of rat tumor EF1 to F-actin displays a sensitivity to pH (Figure 24B). At lower pH, the majority of tumor EF1 is found in the fraction containing crosslinked actin filaments (LSP). As pH is increased most of the EF1

shifts from the LSP to fractions containing single actin filaments (HSP) and unbound EF1 (HSS). In addition, the binding of F-actin by EF1 purified from rat liver displays a pattern similar to tumor EF1 (Figure 24C): as pH increases liver EF1 redistributes from the crosslinked filament fraction to single filament or free fractions. In comparing the F-actin binding profiles of tumor and liver EF1 there is a 10-20% decrease in the amount of bound tumor EF1 at pH greater than 7.5. This difference in binding suggests that tumor EF1 has a lower affinity for F-actin compared to EF1 isolated from normal tissues. Irrespective of variable affinities, it is evident that the pH-sensitive binding of F-actin by EF1 is conserved for these two vertebrate proteins.

The ionic conditions of the co-sedimentation assays described above were chosen to allow direct comparisons with the F-actin binding activity of EF1 from Dictyostelium (Edmonds et al., 1995). These conditions are physiological for a free living amoeba, but are of low ionic strength with respect to mammalian systems. To ascertain the F-actin binding behavior of vertebrate EF1 under more appropriate mammalian physiological conditions, co-sedimentation assays were performed with liver EF1 in a buffer designed to mimic the intracellular composition of a typical mammalian cell (Alberts et al., 1994). Polyethylene glycol (M_r 8 x 10^3; 70 mg/ml) was included to simulate the high intracellular total protein concentration (Minton 1983) which we measured in MTC and MTLn3 cells as 90 or 100 mg/ml, respectively. As shown in Figure 24D, the relative binding of liver EF1 to F-actin is stimulated over 5-fold compared to the Dictyostelium-based low salt buffer. Also, the binding of liver EF1 to F-actin is sensitive to increases in pH under these generic mammalian conditions (data not shown). Thus, it appears that vertebrate EF1 has the potential to bind F-actin in vivo. In combination, the above data confirm previous results indicating similar actin binding activity by EF1 from divergent species and strongly imply that actin binding is a universal property of all EF1 s.

Localization of EF1 in resting and stimulated tumor cells

EF1 from Dictyostelium is associated with actin-containing cytoskeletal structures important for sheparding a chemotactic response to hormone stimulation (Dharmawardhane et al., 1991; Okazaki and Yumura 1995). MTLn3 cells, which are chemotactic to EGF, respond within minutes to exposure to EGF by extending actin-rich lamellipodial projections (Segall et al., 1996). Thus, it was of interest to determine if EF1 in MTLn3 cells displayed an association with dynamic cytoskeletal structures similar to EF1 in Dictyostelium.

The intracellular distribution of EF1 and F-actin was assessed by confocal immunofluorescence microscopy. The distribution of F-actin in unstimulated MTLn3 cells (Figure 25C) is associated most strongly with prominent actin bundles resembling stress fibers and surface projections; i.e., ruffles, filopodia and lamellipodia (arrows). Within 3 minutes after stimulation with EGF, MTLn3 cells undergo a uniform flattening with the formation of broad lamellipodia that display an intense F-actin rim at the leading edge (Figure 25F, arrowhead)(see also Segall et al., 1996; Chan et al., submitted).

The distribution of EF1 parallels that of F-actin in MTLn3 cells. In unstimulated cells (Figure 25B), EF1 is diffuse throughout the cytoplasm with increased levels in surface projections (arrows) which contain F-actin (compare to panel C). There appears to be little

nuclear staining; however, the perinuclear signal probably is associated with the endoplasmic reticulum (Sanders et al., 1996). After stimulation with EGF, a strong EF1 signal is associated with the F-actin rich zone at the leading edge of de novo lamellipods (Figure 25E, arrowhead). Therefore, similar to results reported for *Dictyostelium* (Dharmawardhane et al., 1991; Okazaki and Yumura 1995), the distribution of EF1 within MTLn3 cells is responsive to cytokine stimulation and co-localizes with the actin cytoskeleton in situ.

To delineate more closely the intracellular location of EF1 with respect to F-actin it was necessary to reduce the immunofluorescence due to soluble EF1 . This reduction was accomplished by extracting cells for 15 seconds with saponin prior to fixation. After extraction, as shown in Figure 26, EF1 in MTLn3 cells is associated with a subset of F-actin-containing fibers (arrows) in addition to the leading edge.

While the MTC cell line is not chemotactic to EGF (Segall et al., 1996) these cells do display greater overall motility than MTLn3 cells (J. Wyckoff, unpublished observations). In contrast to MTLn3 cells, the organization of the actin cytoskeleton is very different in MTC cells. The most striking difference is the absence of prominent stress fibers and an overall reduced rhodamine-phalloidin staining of F-actin in motile MTC cells (Figure 27B, D). These observations agree well with the reduced amount of total actin measured in these cells (Table 3). Yet even though the amount of F-actin in MTC cells is reduced, there is the presence of an F-actin rich zone associated with the leading edge (Figure 27B, D) and this region displays a strong EF1 immunofluorescence signal (Figure 27A, C) similar to that observed in MTLn3 cells. MTC cells extracted with saponin also show a prominent staining for F-actin and EF1 in the leading edge (Fig. 27C, D).

An increase in actin polymerization is a typical response to stimulation in many motile cells (Condeelis 1993). In *Dictyostelium* and MTLn3 cells, this increase in F-actin is associated with the formation of surface projections; i.e., filopodia and lamellipodia. In *Dictyostelium* the incorporation of EF1 into the cytoskeleton closely follows this increase in F-actin (Dharmawardhane et al., 1991; Okazaki and Yumura 1995). Similarly, in MTLn3 cells a peak of F-actin formation at the leading edge is observed within 2 minutes of stimulation with EGF (Segall et al., 1996; Chan et al., submitted). As shown in Figure 28, this peak of F-actin polymerization is followed by a gradual depolymerization, or loss of F-actin, which by 5 minutes returns the total amount of cellular F-actin to pre-stimulus levels. The association of EF1 with the cytoplasmic fraction containing F-actin displays a peak at 3 minutes after EGF stimulation and then rapidly declines to prestimulus levels within 1 minute. Thus, EF1 enters the cytoskeletal fraction soon after an increase in F-actin and then leaves this fraction simultaneously with a decrease in the amount of F-actin. This result suggests a dependence on F-actin for EF1 to associate with the cytoskeletal fraction.

Further corroboration that the association of EF1 with the cytoskeleton is mediated by actin was obtained by monitoring changes in the cytoplasmic partitioning of EF1 following disruption of the actin cytoskeleton. Cytochalasin D, an agent which blocks actin polymerization and blunts the morphological and chemotactic responses of MTLn3 cells to EGF stimulation (Segall et al., 1996), prevents the increase in EF1 associated with the Triton-insoluble cytoskeleton following EGF stimulation (Figure 29B). This loss of partitioning of EF1 into the cytoskeleton after stimulation with EGF appears to be specific for F-actin in that the amount of actin associated with the cytoskeleton also is reduced by cytochalasin D treatment (Figure 29A). Exposure to buffer controls containing only DMSO did not affect the

normal response to stimulation with EGF. These observations confirm that the increase in the association of EF1 with the cytoskeleton following stimulation with EGF is linked to changes in F-actin.

DISCUSSION

Part 1 :

      The major result of this study is that stimulation of metastatic MTLn3 cells with EGF causes an increase in actin nucleation activity resulting from the appearance of barbed filament ends at the leading edge of growing lamellipods. The number of barbed ends increases by approximately 6×10^3 within 1 minute of stimulation, a reasonable value considering the broad range of values that have been measured in other systems. For example, in neutrophils about 2×10^5 new filaments appear within 90 sec of stimulation with FMLP (Cano et al., 1991) approximately 4×10^4 barbed ends appear within 5 sec in Dictyostelium in response to stimulation with cAMP (J. Han and J.Condeelis, unpublished) and 500 barbed ends appear within 20 sec following thrombin stimulation of platelets (Hartwig, 1992).

      The timing and location of the stimulated actin nucleation activity in MTLn3 cells can account for the observed accumulation of F-actin at the leading edge of extending lamellipods as documented in a previous study of MTLn3 cells (Segall et al., 1996). The finding that the nucleation activity is transient, occurs before the onset of lamellipod extension and is localized to the leading edge supports the hypothesis that extension is caused by localized actin polymerization at the leading edge (Condeelis (1993), Segall et al.(1996)).

      Unlike A431 cells (Rijken et al, 1991), EGF stimulation of MTLn3 cells does not cause a continual increase in cellular F-actin. Rather, the F-actin content peaks at 1 minute and returns to resting levels within several minutes. These results predict that EGF stimulates both actin polymerization and depolymerization. This conclusion is supported by the observations that in cells treated with cytochalasin D, F-actin content decreases in response to EGF stimulation below that present in control cells (Segall et al., 1996), and that addition of capping protein or cytochalasin D to EGF-stimulated saponin permeabilized cells causes a decrease in rhodamine-actin incorporation below that observed in control cells. Both observations can be explained as an EGF-stimulated depolymerization of actin filaments resulting in a loss of F-actin content (Segall et al., 1996) and loss of pointed ends, which are capable of incorporating rhodamine-actin in the presence of capping protein or cytochalasin D. The presence of EGF-stimulated depolymerization activity is consistent with the accumulation of F-actin at the leading edge if actin polymerization there exceeds depolymerization compared to other regions of the cell where both reactions may be balanced.

      Currently, three mechanisms have been postulated to explain the rapid appearance of barbed ends in response to agonist stimulation (Condeelis (1993), Zigmond (1996), and Schafer et al, 1996): A) Uncapping of pre-existing filaments leading to an increase in the filament length distribution; B) de novo nucleation of actin polymerization from a template molecule to form new barbed ends without affecting pre-existing filaments; and C) severing of pre-existing filaments to form more uncapped filament ends, causing a decrease in the filament length distribution. Mechanism C explains the EGF stimulated depolymerization of F-actin in both intact and permeabilized cells treated with cytochalasin and capping protein, since EGF-induced severing would shorten the filament length distribution and result in the disappearance of filaments due to depolymerization if barbed ends could not elongate. This conclusion is consistent with studies by Zigmond and coworkers (Cano et al., 1991) who measured an increase in the number of short filaments in neutrophils following stimulation.

Mechanism A is consistent with PIP2- mediated uncapping of actin filaments by gelsolin (Hartwig, 1992) and capping protein (Hartwig et al. (1995), Schafer et al, (1996)). Both gelsolin, a PIP2- regulated barbed end capping protein which severs and then caps the newly created barbed end (Hartwig, 1992) and capping protein, a heterodimeric barbed end capper that is regulated by PIP2 (Schafer et al, 1996) have been proposed to control the availability of barbed ends by uncapping as PIP2 levels increase in the plasma membrane following stimulation. The location, very close to the plasma membrane of the leading edge, of nucleation sites for rhodamine-actin incorporation is consistent with a role for a phosphoinositol-regulated uncapping mechanism (Hartwig et al, 1995). However, it remains to be established if uncapping of actin filaments is a major mechanism for generating free-barbed ends after agonist stimulation. Gelsolin null cells can mobilize free barbed ends after stimulation (Witke et al., 1995) and conflicting results have been reported concerning whether capping protein is released from actin filaments in cells following stimulation as required by mechanism A(Nachmias et al.(1996), Barkalow et al (1996).

The appearance of nucleation sites proximal to the membrane of the leading edge in EGF-stimulated MTLn3 cells as reported here is consistent with previous observations in A431 and Cos-7 cells where accumulation of F-actin following EGF stimulation is proximal to the EGF- receptor in the plasma membrane (Wiegant et al. (1986), Gonzalez et al. (1993)) and a report that EGF-R signals PIP2 regulated actin binding proteins like gelsolin (Chen et al, 1996). The significance of co-localization between the EGF- receptor and F-actin is unclear but the conclusions that the EGF -R is itself an actin binding protein (den Hartigh et al, 1992) that F-actin in association with the EGF-R may form an active signaling complex (Diakonova et al. (1995), van Delft et al. (1995), and that actin nucleation sites form immediately adjacent to the plasma membrane after EGF-stimulation as reported here, provide clues for future research.

Part II:

Metastatic cells display ameboid chemotaxis

It has been long illustrated that tumor cell motility or protrusive activity is generally correlated to the expression of a high invasive and metastatic potential. Likewise, tumor cell ability to migrate in two or three dimensions *in vitro* in assays as different as Boyden chambers, wound healing or collagen matrices invasion () is no longer controversed, nor is the fact that such motile behaviors can be triggered by cytokines such as EGF or HGF. However, while cell motility and chemotaxis have been widely studied in ameboid cells such as *Dictyostelium* and neutrophils, little is known about the molecular mechanisms underlying the directed movement of mammalian metastatic cells. We demonstrate here that metastatic tumor cells display chemotaxis *in vitro* in a way which is directly comparable to what has been observed for ameboid cells. Metastatic MTLn3 cells move at the average rate of 1.5 μm/mn, which is approximately 5 times slower than the rate of movement of ameboid cells such as Dictyostelium, or neutrophils. In this regard, it is worth mentioning that, unlike those ameboid cells, MTLn3 cells display strong adhesions to the substrate, correlated with the presence of a consistent number of mature focal contacts as well as well-organized stress fibers. This pattern of stress fibers and focal contacts is maintained throughout the motion, which might be part of the explanation for the slow rate of movement of these cells. Movement towards the pipette was shown to encompass cycles of protrusions at the front of the cell, mainly in the form of extension of a broad lamellipodia, as well as retraction

processes at the rear. The result was net movement. Some of the cells could express some extent of ruffling at the front during cycles of protrusive activity, but most of the time, ruffling did not appear to be a major event during lamellipod extension, as opposed to what was observed for the progression of leading lamella in fibroblasts (Abercrombieet al. (1970, I and II), Rinnerthaler,et al,, 1988). We were able to show that retraction at the rear may involve ripping of the tail of the cell, as described during random motion of fibroblasts (Schmidt et al, 1993). This ripping of the cell may result in the cell leaving small fragments of its membrane behind, as shown by IRM time-lapse monitoring (data not shown). This ripping process appear to be mainly due to the presence of focal contacts at the rear of the cell which do not disassemble completely while the cell is moving and are dragged by the cell to allow retraction at the rear and resume net cell movement.

Relationship between adhesion and protrusion during chemotaxis

We previously showed that stimulation of MTLn3 cells with a homogeneous concentration of EGF led to the rapid extension of a lamellipod. This lamellipod extension could be quantitated as an overall increase in cell area. We then investigated whether this lamellipod extension assay could be used as a convenient model to mimic the major aspects of the chemotactic process. The data we present here show that upshift in EGF resulted in 3 subsequent major events, i.e. protrusion (lamellipod extension), new focal contact formation, and destabilization of the preexisting mature contacts. Those three events correspond to the three major assumed steps involved in chemotaxis (Lauffenbuerger and Horwitz, 1995), thus comforting us in our use of the upshift assay as a model to study directed cell motility.

Contact formation is not required for cell protrusion

EGF induces lamellipod extension by an actin-dependent mechanism. Lamellipod extension is accompanied by the elaboration of a dense F-actin rich zone located at the leading edge underneath the cell membrane. The intensity and thickness of this F-actin rich zone is maximum at 3 minutes after EGF stimulation when the lamellipod reaches maximal extension. This is actually the result of the EGF triggering a rapid burst of actin polymerization (within 1 minute) which is mainly located beneath the cell margin (Chan et al, manuscript in preparation). It had been suggested that polymerization of actin alone and derived forces could be sufficient to drive the protrusive activity (Mitchinson et Cramer (1995), Condeelis, (1993)). However, IRM studies of the leading lamella of chick embryo fibroblasts and other cells suggested that, while evidence showed that the establishment of focal contacts was not a prerequisite to the extension of the lamellipodia, forward protrusion of the leading lamella required close contacts formation, predominantly at the base of the leading edge (Izzard & Lochner, 1976, 1980; Couchman & Rees, 1979; Haemmerli et al, 1980; Bereiter-Hahn et al, 1980). While the extreme margin of the lamella was found to first extend free off the substrate, close contacts were rapidly formed by the extended lamellipodium, which have been proposed to provide the adhesion required to transmit to the substrate the forces involved in the forward movement of the cytoplasm and advance of the leading lamella (Izzard & Lochner, 1980). Focal contacts appeared later, followed by movement of the cell body which was believed to occur through traction forces developed thanks to the establishment of the focal contacts and stress fibers (Izzard & Lochner, 1980). Our first observations appeared consistent with these former assumptions: both IRM and immunofluorescence studies showed that the new focal contacts were forming unambiguously

after the lamella had reached maximal extension, and the extension itself was accompanied by the formation of large zones of close contact. Only the extreme margin of the lamella would appear free off the substrate, which represent approximately 1 µm while the total extension of the lamellipod after stimulation could reach 8 µm (data not shown). However, further studies showed that the cells were able to express remarkable protrusive activity when stimulated in suspension, i.e. when devoid of any contact with a substrate. Protrusive activity was also stimulated by EGF on adherent cells over the dorsal surface where the cells had obviously no contacts with the substrate. Even though we were not able to demonstrate that the protrusions seen in suspension, or over the dorsal surface of adhering cells, were actually of the same nature as the broad lamellipod extension over the substrate, this was highly suggestive that lamellipod extension might be, at least partly, independent of any contact with the substrate. We then underwent experiments to determine if adherent cells could actually extend their lamellipod independently of any contacts with the substrate, using both adhesion-inhibiting peptides and patterned coverslips. Both experiments showed very comparable results: adhering cell stimulated with EGF under those particular conditions still extend a lamellipod, with identical kinetics and to a comparable extent when compared to cells on a regular substrate, even though they were not allowed to make any contacts with the substrate all over this new extension. Thus it appears that contact formation is not required for protrusive activity, whatever the shape of the resulting protrusion.

Contact formation stabilizes protrusions against retraction. Cells in suspension do generate protrusive activity after EGF stimulation but this activity is already down by 30% after 5 minutes. Similarly, stimulated adherent cells extend a lamellipod over a non adhesive substrate with the same kinetics that they do over an adhesive substrate, but this extension is only transient: the lamellipod reaches maximal extension at 3-4 mn but then the cells retract back to their original size over the course of 5 minutes, instead of stabilizing in extended shape. Thus, while EGF stimulated protrusive activity does not require any contact with the substrate, it appears that contacts are necessary to stabilize the generated protrusions against retraction. This was actually well illustrated by the experiment on patterned coverslips where the cell retracted the extended parts that were over the non adhesive surface, while the extensions over the adhesive lanes got stabilized, resulting in a net increase in cell length. Comparable lamellipodial stabilization by contact with the extracellular matrix has been demonstrated in mesenchymal cells migrating toward a gradient of PDGF. From the sequence of events that we observed, it appears that the establishment of new focal contact is not the primary adhesive event occurring to stabilize the extension. Indeed, new focal contacts are detected as long as two minutes after the lamellipod had reached maximal extension and started to retract if not in contact with the substrate. It is unlikely that this delay in new focal contact detection is due to a lack of sensitivity in the techniques we used to identify the focal contacts, since both IRM and immunofluorescence gave us concordant results. According to our IRM studies, close contacts are enough to stabilize the lamellipod at least for the first two minutes after it had reached maximal extension. This is accordance with the observations made on leading lamella in fibroblasts, where it was shown that close contacts were rapidly formed by the extended lamellipodium, the focal contacts appearing later (Izzard & Lochner, 1980). It remains however still unclear if close contacts are necessary *and* sufficient for further maintenance of the extension, or if long term stabilization requires focal contacts formation. It has been shown that cells with fewer focal contacts are more motile, and actually highly motile cells like neutrophils or Dictyostelium cells do not form focal contacts. This was

highly suggestive of the focal contacts just hampering the cell movement. On the other hand, it has been suggested that focal contacts at the tips of stress fibers could be involved more in generating traction forces necessary to pull the cell body forward to resume net movement (Izzard & Lochner, 1980). It is conceivable that focal contacts may indeed play such a role in epithelial tumor cells. This would be consistent with other results showing a correlation between the number of focal adhesion plaques and the migration rate in mammalian cells. The process of retraction of the lamellipod in two different kinds of systems was shown to occur by levels, twice as slowly as the extension. This is actually reminiscent of old observations on the leading lamella of fibroblasts showing that the lamella undergoes cycles of protrusion and retraction, the result being net movement (Abercombie, 1970). It looked as though extension and retraction are two mutually exclusive mechanisms that can't be done by the cell at the same time. It is possible that some level of protrusive activity is still present in the lamellipodium after maximal extension, and this activity would counteract the retraction forces at some point, resulting in discontinuous retraction.

Contact formation amplifies protrusive activity. Is the substrate only stabilizing the protrusions or can it play a more active role in the persistence of the protrusion? Protrusion activity after stimulation in suspension peaks at 2 minutes. However, while protrusive activity on the dorsal surface of adherent cells also peaks at 2 minutes after stimulation, the major protrusive activity in adherent cells, i.e. lamellipod extension, peaks at 3-4 minutes after stimulation. One simple explanation would have been that contact with the substrate stabilizes the protrusion as it goes on, thus allowing a wider and somehow delayed final extension. However, our results in experiments where cell were allowed to extend their lamellipod only over a non adhesive substrate show that this is not the case. Cells on patterned coverslips or in presence of adhesion-inhibiting peptides extend their lamellipod with the same kinetics as cells on a regular substrate, reaching maximum extension at 3-4 minutes after stimulation. Contact with the substrate during the extension *per se* is thus probably not affecting the kinetics of the extension. However, in the case of stimulated cells on vitronectin extending their lamellipod in presence of adhesion-inhibiting peptides, the maximal extension measured reached only 70% of the control extension. This leads us to conclude that contact with the substrate can amplify the lamellipod extension, i.e. can potentiate the protrusive activity over the substrate. Indeed, it is well known that signals can be transmitted from the substrate to the inside of the cell, affecting many cell processes such as division, differentiation, apoptosis or motility (Hall, C. et al (1994) Dedhar (1995); Akiyama et al (1995); Parsons, (1996); Leavesly et al (1993)). One of the major family of membrane molecules involved in these processes is the family of the integrin receptors (Dedhar, (1995); Parsons, (1996)). Many of these receptors are known to trigger downstream signaling inside the cell, and some of them have been shown to affect actin polymerization and lamellipod extension, although the exact pathways involved are presently still unclear. In our particular experiment, it is conceivable that contact of the vitronectin receptor with its ligand triggers a signal which leads to potentiation of actin polymerization and thus subsequent increase in the level of protrusive activity. Indeed, it has been shown that activation the integrin alphav-beta3, which is one of the major vitronectin receptors in epithelial cells, can trigger a downstream signal which will affect actin polymerization and cell motility through the means of phosphokinase C activation (Chersesh, 1995).

The shape of the protrusion is modulated by the cell's relationship to the substrate. One of the peculiar results of our study is that adherent cells which are allowed to protrude only over a non adhesive substrate still extend a flat broad lamellipod. One commonly accepted idea about cell spreading was that the cells placed on a substrate were actually extending protrusions from all over their cortex in a random fashion, similarly to what we showed for cells stimulated in suspension. However, only those extension that would come in contact with the substrate would be stabilized, and further generate the spreading. The data we present here demonstrate that lamellipod extension during chemotaxis is a different mechanism, and can not be assimilated as simple spreading. Cells stimulated over a substrate show some extent of protrusive activity over their dorsal surface, but the major event of protrusion remains lamellipod extension, whether or not the cells are able to make contacts with the substrate during extension. Similarly, cells adhering over a pattern substrate preferentially extend over the adhesive surface. The results presented here and complementary observations thus led us to conclude that the initial status of the cell, i.e. in contact or not with a substrate, is influencing the shape of the protrusion to be generated after stimulation. It is possible that the special conformation of the actin meshwork in the lamella of spread adhering cell (see refs. in Micthinson and Crammer, Cell (1995); Small, (1988)), as well as the fact that this part of the cell is already in close contact with the substrate (which could potentiate the stimulated protrusive activity, see above), allows for a more important burst of actin polymerization in the lamella as compared with other parts of the cells. Concomitant stabilization and amplification of the protruding activity in the lamellipod as it extends over the substrate generates membrane extension, which in turns may create sufficient tension to inhibit protrusions over the dorsal surface. On the other hand, those protrusions may be transient because they do not get stabilized by contact with the substrate. However, the first explanation is more likely to us since those protrusions on the dorsal surface almost completely disappear within one minute, while protrusions in suspension persist for at least five minutes after EGF stimulation.

Preexisting contacts are remodeled during protrusion. We showed that the cells are not completely disassembling their preexisting focal contacts during movement after stimulation. Rather, while some of the focal contacts can diffuse and progressively get converted to close contacts, many of the focal contacts, and especially at the rear, got dragged by the cells. During this dragging part, the focal contacts get remodeled or fused, some of them slowly disappearing. As the cell pulls hard on the rear to drag the focal contact, part of the tail can rip. Ripping has been shown to be a common phenomenon during random movement of. To our knowledge, this is the first time that this is reported for metastatic cancer cells. Furthermore, focal contacts have been generally assumed to be fixed structures which would stay stable during cell movement and would thus require complete disassembly in order for the cell to progress. We show here that they can move with the cell and keep their original shape for at least a few minutes while moving (present data and data not shown). We propose that maintenance of the focal contacts might be necessary for the cell to maintain a reasonable shape during movement, while the brutal disassembly of focal contacts at the rear during tension might results in the cell slipping back like an elastic and detaching from the substrate. Considering the kinetics that we observed, it is likely that the remodeling of the preexisting contacts, especially at the rear, is initiated by a signal generated by the formation of the new contacts at the front rather by a direct parallel signal from the chemoattractant. Remodeling starts approximately at the same time as new focal contact assembly, and if it were to be directly triggered by the stimulation with EGF, we should see

remodeling and disappearing of focal contacts, and subsequent cell detachment from the substrate, in the experiments where lamellipod extension was accomplished over a non adhesive substrate, which is not the case (data not shown). Preexisting large focal contacts are not completely disassembled during cell movement but they at least undergo drastic remodeling. We found a correlation between the beginning of remodeling 5 minutes after stimulation and the disappearance of phosphotyrosine staining in large focal contacts as opposed to newly formed ones which are highly enriched in phosphotyrosine at this time. Major components of the focal contacts such as talin or vinculin (data not shown) remained however stable after 5 minutes stimulation in both types of focal contacts. This suggests that dephosphorylation of the major phosphorylated components of the focal contacts is happening in preexisting contacts 5 minutes after stimulation. We would like to propose that this could be linked to a partial destabilization of the contacts, potentially without loss of any major components, which would in turn allow the focal contact remodeling necessary for cell movement. Well-developed stable focal contacts generally present a high content in phosphotyrosine (Burridge et al (1988); Burridge et al, (1992)). A large number of the proteins which compose the focal contacts can be phosphorylated on tyrosine (Jockusch et al, 1995), but it is generally assumed that the two major tyrosine-phosphorylated components are focal adhesion kinase (FAK) and paxillin (Romer et al (1992); Burridge et al, (1992)). The role of paxillin phosphorylation during focal contact assembly and maintenance is presently unknown, but data showing that FAK was activated during cell adhesion and focal contact assembly (Romer et al, (1992); Kornberg et al (1992) ; Burridge et al (1992)), and that tyrosine kinase inhibitors prevent focal contact assembly, first suggested that FAK played a major role in focal contact assembly. Indeed, in melanoma cell lines, FAK expression has been directly correlated to FAK activation and to the number of focal contacts per cell. However, in view of other data, the role of FAK activation in focal contact assembly appear far more complicated. FAK null cells have been generated, which showed a higher number of focal contacts. Conversely, cells overexpressing FAK show increased motility, which one could supposedly relate to focal contacts which are more readily destabilized to facilitate movement. Other data showed that FAK does not mediate focal contact assembly. Those ideas now converge to propose a role for FAK in focal contact disassembly, and at least some of the data are consistent with this hypothesis. Another group however has shown that focal adhesion breakdown was related to an increased in tyrosine phosphorylation, athough not involving the major tyrosine phosphoproteins of the focal contacts, and particularily FAK (Crowley and Horwitz, 1995). It should be kept in mind, however, that the authors were working on unstimulated permeabilized fibroblasts, which could have resulted in overall modifications of the process of adhesion disassembly. Nevertheless, others data are consistent with our findings, which show that a gradual loss of tyrosine phosphorylation coincided with disruption of focal contacts (Matsumoto et al, (1994); Maher (1993)). One possible way to reconcile all these data was proposed by Matsumoto et al, who suggested that disassembly of focal contacts could be initiated by transient hyper-phosphorylation of FAK, and might then be followed by dephosphorylation during the destabilization *per se*. Obviously, more work has to be done before those issues are to be resolved, and in particular, it would be very interesting to be able to follow individual contacts during cell movement and correlate their content in phosphotyrosine with their status (stable or remodeling).

A model for cancer cell chemotaxis process

Based on our results, we would like to propose the following model to describe metastatic epithelial cell chemotaxis. Carcinoma cells move toward a chemoattractant source basically using cycles of protrusion at the front and retraction at the rear. The protrusive activity was mainly in the form of the extension of a broad lamellipodia, but it appeared that the shape of this protrusion can be modulated by the status of the cell in reference to a substrate before stimulation. We assume that the shape of the extension toward the chemoattractant source is the result of a combination of the gradient of chemoattractant for the direction of the protrusion, and of the cell body being in contact with a plane surface for the flat broad pseudopodial shape of the protrusion. The protrusive activity can occur without any contact with the substrate but is then only transient. This leads us to conclude that this activity is mainly driven by the forces generated by actin polymerization, crosslinking and/or gel osmotic pressure (Condeelis, (1993); Lauffenburger and Horwitz, (1996)). However, if contacts are made with the substrate, not only those contacts do stabilize the protrusion, but they can also amplify the protrusive activity so that the final protrusion will be even broader. This amplification mechanism is likely to be triggered by signaling from membrane receptors binding to their ligands on the substrate, and particularly integrin receptors, which can activate downstream signaling pathways to potentiate actin polymerization and resulting protrusive activity. The cell architecture appears to be quite fully conserved during cell movement, and in particular, the cells do not completely loose focal contacts and stress fibers. Rather, the cells do conserve focal contacts, especially at the rear, which we assume can maintain the cell shape during movement. Some of the preexisting focal contacts can diffuse and progressively disappear but it appears that the cells are able to drag the focal contacts, especially at the rear, during movement. This mainly results in the ripping of the tail, and remodeling of the contacts at the rear as the cell progresses. On the other hand, protrusion at the front is first stabilized by the quasi-concomitant establishment of close contacts, and further captured by formation of new focal contacts. These new contacts appear quite stable and are most probably used by the cell as strong anchoring points to generate traction forces to pull the cell body forward. Our results suggest that the remodeling of the preexisting contacts, especially at the rear, is likely to be initiated by a signal generated by the formation of the new contacts at the front rather by a direct parallel signal from the chemoattractant. It thus appears that chemotaxis of carcinoma cells share some of the characteristics common to chemotaxis in typical ameboid cells and to random movement of fibroblastic cells. This process as a whole appears to be highly complex and tightly regulated by the cell, as it involves signals from both the chemoattractant source and contacts with the substrate. We provide here a model which will enable further studies the molecular mechanisms underlying this complex process, and resolve highly discussed issues on how cancer cells move.

Part III:

EF1 is an actin binding protein in vertebrate cells

In this study we have demonstrated that EF1 from metastatic rat mammary adenocarcinoma cells is an actin binding protein. The nature of the interaction between EF1 and F-actin is thought to be charge-dependent based upon the sensitivity to pH and ionic strength (Figure 24B, C, and see Edmonds et al., 1995). The basic pI of EF1 (8.5-9.5) and the acidic pI of actin (4.0-4.5) has lead to the argument that the in vitro interaction of EF1

with actin is nonspecific thereby trivializing any physiological relevance. This argument is inconsistent with the following observations: (i) Rat liver EF1 binds tightly to F-actin under the physiological ionic conditions appropriate for mammalian cells (Fig. 23D); (ii) The intracellular concentrations of F-actin and EF1 are far in excess of measured K_d suggesting the potential for a high degree of interaction. In fact, we observe ~60% of total cellular EF1 in association with the cytoskeletal fraction of whole cell lysates (Table 3), and this association is reduced by cytochalasin D; (iii) Two specific peptide sequences from Dictyostelium EF1 have been identified which bind to F-actin (Liu et al., submitted). The pIs for these peptides are acidic while several other peptides with very basic pI do not interact with F-actin; (iv) Aminoacyl-tRNA, but not deacyl-tRNA, specifically blocks actin binding (Liu et al., submitted). Other exposed faces of the molecule with surface charge distributions similar to the tRNA binding sites do not bind to actin; and (v) EF1 is a prototypical G protein where the rates of guanine nucleotide hydrolysis and exchange play crucial roles in the elongation cycle (Riis et al.,1990). GTP and GDP, but not ATP, affect the F-actin binding by *Tetrahymena* or Dictyostelium EF1 (Kurasawa et al., 1996; Edmonds et al., in preparation). The creation of EF1 mutants that fail to bind to actin, but are fully functional in protein synthesis, will help to resolve the issue of the physiological consequences of EF1 binding to actin in vivo.

The binding of EF1 to actin is related to metastasis

In a direct comparison of metastatic potential with the actin binding activity of EF1 , there is a 30% reduction in the ratio of EF1 : F-actin in the cytoskeletons of highly metastatic MTLn3 cells versus the weakly metastatic MTC cells (Table 3). At present, the explanation for this reduced affinity of MTLn3 compared to MTC EF1 for F-actin is unclear. Presumably, the primary sequences of MTC and MTLn3 EF1 are identical given the high degree of nucleotide sequence conservation between vertebrate EF1 genes (Riis et al., 1990), and the low EF1 gene copy number in the mammalian genome (Opdenakker et al., 1987). Therefore, the different observed affinities for actin binding may be related to competition for actin substrate by other actin binding proteins, to different post-translational modifications, or to different intracellular pH regulation.

Indirect evidence suggests that the first seven amino acids of the amino terminus of actin may be involved partly in the interaction with Dictyostelium EF1 (Edmonds et al., 1995). This region of the actin molecule is a "hot spot" for the binding of several other actin binding proteins, including myosin (Rayment et al., 1993). Thus, if events that induce metastasis affect the expression or activities of competing families of actin binding proteins, then EF1 may not be able to interact as efficiently with actin in metastatic cells as in nonmetastatic cells.

Alternatively, several post-translational modifications of EF1 have been reported including phosphorylation, methylation, and n-ethanolamine addition at glutamic acid residues (Venema et al., 1991; Dever et al., 1989; Sherman and Sypherd, 1989). The functional significance of these modifications is unresolved with respect to translation and their effects on actin binding have not been investigated directly. Further analysis by mass spectroscopy of intact and proteolytic fragments of each tumor EF1 will aid in determining the nature of any modifications.

Stimulation of many cell types results in cytoplasmic alkalinization (Grinstein et al., 1989). In *Dictyostelium,* an increase in intracellular pH results in a decrease in EF1 associated

with the cytoskeleton (Edmonds et al., 1995); therefore, the reduced affinity of MTLn3 EF1 for actin may reflect a higher MTLn3 cytoplasmic pH compared to MTC cells. As MTC cells lack the EGF receptor (Kaufmann et al., 1994), perhaps the amount of other protein components of the MTC cell membrane are altered compared to MTLn3 cells. Differences in the complement of membrane proteins between MTC and MTLn3 cells may include ion channels and transporters, such that proton homeostasis is different. This issue requires further study.

Links between EF1 binding to actin and metastasis

Given that MTLn3 EF1 binds less tightly to actin than MTC EF1 , how might this difference relate to the observed differences in metastatic potential between these two cell lines? Two possible roles for EF1 which may be related to metastatic potential are: (i) to influence the organization of the actin cytoskeleton, and/or (ii) to synthesize locally proteins important for maintaining an appropriate intracellular environment necessary for propagating the motile process.

Ultrastructural studies of *Dictyostelium* have shown that EF1 is associated with actin bundles in situ (Liu et al., 1996). These EF1 : F-actin bundles may exhibit an unique organization which would tend to exclude other known actin binding proteins (Owen et al., 1992). This property alone suggests that EF1 could play a unique role; however, EF1 also can affect the dynamics of actin filaments. Specifically, EF1 slows the rate of actin polymerization and depolymerization and decreases the critical concentration for actin polymerization in vitro (Murray et al., 1996). The net effect of this activity in the EF1 / actin compartment would be to produce actin filaments more slowly, and once formed those filaments bound to EF1 would remain more stable. The differences in the affinity of EF1 for actin between MTLn3 and MTC cells may alter the coordination of actin dynamics in the cytoskeleton thereby leading to a change in the efficiency of directed movement.

The compartmentation of EF1 also may have significance for EF1 function in protein synthesis. In myoblasts and fibroblasts, -actin mRNA has been shown to localize to the leading edge, to be actively translated there, and to redistribute with actin in response to various second messenger pathways (Lawrence and Singer 1986; Kislauskis et al., 1994; Latham et al., 1994). These observations suggest a mechanism whereby cytokines could influence metastasis by compartmentalizing specific proteins required for chemotaxis through modulation of their localized synthesis. For example, if the localization of -actin mRNA or the synthesis of actin protein at the leading edge were compromised then the efficiency of directed motility might be affected. In fact, mislocalization of -actin mRNA has been shown to disrupt cell polarity (Kislauskis et al., 1994).

In human fibroblasts, over 70% of total poly (A)-containing mRNA is associated with the actin cytoskeleton (Taneja et al., 1992). This observation implies that actin somehow is involved in the biology of cytoplasmic mRNA. Therefore, changes in the amount of cellular actin or the organization of the actin cytoskeleton might affect the synthesis of many different proteins. Because MTC cells have less total actin (Table 3) and lack prominent stress fibers compared to MTLn3 cells, a dichotomy may exist in the complexion of proteins synthesized between these two cell types. Observations from differential hybridization screens of these two cell lines support this idea (Pencil et al., 1993). Because the leading edge is present in both cell types and stress fibers are lacking in the weakly metastatic MTC cells, perhaps the

synthesis of proteins in the stress fiber compartment of the MTLn3 cells is related to their transformation to the metastatic state. In addition, as only a subpopulation of stress fibers display an association with EF1 in MTLn3 cells, there is the potential for the regional synthesis of a set of actin-bound mRNAs distinct from those at the leading edge.

One current model for the involvement of the actin cytoskeleton in protein synthesis depicts the sequestration of EF1 away from other components of the translational machinery by F-actin (Liu et al., 1996). Actin and tRNA are ligands which compete for binding to EF1, such that when EF1 is complexed with tRNA, binding to actin is excluded (Liu et al., submitted). Under one scenario the generation of an appropriate intracellular signal (e.g., cytoplasmic alkalinization) by the binding of a cytokine might weaken the interaction of EF1 with F-actin thereby favoring the binding of tRNA to EF1 and the promotion of polypeptide elongation. One prediction of this model is that the rates of translation for certain mRNAs associated with the cytoskeletal compartment may be different in MTC versus MTLn3 cells based upon the different affinities of EF1 for F-actin in these cells. However, interpretation of such experiments could be complicated by the possibility that other steps in translation may be affected by transformation to the metastatic state. It remains to be determined if protein synthetic components other than EF1 also are up-regulated in metastatic cells.

CONCLUSIONS

In this report, we have provided the following data regarding responses to EGF in MTLn3 cells. In Part I, we have demonstrated that the site of actin nucleation in lamellipods induced by EGF is at the leading edge of the lamellipod. These sites are inhibitable by capping protein and cytochalasin D, indicating that the barbed ends of the actin filaments are the sites of polymerization. In Part II, we have demonstrated that talin is a strong candidate for a nucleating factor, given its localization at the leading edge of the lamellipod (where the sites of nucleation are). In addition, the extension of lamellipods does not appear to require an adhesive surface. However, stabilization of lamellipods and formation of new focal contacts does require an adhesive surface. Addition of EGF destabilizes old focal contacts as well as stimulating the formation of new focal contacts at the leading edge. In Part III, we show that EF1alpha is also present in lamellipods, but is not concentrated at the leading edge. It is slightly enriched in metastatic cells compared to nonmetastatic cells.

These results provide important data regarding the process of lamellipod extension in metastatic cells. Talin is identified as a strong candidate for regulating or activating lamellipod extension. Further studies are planned (as part of Technical Objectives 4 and 5) to directly test the role of talin by suppressing its expression in MTLn3 cells and determining the effects of such suppression on metastasis. If there is a strong effect on the metastatic ability of these cells, then talin would be a strong candidate for pharmaceutical approaches to the inhibition of metastasis.

REFERENCES

Abercrombie, M., Heaysman, J.E.M. and Pegrum, S.M. The locomotion of fibroblasts in culture. I. Movements of the leading edge. Expl. Cell Res.59, 393-398, 1970.

Abercrombie, M., Heaysman, J.E.M. and Pegrum, S.M. The locomotion of fibroblasts in culture. II. "Ruffling". Expl. Cell Res.60, 437-444, 1970.

Akiyama, S.K., Olden, K. and Yamada, K.M. Fibronectin and integrins in invasion and metastasis. Cancer Metastasis Rev. 14, 173-189, 1995.

Alberts, B., Bray, D., Lewis, J., Raff, M., Roberts, K. and Watson, J.(1994). *Molecular Biology of the Cell*, p.508. Garland Publishing, New York.

Barkalow K., Witke W., Kwiatkowski DJ., Hartwig JH. 1996. Coordinated regulation of Platelet actin filament barbed ends by gelsolin and capping protein. *J. Cell. Biol.*134: 389-399

Bektas, M., Nurten, R., Gürel, Z., Sayers, Z., and Bermek, E. (1994). Interactions of eukaryotic elongation factor 2 with actin: a possible link between protein synthetic machinery and cytoskeleton. *FEBS Lett.* 356, 89-93.

Blay J.,Brown KD. 1985. Epidermal growth factor promotes the chemotactic migration of cultured rat intestinal epithelial cells. *J Cell Physiol*, 124: 107-12

Boonstra J., Rijken P., Humbel B., Cremers F., Verkleij A., Van Bergen En Henegouwen P. 1995. The epidermal growth factor. *Cell Biol Inte* 19: 413-430.

Burridge, K., Fath, K., Kelly, T., Nuckolls, G. and Turner, C. Focal adhesions: transmembrane junctions between the extracellular matrix and the cytoskeleton. Ann. Rev. Cell Biol. 4, 487-525, 1988.

Burridge, K., Turner, C.E. and Romer, L.H. Tyrosine phosphorylation of paxillin and pp125[FAK] accompanies cell adhesion to extracellular matrix: a role in cytoskeletal assembly. J Cell Biol. 119, 893-903, 1992.

Cano ML., Lauffenburger DA., Zigmond SH. 1991. Kinetic analysis of F-actin depolymerization in polymorphonuclear leukocyte lysates indicates that chemoattractant stimulation increases actin filament number without altering the filament length distribution. *J. Cell. Biol.* 115: 677-87

Carroll, S. B. and Stollar, B. D. (1983) Antibodies to calf thymus RNA polymerase II from egg yolks of immunized hens. *J. Biol. Chem.* 258, 24-26.

Carvalho, M. G. C., Carvalho, J. F. and Merrick, W. C. (1984). Biological characterization of various forms of elongation factor 1 from rabbit reticulocytes. *Arch. Biochem. Biophys.* 234, 603-611.

Chen, P., Gupta, K and Wells, A. Cell movement elicited by epidermal growth factor receptor requires kinase and autophosphorylation but is separable from mytogenesis. J. Cell Biol. 124, 547-555, 1994.

Chen P., Murphy-Ullrich JE., Wells A. 1996. A role for gelsolin in actuating epidermal growth factor receptor-mediated cell motility. *J.Cell Biol.* 134: 689-98

Chi, K., Jones, D. V. and Frazier, M. L. (1992). Expression of an elongation factor 1 gamma-related sequence in adenocarcinomas of the colon. *Gasteroenterolgy* 103, 98-102.

Collings, D. A., Wasteneys, G. O., Miyazaki, M., and Williamson, R. E. (1994). Elongation factor 1 is aa component of the subcortical actin bundles of characean algae. *Cell. Biol. Intl.* 18, 1019-1024.

Condeelis, J., Geosits, S., and Vahey, M. (1982). Isolation of a new actin-binding protein from Dictyostelium *discoideum. Cell Motil.* 2, 273-285.

Condeelis, J., Jones, J. and Segall, J. E. (1992). Chemotaxis of metastatic tumor cells: clues to mechanisms from the Dictyostelium paradigm. *Cancer Metastasis Rev.* 11, 55-68.

Condeelis, J. (1993). Life at the leading edge: the formation of cell protrusions. *Ann. Rev. Cell Biol.* 9, 411-444.

Cooper JA., Walker SB., Pollar TD. 1983. Pyrene actin: documentation of the validity of a sensitive assay for actin polymerization. *J. Muscle Res. Cell Motil.* 4: 253-262

Crowley, E., and Horwitz, A.F. Tyrosine phosphorylation and cytoskeletal tension regulate the release of fibroblast adhesions. J. Cell. Biol. 131, 525-537, 1995.

Dadabay CY., Patton E., Cooper JA., Pike LJ.1991. Lack of correlation between changes in polyphosphoinositide levels and actin/gelsolin complexes in A431 cells treated with epidermal growth factor. *J Cell Biol,* 112, 1151-6.

Dedhar, S. Integrin mediated signal transduciton in oncogenesis: an overview. Cancer Metastasis Rev. 14, 165-172, 1995.

Demma, M., Warren, V., Hock, R., Dharmawardhane, S. and Condeelis, J. (1990). Isolation of an abundant 50,000-Dalton actin filament bundling protein from Dictyostelium amoebae. *J. Biol. Chem.* 265, 2286-2291.

Dever, T. E., Costello, C. E., Owens, C. L., Rosenberry, T. L. and Merrick, W. C. (1989). Location of seven post-translational modifications in rabbit elongation factor 1 including dimethyllysine, trimethyllysine and glycerylphosphorylethanolamine. *J. Biol. Chem.* 264, 20518-20525.

Devreotes, P. N. and Zigmond, S. H. (1988). Chemotaxis in eukaryotic cells: a focus on leukocytes and Dictyostelium. *Ann. Rev. Cell Biol.* 4, 649-686.

Dharmawardhane, S., Demma, M., Yang, F. and Condeelis, J. (1991). Compartmentalization and actin binding properties of ABP-50: the elongation factor-1 alpha of Dictyostelium. *Cell Motil. Cytoskel.* 20, 279-288.

Diakonova M., Payrastre B., Van Velzen AG., Hage WJ., van Bergen en Henegouwen PM., Boonstra J., Cremers FF., Humbel BM. 1995. Epidermal growth factor induces rapid and transient association of phospholipase C -γ 1 with EGF-receptor and filamentous actin at membrane ruffles of A431 cells. *J. Cell Sci.* 108: 2499-2509.

Eddy RJ., Han JH., Roger AS., Condeelis JS. 1996. A major agonist- related capping activity in Dictyostelium is due to the capping protein, cap 32/34. *Biochem. Biophys. Acta.* In press

Edmonds, B. T., Murray, J. and Condeelis, J. (1995). pH regulation of the F-actin binding properties of Dictyostelium elongation factor-1 . *J. Biol. Chem.* 270, 15222-15230.

Gilmore, A.P. and Romer, L.H. Inhibition of focal adhesion kinase (FAK) signaling in focal adhesions decreases cell motility and proliferation. Mol. Biol. Cell 7, 1209-1224, 1996.

Gonzalez FA., Seth A., Raden DL., Bowman DS., Fay FS., Davis RJ. 1993. Serum-induced translocation of mitogen-activated protein kinase to the cell surface ruffling membrane and nucleus. *J.Cell Biol.* 122: 1089-1101

Grinstein, S., Rotin, D. and Mason, M. J. (1989). Na$^+$ / H$^+$ exchange and growth factor-induced cytosolic pH changes. Role in cellular proliferation. *Biochim. Biophys. Acta* 988, 73-97.

Grotendorst GR., Soma Y., Takehara K., Charette M. 1989. EGF and TGF-alpha are potent chemoattractants for endothelial cells and EGF-like peptides are present at sites of tissue regeneration. *J Cell Physiol*, 139: 617-23

Hall, C.L.,Wang, C., Lange, L.A. and Turley, E.A. Hyaluronan and the hyaluronan receptor RHAMM promote focal adhesion turnover and transient tyrosine kinase activity. J. Cell Biol. 126, 575-588, 1994.

den Hartigh J C., van Bergen en Henegouwen PM., Verkleij A J., Boonstra J. 1992. The EGF receptor is an actin-binding protein. *J. Cell. Biol.* 119: 349-355.

Hartwig JH. 1992. Mechanisms of actin rearrangements mediating platelet activation. *J. Cell. Biol.* 118: 1421-1442

Hartwig JH., Bokoch GM., Carpenter CL., Janmey PA., Taylor LA., Toker A., Stossel TP. 1995. Thrombin receptor ligation and activated Rac uncap actin filament barbed ends through phosphoinositide synthesis in permeabilized human platelets. *Cell* 82: 643-53

Hesketh, J. E. and Pryme, I. F. (1991). Interaction between mRNA, ribosomes and the cytoskeleton. *Biochem. J.* 277, 1-10.

Hoelting T., Siperstein AE., Clark OH., Duh QY. 1994. Epidermal growth factor enhances proliferation, migration, and invasion of follicular and papillary thyroid cancer *in vitro* nd *in vivo. J Clin Endocr Metab.* 79: 401-8.

Izzard, C.S. and Lochner, L.R. Formation of cell-to-susbtrate contacts during cell motility: an interference-reflexion study. J. Cell Sci.42, 81-116, 1980.

Jockusch, B.M., Bubeck, P., Giehl, K., Kroemker, M., Moschner, J., Rothkegel, M., Rüdiger, M., Schlüter, K., Stanke, G., and Winkler, J. The molecular architecture of focal adhesions. Annu. Rev. Cell Dev. Biol. 11, 379-416, 1995.

Kaufmann AM., Khazaie K., Wiedemuth M., *et al.* 1990. Expression of epidermal growth factor receptor correlates with metastatic potential of 13762 NF rat mammary adenocarcinoma cells. *Int J Oncol.* 4: 1149-55

Kaufmann, A. M., Khazaie, K., and Weidemuth, M. (1994). Expression of epidermal growth factor receptor correlates with metastatic potential of 13762NF rat mammary adenocarcinoma cells. *Int. J. Oncol.* 4, 1149-1155.

Kislauskis, E. H., Zhu, X. and Singer, R. H. (1994). Sequences responsible for intracellular localization of beta-actin messenger RNA also affect cell phenotype. *J. Cell Biol.* 127, 441-451.

Kornberg, L., Earp, H.S., Parsons, J.T., Schaller, M. and Juliano, R.L. Cell adhesion or integrin clustering increases phosphorylation of a focal adhesion-associated tyrosine kinase. J. Biol. Chem. 267, 23439-23442, 1992.

Kundra, V., Escobedo, J.A., Kazlauskas, A., Kim, H.K., Rhee, S.G., Williams, L.T. and Zetter, B.R. *Nature* 367: 474-476, 1994.

Kurasawa, Y., Hanyu, K., Watanabe, Y., and Numata, O. (1996). F-actin bundling activity of Tetrahymena elongation factor 1 is regulated by Ca^{2+} / calmodulin. *J. Biochem.* 119, 791-798.

Latham, V. M., Kislauskis, E. H., Singer, R. H. and Ross, A. F. (1994). Beta-actin mRNA localization is regulated by signal transduction mechanisms. *J. Cell Biol.* 126, 1211-1219.

Lauffenburger, D.A. and Horwitz, A.F. Cell migration: a physically integrated molecular process. Cell 84, 359-369, 1996.

Lawrence, J. B. and Singer, R. H. (1986). Intracellular localization of messenger RNAs for cytoskeletal proteins. *Cell* 45, 407-415.

Leavesley, D.I., Schwartz, M.A., Rosenfeld, M. and Cheresh, D.A. Integrin beta1-and beta3-mediated endothelial cell migration is triggered through distinct signaling mechanisms. J. Cell Biol. 121, 163-170, 1993.

Lew, Y., Jones, D. V., Mars, W. M., Evans, D., Byrd, D. and Frazier, M. L. (1992). Expression of elongation factor-1- related sequence in human pancreatic cancer. *Pancreas* 7, 144-152.

Lichtner RB., Wiedemuth M., Kittmann A., Ullrich A., Schirrmacher V., Khazaie K.1992. Ligand-induced activation of epidermal growth factor receptor in intact rat mammary adenocarcinoma cells without detectable receptor phosphorylation. *J Biol Chem.* 267, 11872-80.

Liu, G., Edmonds, B. T. and Condeelis, J. (1996). pH, EF1 and the cytoskeleton. *Trends Cell Biol.* 6, 168-171.

Matsumoto, K., Matsumoto, K., Nakamura, T. and Kramer, R.H. Hepatocyte growth factor/scatter factor induces tyrosine phosphorylation of focal adhesion kinase (p125^{FAK}) and promotes migration and invasion by oral squamous cell carcinoma cells. J. Biol. Chem. 269: 31807-31813, 1994.

Matsumoto, K., Ziober, B.L., Yao, C-C and Kramer, R.H. Growth factor regulation of integrin-mediated cell motility. Cancer Metastasis Rev. 14, 205-217, 1995.

Minton, A. P. (1983). The effect of volume occupancy upon the thermodynamic activity of proteins: some biochemical consequences. *Mol. Cell. Biochem.* 55, 119-140.

Mitchison, T.J. and Cramer, L.P. Actin-based cell motility and cell locomotion. Cell 84, 371-379, 1996.

Murray, J., Edmonds, B. T., Liu, G., and Condeelis, J. (1996) Elongation factor-1 alters the initial rates and final extent of actin polymerization and depolymerization. *J. Cell Biol.* (in press).

Nachmias V T., Golla R., Casella JF., Barron-casella E. 1996. Cap Z, a calcium insensitive capping protein in resting and activated platelets. *FEBS Lett.* 378: 258-262.

Neri, A., Welch, D., Kawaguchi, T. and Nicolson, G. L. (1982). Development and biologic properties of malignant cell sublines and clones of a spontaneously metastasizing rat mammary adenocarcinoma. *J. Natl. Cancer Inst.* 68, 507-517.

Okazaki, K. and Yumura, S. (1995). Differential association of three actin-bundling proteins with microfilaments in Dictyostelium amoebae. *Eur. J. Cell Biol.* 66, 75-81.

Olmsted, J. B. (1981). Affinity purification of antibodies from diazotized paper blots of heterogeneous protein samples. *J. Biol. Chem.* 256, 11955-11957.

Opdenakker, G., Cabeza-Arvelaiz, Y., Fiten, P., Dijkmans, R., Van Damme, J., Volckaert, G., Billiau, A., Van Elsen, A. and Cassiman, J-J. (1987) Human elongation factor 1 a polymorphic and conserved multigene family with multiple chromosomal localizations. *Hum. Genet.* 75: 339

Open, C. H., DeRosier, D. J. and Condeelis, J. (1992). Actin crosslinking protein EF-1 of Dictyostelium *discoideum* has a unique bonding rule that allows square-packed bundles. *J. Struct. Biol.* 109, 248-254.

Parsons, J.T. Integrin-mediated signalling: regulation by protein tyrosine kinases and small GTP-binding proteins. Current Opinions Cell Biol. 8, 146-152, 1996.

Pedersen PH., Ness GO., Engebraaten O., Bjerkvig R., Lillehaug JR., Laerum OD. 1994. Heterogeneous response to the growth factors [EGF, PDGF (bb), TGF-alpha, bFGF, IL-2] on glioma spheroid growth, migration and invasion. *Int J Cancer*. 56: 255-61.

Pencil, S. D., Toh, Y. and Nicolson, G. L. (1993). Candidate metastasis-associated genes of the rat 13762NF mammary adenocarcinoma. *Breast Cancer Res. Treat*. 25, 165-174.

Peppelenbosch MP., Tertoolen LG., Hage WJ., de Laat SW. 1993. Epidermal growth factor-induced actin remodeling is regulated by 5-lipoxygenase and cyclooxygenase products. *Cell*. 74, 565-75.

Pollard TD. 1986. Rate constants for the reactions of ATP- and ADP-actin with the ends of actin filaments. *J. Cell. Biol.* 103: 2747-54

Price JE., Sauder DN., Fidler IJ., 1988. Tumorigenicity and metastatic behavior in nude mice of two human squamous cell carcinoma lines that differ in production of cytokine ETAF/IL-1. *J Invest Dermatol*. 91: 258-62

Rayment, I., Holden, H. M., Whittaker, M., Yohn, C. B., Lorenz, M., Holmes, K. C. and Milligan, R. A. (1993). Structure of the actin-myosin complex and its implications for muscle contraction. *Science* 261, 58-65.

Riis, B., Rattan, S. I. S., Clark, B. F. C. and Merrick, W. C. (1990). Eukaryotic protein elongation factors. *Trends Biol. Sci.* 15, 420-424.

Rijken PJ., Hage WJ., van Bergen en Henegouwen PM., Verkleij AJ., Boonstra J. 1991. Epidermal growth factor induces rapid reorganization of the actin microfilament system in human A431 cells. *J. Cell Sci.* 100: 491-499

Rijken PJ., Post SM., Hage WJ., Van Bergen En Henegouwen PM., Verkleij AJ., Boonstra J. 1995. Actin polymerization localizes to the activated epidermal growth factor receptor in the plasma membrane, independent of the cytosolic free calcium transient. *Exp. Cell Res*. 218: 223-32

Rinnerthaler, G., Geiger, B, and Small, J.V. Contact formation during fibroblasts locomotion: involvement of membrane ruffles and microtubules. J. Cell. Biol. 106, 747-760, 1988.

Romer, L.H., Burridge, K. and Turner, C.E. Signaling between the extracellular matrix and the cytoskeleton: tyrosine phosphorylation and focal adhesion assembly. Cold Spring Harbor Symposia on Quantitative Biology, vol. LVII, 193-202, 1992.

Royce LS., Baum BJ., 1991. Physiologic levels of salivary epidermal growth factor stimulate migration of an oral epithelial cell line. *Biochim Biophys Acta*. 1092:401-3

Sanders, J., Brandsma, M., Janssen, G. M. C., Dijk, J. and Moller, W. (1996). Immunofluorescence studies of human fibroblasts demonstrate the presence of the complex of elongation factor-1 in the endoplasmic reticulum. *J Cell Sci*. 109, 1113-1117.

Schafer D., Jennings P., Cooper J. 1996 Dynamics of capping protein and actin assembly in vitro: uncapping barbed ends by PIP2. *J. Cell. Biol.* in press

Schmidt, C.E., Horwitz, A.F., Lauffenburger, D.A., and Sheetz, M.P. Integrin-cytoskeletal interactions in migrating fibroblasts are dynamic, asymetric, and regulated. J. Cell Biol. 123, 977-991, 1993.

Segall, J. E., Tyerech, S., Boselli, L., Masseling, S., Helft, J., Chan, A., Jones, J. and Condeelis, J. (1996). EGF stimulates lamellipod extension in metastatic mammary adenocarcinoma cells by an actin-dependent mechanism. *Clin. Exp. Metastasis.* 14, 61-72.

Shepherd, J. C. W., Walldorf, U., Hug, P. and Gehring, W. J. (1989). Fruit flies with additional expression of the elongation factor EF1 live longer. *Proc. Natl. Acad. Sci. USA,* 86, 7520-7521.

Sherman, M. and Sypherd, P. S. (1989). Role of lysine methylation in the activities of elongation factor 1 . *Arch. Biochem. Biophys.* 275, 371-378.

Silletti S., Raz A., 1993. Autocrine motility factor is a growth factor. *Biochem Biophys Res Commun.* 194: 446-57

Singer, R. H. (1992). The cytoskeleton and mRNA localization. *Curr. Opin. Cell Biol.* 4, 15-19.

Small, J.V. The actin cytoskeleton. Electron Microsc. Rev. 1, 155-174, 1988.

Spudich JA., Watt S. 1971. The regulation of rabbit muscle contraction. I. Biochemical studies of the interaction of the tropomyosin-troponin complex with actin and the proteolytic fragments of myosin. *J. Biol. Chem.* 246: 4866-4871.

Stracke M., Liotta LA., Schiffmann E. 1993. The role of autotaxin and other motility stimulating factors in the regulation of tumor cell motility. *Symp Soc Exp Biol.* 47: 197-214.

Symons MH., Mitchison TJ., 1991. Control of actin polymerization in live and permeabilized fibroblasts. *J.Cell Biol.* 114: 503-513

Taneja, K. L., Lifshitz, L. M., Fay, F. S., and Singer, R. H. (1992). Poly (A) RNA codistribution with microfilaments: evaluation by in situ hybridization and quantitative digital imaging microscopy. *J. Cell Biol.* 119, 1245-1260.

Taniguchi, S., Miyamoto, S., Sadano, H. and Kobayashi, H. (1992). Rat elongation factor 1 alpha: sequence of cDNA from highly metastatic fos-transferred cell line. *Nuc. Acid Res.* 19, 6949.

Tatsuka, M., Mitsui, H., Wada, M., Nagata, A., Nojima, H. and Okayama, H. (1992). Elongation factor-1 alpha gene determines susceptibility to transformation. *Nature* 359, 333-336.

Van Delft S., Verkleij AJ., Boonstra J., van Bergen en Henegouwen PM. 1995. Epidermal growth factor induces serine phosphorylation of actin. *FEBS Letters.* 357: 251-254

Venema, R. C., Peters, H. I. Traugh, J. A. (1991). Phosphorylation of elongation factor 1 (EF-1) and valyl-tRNA synthetase by protein kinase C and stimulation of EF-1 activity. *J. Biol. Chem.* 266, 12574-125880.

Wang X., Kamiyama K., Iguchi I., Kita M., Imanishi J. 1994. Enhancement of fibronectin-induced migration of corneal epithelial cells by cytokines. *Invest Ophthalmol Vis Sci.* 35: 4001-7

Welch, D. R., Neri, A. and Nicolson, G. L. (1983). Comparison of 'spontaneous' and 'experimental' metastasis using rat 13762 mammary adenocarcinoma metastatic cell clones. *Invasion Metastasis* 3, 5-80.

Wiegant FA., Blok FJ., Defize LH., Linnemans WA., Verkley AJ., Boonstra J. 1986. Epidermal growth factor receptors associated to cytoskeletal elements of epidermoid carcinoma (A431) cells. *J. Cell. Biol.* 103: 87-94

Winkler, M. (1988). Translational regulation in sea urchin eggs: a complex interaction of biochemical and physiological regulatory mechanisms. *Bio. Essays* 8, 157-161.

Witke W., Sharpe AH., Hartwig JH., Azuma T., Stossel TP., Kwiatkowski DJ. 1995. Hemostatic, inflammatory, and fibroblast responses are blunted in mice lacking gelsolin. *Cell.* 81: 41-51.

Xie, H.,Turner, T., Wang, M.H., Singh, R.K., Siegal, G.P. and Wells, A. *Clin. Expl. Metastasis* 13: 407-419, 1995.

Yang, F., Demma, M., Warren, V., Dharmawardhane, S., and Condeelis, J. (1990). Identification of an actin-binding protein from Dictyostelium as elongation factor 1 . *Nature* 347, 494-496.

Yang, W., Burkhart, W., Cavallius, J., Merrick, W. C., and Boss, W. F. (1993). Purification and characterization of a phosphatidylinositol-4-kinase activator in carrot cells. *J. Biol. Chem.* 268, 393-398.

Zigmond SH.1996. Signal transduction and actin filament organization. *Curr Opin Cell Biol.* 8: 66-73

APPENDIX

TABLES

Table 1: Quantitation of Morphological Changes in Response to EGF

Treatment	Lamellipod with F-actin Tip[a]	Lamellipod with rhodamine-actin tip[b]
buffer	9/64	8/64
5nM EGF	43/61	58/61

Six fields of cells as shown in Figure 2 were counted. The total number of cells counted in all fields is the denominator.

a: Cells were scored for lamellipods that contained F-actin localized to the lamellipod tip as shown in Figure 2 D

b: Cells were scored for lamellipods that contained a continuous rhodamine-actin zone as in Figure 2 F

Table 2. Metastatic involvement of tissues from rats inoculated with MTLn3 or MTC cell lines[1].

	MTLn3			MTC		
weeks[2]	IPL	CPL	Lung	IPL	CPL	Lung
3	2/2	0/2	0/2	-	-	-
4	4/4	4/4	4/4	0/3	0/3	0/3
5	7/8	4/7	7/8	4/4	0/4	0/4

[1] expressed as number of positive animals per total number of animals examined

[2] time following inoculation of mammary fat pads with specified cell type

IPL: ipsilateral axillary lymph node

CPL: contralateral axillary lymph node

Table 3. Levels of expression of EF1 in cell lines and whole tumors.

I. MTLn3

	% Total Protein	[1]μM	[1]EF1 :Actin	[2]μM	[2]EF1 :F-actin	[3]$K_d$app
EF1	2.9	57	-	35	-	26 μM
Actin	6.5	153	0.37	76	0.46	-

II. MTC

	% Total Protein	[1]μM	[1]EF1 :Actin	[2]μM	[2]EF1 :F-actin	[3]$K_d$app
EF1	2	37	-	21	-	7 μM
Actin	3	65	0.57	31	0.68	-

III. Rat mammary tumors and normal liver

	[4]Level of Expression
MTLn3 primary tumor	1.86
MTC primary tumor	1.06
Normal rat liver	1.00

[1] from whole cell lysates.

[2] from the Triton-insoluble cytoskeletal fraction.

[3] calculated from: apparent K_d = (EF1)$_{free}$ (F-actin)$_{free}$ / (EF1)$_{bound}$ in the Triton-insoluble cytoskeletal fraction.

[4] relative to the amount in normal rat liver.

FIGURE LEGENDS

Figure 1 (A). Number of barbed ends in cell lysates varies with time after stimulation. ■ represent data from EGF-stimulated cells; each point is the average of four independent determinations. □ are data from buffer-stimulated cells. (Inset) Relative rate from a trial with EGF- stimulated cells in which either 100 nM cytochalasin D (O) or DMSO (carrier, □) was added before the introduction of pyrene actin to the cell lysate. Relative rate is the initial rate of actin polymerization in lysates from EGF-stimulated cells divided by the initial rate from the unstimulated cells in the same experiment. (B) The content of F-actin in MTLn3 cells increases transiently following EGF-stimulation. F-actin content was measured using the NBD-phallicidin binding assay as described in Materials and Methods. Error bars show SEM.

Figure 2. Rhodamine-actin polymerizes preferentially at the tips of lamellipods in EGF-stimulated cells. MTLn3 cells were stimulated for 1 minute with either buffer (A,C,E) or 5 nM EGF (B,D,F); permeabilized with 0.2 mg/ml saponin together with 0.45 uM rhodamine-labeled actin in permeabilization buffer and incubated for 5 min. Permeabilized cells were fixed and stained with fluorescein-phalloidin. (A,B) phase-contrast, (C,D) fluorescein - phalloidin channel showing total F-actin and (E,F) rhodamine-labeled actin channel showing incorporated exogenous rhodamine-actin. All images were obtained at identical settings in each channel. Bar = 10 um

Figure 3. EGF stimulates lamellipod extension and accumulation of F-actin and rhodamine-actin at the lamellipod tips. This figure is an overlay image of the fluorescein-phalloidin(green) and rhodamine-actin(red) channels from two confocal images. (A), control cells have incorporated rhodamine - actin only at sites of protrusive activity. (B), EGF-stimulated cells extend broad and almost encompassing lamellipods with intense and continuous rhodamine-actin at the lamellipod tips. The rhodamine-actin cortex as seen in red (arrowhead) is more proximal to the plasma membrane than the broad green F-actin zone. Both EGF-stimulated and control cells have rhodamine-actin incorporating at the ends of stress fibers (arrow). Bar = 10 um

Figure 4. Rhodamine-labeled actin incorporation in permeabilized MTLn3 cells is not diffusion limited. Changes in fluorescence intensity as a function of the incubation time, A) rhodamine-actin intensity at the tip of the lamellipods. B) rhodamine-actin intensity at the cell center. Data for each time point is the average and SEM of 15 different cells. Images A and B demonstrate where on cells the measurements were taken.

Figure 5. The pattern of rhodamine-labeled actin incorporation in saponin permeabilized MTLn3 cells does not change over time. A) Cells were stimulated with 5 nM EGF for 1 minute, incubated in permeabilization buffer containing 0.45 uM rhodamine-actin for 1 minute or B) for 5 minutes. To visualize only the rhodamine-labeled actin incorporation pattern, MTLn3 cells were not stained with fluorescein phalloidin.

Figure 6. Distribution of rhodamine labeled- actin fluorescence measured as a function of distance from the leading edge of the lamellipod. Measurements of 10 cells taken from SIT

camera images. ■ cells stimulated with EGF for 1 minute. ●: control cells after treatment with buffer for 1 minute; □: cells stimulated with EGF for 1 min and then exposed to 20 nM of capping protein before addition of rhodamine-actin; O: control cells treated with buffer for 1 min and then exposed to 20 nM of capping protein before addition of rhodamine-actin. ▲, fluorescein phalloidin staining in cells stimulated with EGF for 1 minute.

Figure 7. Capping protein inhibits the incorporation of rhodamine labeled-actin in permeabilized EGF-stimulated MTLn3 cells. Cells were stimulated with 5 nM EGF for 1 minute, permeabilized in the presence (B, D,F) or absence (A,C,E) of 20 nM capping protein and subsequently incubated for 5 minutes with 0.45 uM rhodamine-actin in permeabilization buffer, fixed and stained with fluorescein-phalloidin. (A,B) phase-contrast, (C,D) fluorescein - phalloidin channel and (E,F) rhodamine-labeled actin channel. No fluorescence is observed in the rhodamine channel in (F) indicating no cross over from the fluorescein to the rhodamine channel, under the imaging conditions used in this study. Bar = 10um

Figure 8. Cytochalasin D inhibits the incorporation of rhodamine labeled-actin in permeabilized EGF-stimulated MTLn3 cells. Cells were stimulated, permeabilized in the absence (A, C) or presence of (B,D) of 100 nM Cytochalasin D and then incubated for 5 minutes with rhodamine-actin in permeabilization buffer. To evaluate cross channel fluorescence, these cells were not stained with fluorescein-phalloidin. Under these circumstance the rhodamine -actin images is unchanged indicating no contribution from the fluorescein-phallioidin channel. No fluorescence was observed in the fluorescein channel (not shown) demonstrating that the fluorescein-phallioidin image is not affected by the rhodamine-actin fluorescence. (A,B) Phase-contrast and (C,D) rhodamine channel. Bar = 10 uM

Figure 9: Metastatic cells display ameboid chemotaxis. *A*, a pipette filled with a solution of 1 μM EGF was placed near an MTLn3 metastatic cell. The cell rapidly undergoes shape changes to crawl toward the pipette at an average rate of 1.5 um/mn, and can rapidly change direction when the pipette is moved (arrow on image 16:31:04). Real timing is indicated on the top left corner of each images. *B*, *DIAS* computer program was used to generate the difference movie corresponding to the phase contrast images in *A*. The ameboid movement of the cells is characterized by a cycle of lamellipod extension at the front of the cells (displayed in green) and retraction at the rear (in red). Parts common to the previous images for each time are shown in gray. The calculated trajectory for the cells is indicated for each time by arrows. Time is indicated in the lower left corner as minutes after stable positioning of the pipette next to the cell. Insert, the cell path over the course of the experiment is shown as traces of the position of the centroid of the cell once every minute. The change in direction displayed by the cell to follow the pipette is shown as a net turn in the cell path.

Figure 10: Lamellipod extension and modifications of cell contacts with the substrate after an homogeneous upshift in EGF. MTLn3 cells were stimulated with a final concentration of 5 nM EGF and the changes in cell shape and contacts with the substrate were monitored by interference reflection microscopy. Images were recorded every 30 seconds using a low light level cooled CCD camera and assembled as a movie using *NIH Image* program. The sequence show

representative images of the same cell immediately before and 14 minutes after EGF stimulation (time is indicated as minutes after stimulation in the upper right corner of the images). EGF stimulation triggers a rapid and drastic lamellipod extension which is maximum around 3 minutes after stimulation. This extension is accompanied by the simultaneous establishment of close contacts in the newly extended area. After 5 minutes, new focal contacts are forming, which are then increasing in size over the course of the experiment. In the meantime, many of the previously existing focal contacts are remodeled: some of them are diffusing and are no longer visible after 20 minutes, while those located at the rear are dragged for a while by the cell and then disassembled, at least partly, as the cell rips the tail.

Figure 11: Kinetics of lamellipod extension after EGF stimulation. MTLn3 cells were stimulated with 5 nM EGF and the changes in cell shape were monitored phase contrast microscopy. Images were recorded every minute. Lamellipod extension was quantitated as modifications of the total area of the cells. Recording was done for 5 minutes prior EGF stimulation (at 5 minutes). Control cells were stimulated in parallel with control medium without EGF. Circles, stimulated cells; triangles, control cells. Results are the mean of respectively 50 and 40 cells for the stimulated and control experiments (SEM less than 5% for both experiments).

Figure 12: Talin is present at the growing edges of lamellipods. Cells were stimulated with EGF for 3 minutes and then stained for talin (left) and F-actin (right). There is a fine punctate localization of talin at the leading edge of the lamellipods which is narrower than the F-actin staining seen. The brighter central staining points seen are identified as focal contacts (see Results).

Figure 13: EGF stimulation triggers focal contact assembly. MTLn3 cells were stimulated with EGF for different amounts of time, and were then fixed, permeabilized and immunostained with antibodies against talin to visualize focal contacts. top left, unstimulated MTLn3 cell stained for talin. Note large preexisting focal contacts (arrowheads). top right, same cell as viewed by IRM. Note that the talin-based focal contact pattern matches exactly the focal contact pattern revealed by IRM. bottom left, numerous newly formed focal contacts are visible 5 minutes after EGF stimulation. bottom right, 20 minutes after EGF stimulation, the new focal contacts have grown to the size of mature focal contacts.

Figure 14: Focal contact distribution following EGF stimulation. MTLn3 cells were stimulated with EGF for different amounts of time, and were then fixed, permeabilized and immunostained with antibodies against talin to visualize focal contacts. The number (triangles) and the size (circles) of the focal contacts were assessed for individual cells at each time on single optical sections taken with the confocal microscope. The results for focal contact numbers are the sum of two comparable experiments, and each point shows the mean for 15 to 55 cells. The size of the focal contacts was evaluated on four representative cells for each time point. The SEM was less than 10% in each series.

Figure 15: Large preexisting focal contacts lose phosphotyrosine staining after EGF stimulation. MTLn3 cells were stimulated with EGF for different amounts of time, and were then fixed, permeabilized and double stained with antibodies against talin (left) and phosphotyrosine (right) to

visualize focal contacts. top: unstimulated cell. bottom: cell stimulated for 5 minutes. Unstimulated cells show almost identical focal contact patterns as revealed by talin or phosphotyrosine staining (compare top images). On the contrary, after stimulation with EGF for 5 minutes, some cells display a lower intensity of phosphotyrosine staining in large focal contacts, while other cells have completely lost phosphotyrosine staining in large preexisting contacts (bottom). Note that the phosphotyrosine staining remains unchanged in newly formed small focal contacts in the same cells.

Figure 16: Quantitation of the decrease in phosphotyrosine staining in the large preexisting focal contacts 5 minutes after EGF stimulation. MTLn3 cells, unstimulated or stimulated with EGF for 5 minutes were fixed, permeabilized and double stained with antibodies against talin and phosphotyrosine to visualize focal contacts. Parallel images were taken from single optical sections with the confocal microscope using identical constant settings for each set of images. The integrative density of respectively talin and phosphotyrosine fluorescence was then measured for each focal contact in individual. The ratio of those integrative densities (talin versus phosphotyrosine) were then plotted as a function of the area for each focal contact. *A*, unstimulated cells (9 representative cells analyzed, total number of focal contacts: 347). *B*, cells 5 minutes after EGF stimulation (10 representative cells analyzed, total number of focal contacts: 1014). Note the larger number of very small focal contacts at 5 minutes, reflecting the formation of new focal contacts at this time (see Figure 15). In unstimulated cells, the ratio of both fluorescence appears to be constant, whatever the size of the focal contacts (*A*). On the contrary, 5 minutes after EGF stimulation, this ratio remains the same in small focal contacts but tends to increase in the larger focal contacts, showing specific loss of phosphotyrosine staining in those contacts. Comparison of the two independent slopes from each individual linear regression analysis showed a strong statistical significance (p<0.00001).

Figure 17: EGF stimulates protrusive activity in cells in suspension. MTLn3 cells were stimulated in suspension with EGF for different amounts of time, and were then fixed, permeabilized and stained with rhodamine-labeled phalloidin. They were then analyzed under regular microscopy (panel *A*) or confocal microscopy followed by 3-dimensional reconstruction (panel **B**). *A*, representative MTLn3 cells, either unstimulated (EGF0) or stimulated for 2 or 5 minutes (EGF2 and EGF5). The upper panel shows the DIC images, while the lower panel shows the corresponding actin fluorescence images for each cell. Note the large actin-rich protrusions on the surface of the cells after a 2 minute stimulation, which tend to decrease after 5 minutes. *B*, 3-D reconstructions of representative cells after stimulation in suspension. Note that the protrusive activity on the surface is very low in unstimulated cells (EGF0), but becomes very prominent after a 2 minute EGF stimulation (EGF2). However, it is slowly going back to normal after 5 minutes (EGF5).

Figure 18: Quantitation of the protrusive activity in suspension after EGF stimulation. MTLn3 cells were stimulated in suspension with EGF for different amounts of time, and were then fixed, permeabilized and stained with rhodamine-labeled phalloidin. The percent of cell with protrusive activity was evaluated using DIC (see Figure 17). Results are the mean of three different experiment where 268 to 497 cells were counted for each time point in each experiment; they are expressed as mean±SEM.

Figure 19: Kinetics of protrusive activity on the dorsal surface of cells adhering to a substrate. Adherent MTLn3 cells were stimulated in suspension with EGF for different amounts of time, and were then fixed, permeabilized and stained with rhodamine-labeled phalloidin. Three-dimensional reconstructions of the cell shape were done using confocal microscopy images (*A*). The percent of cell with protrusive activity on the dorsal surface was evaluated using regular fluorescence (*B*). *A*, 3-D reconstruction of representative adhering MTLn3 cells, either unstimulated (EGF0) or 2 minutes after EGF stimulation (EGF2). *Top panel*: elevation view of the whole cells; *lower panel*: corresponding direct above view of the dorsal surface. Note the intense protrusive activity on the dorsal surface after 2 minutes stimulation. C. Percentage of cells adhering to a substratum with dorsal protrusions as a function of time after exposure to EGF. Phalloidin-stained cells were examined for the presence of dorsal protrusions.

Figure 20: MTLn3 cells are able to display lamellipod extension after stimulation in the presence of adhesion-inhibiting peptides. MTLn3 cells were plated for two hours on vitronectin and stimulated with 5 nM EGF either in regular medium (diamonds) or in presence of 1.5 mM of the adhesion-inhibiting GRGDSP peptide (squares) or the control GRADSP peptide (triangles). Changes in cell shape were monitored using phase contrast microscopy and lamellipod extension was quantitated. Recording started 4 minutes prior EGF stimulation (at 4 min). Results are the mean of 10 cells for each experiment. Note that in presence of the inhibitory peptide, the cells are able to extend a lamellipod with the same kinetics as control cells but this extension is not stable and retracts immediately after reaching a maximum 3 minutes after stimulation.

Figure 21: MTLn3 cells are able to display lamellipod extension over a non adhesive substrate. MTLn3 cells were plated on gold-coated glass coverslips which were patterned with hexadecanethiol and EG6-thiol to generate 10 μm lanes of adhesive substrate. They were then stimulated with 5 nM EGF and changes in cell shape were monitored using phase contrast microscopy, and the corresponding images were digitized and analyzed. Recording started 2 minutes prior EGF stimulation. *A*, representative sequence of a cell stimulated on 10 μm lane-patterned coverslips. The cell is shown before stimulation (EGF0), and respectively 4 and 8 minutes after stimulation (EGF4, EGF8). Note the maximal lamellipod extension at 4 minutes (arrows). Net increase in cell length after 8 minutes can be observed. *B*, quantitation of the changes in cell shape after stimulation. Three parameters were quantitated for each cell: maximum length (diamonds), maximum width (squares), and central width (triangles). A representative experiment is shown, where the results are the mean of 14 cells (SEM less than 10%). Note that the main extension occurs longitudinally over the cell length along the adhesive lane (see *A*). *Insert*, narrowed scale showing more precisely the modifications in the maximal width and central width over the same time course. The central width is decreasing as the cell is stretched as a result of the increase in cell length after stimulation. Note that the maximal width is increasing after stimulation, showing that the cells are able to extend their lamellipod above the limits of the lane over the non adhesive substrate (for a distance of about two microns on each side of the lane). This extension is followed by a rapid retraction, which brings back the maximal width of the cells within the limits of the adhesive lane (see *A*).

Figure 22: EGF-stimulated lamellipod extension over a non adhesive substrate. MTLn3 cells were plated on gold-coated glass coverslips which were patterned with hexadecanethiol and EG6-thiol to generate 10 μm lanes of adhesive substrate. Preparations were stimulated with EGF for 3 minutes, fixed, permeabilized and double stained with rhodamine-labeled phalloidin to visualize the cell cytoskeleton and antibodies against vitronectin to visualize the adhesive lanes. Parallel images of single optical sections were taken with the confocal microscope and overlayed. *In green*, vitronectin staining; *in red*, actin staining. The cell shows prominent lamellipod extension over the non adhesive surface (arrows; matched arrowheads, limits of the adhesive surface). A faint green fluorescence can be see over the whole cell body due to vitronectin from the foetal calf serum that has adsorbed all over the cell surface.

Figure 23. (A) Immunodetection of EF1 in a total homogenate from rat tumors derived from injected MTLn3 cells (a,b); and in a total homogenate from normal rat liver(c.d). (a,c) Coomassie Blue-stained SDS-PAGE gel and (b,d) corresponding lanes western blotted and probed with an anti-EF1 peptide antibody. Arrowheads indicate molecular weight markers (kDa) from top to bottom: 200, 116.3, 97.4, 66.3, 55.4, 36.5, 31.0. (B) Coomassie Blue-stained SDS-PAGE gel of EF1 purified from rat liver and whole MTLn3-derived tumors. (C) In vitro polyphenylalanine synthesis by EF1 purified from rat liver and MTLn3-derived tumors. In control experiments, no poly(U) message was added.

Figure 24. Effect of pH on F-actin binding by EF1 purified from MTLn3-derived rat mammary tumors and normal rat liver. (A, inset) EF1 : F-actin co-sedimentation assay at pH 6.5 where actin filaments crosslinked by EF1 (low speed pellet, LSP) were separated from EF1 bound to single actin filaments (high speed pellet, HSP) and free EF1 (high speed supernatant, HSS) by differential centrifugation. Lanes a - j: Coomassie Blue-stained SDS-PAGE gel, lanes a - e: EF1 alone; f - j: mixture of tumor EF1 (1 μM) and rabbit skeletal muscle F-actin (3 μM). Lanes f' - j': corresponding western blot of lanes f - j probed with an anti-EF1 antibody. Lanes a, f, f' = total reaction mixture; lanes b, g, g' = low speed supernatant; lanes c, h, h' = LSP; lanes d, i, i' = HSS; lanes e, j, j' = HSP. (B) rat tumor or (C) rat liver EF1 (1 μM) was co-polymerized with rabbit skeletal muscle actin (3 μM) at the indicated pH. ( ) LSP, ( ) HSP, ( ) HSS. Data are representative of 3 experiments. (D) Liver EF1 (2 μM) and muscle F-actin (12 μM) co-sedimentation assays performed under physiological conditions. The low salt buffer conditions utilized in panels A - C were compared to a physiological salt solution designed to mimic mammalian intracellular ionic conditions (see Methods).

Figure 25. Immunofluorescent images acquired by confocal microscopy of EGF-mediated changes in EF1 and F-actin distribution in MTLn3 cells. Panels A - C: unstimulated; D - F: after 3 min stimulation with 5 nM EGF. Panels A, D: phase contrast; B, E: fluorescein-EF1 ; C, F: F-actin visualized by rhodamine-phalloidin; G: anti-EF1 antibody preabsorbed against EF1 purified from rat liver; H: rhodamine-phalloidin staining of same cell shown in panel G. Arrowheads indicate regions of lamellipodial extension in response to stimulation with EGF; arrows indicate EF1 -rich surface projections. Bar = 10 μm.

Figure 26. Immunofluorescence images of the distribution of EF1 and F-actin in EGF-stimulated MTLn3 following extraction with saponin. Single optical sections acquired by confocal microscopy of (A) fluorescein-EF1 and (B) the corresponding rhodamine-phalloidin. Arrows indicate regions where stress fibers are prominent. Bar = 10 μm.

Figure 27. Immunofluorescent images acquired by confocal microscopy of the distribution of EF1 and F-actin in MTC cells. Single optical sections of (A, C) fluorescein-EF1 and (B, D) rhodamine-phalloidin were imaged at the plane of the substratum. (C-D) MTC cells were extracted with saponin as in Figure 25. Bar = 10 μm.

Figure 28. EGF-mediated changes in the amount of EF1 and F-actin associated with Triton-insoluble cytoskeletons from MTLn3. The amount of EF1 (circles) and F-actin (squares) was determined by densitometry analysis of western blots and corresponding Coomassie Blue-stained SDS-PAGE gels of cytoskeletal fractions acquired before and after stimulation with 5 nM EGF. The data is normalized to pre-stimulus levels of the respective protein. The error bars represent the standard deviation of 3 separate samples.

Figure 29. The effect of cytochalasin D on the association of EF1 and F-actin with the Triton-insoluble cytoskeleton following stimulation with EGF. The changes in the amounts of (A) F-actin and (B) EF1 180 sec following stimulation with 5 nM EGF were quantitated as in Figure 6 and expressed relative to amounts before stimulation (0 sec). Error bars represent the standard deviation of 3 separate experiments.

Figure 1
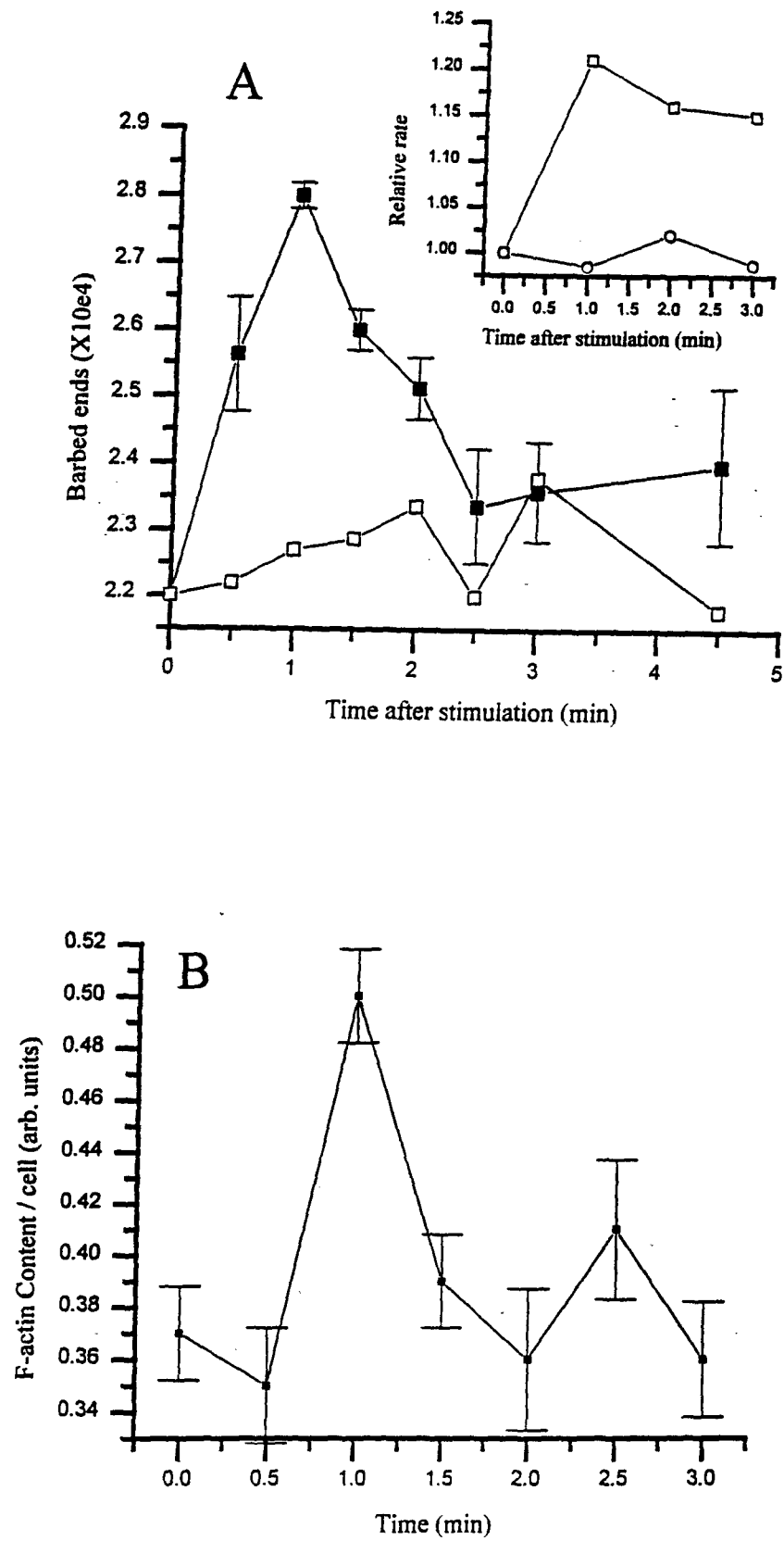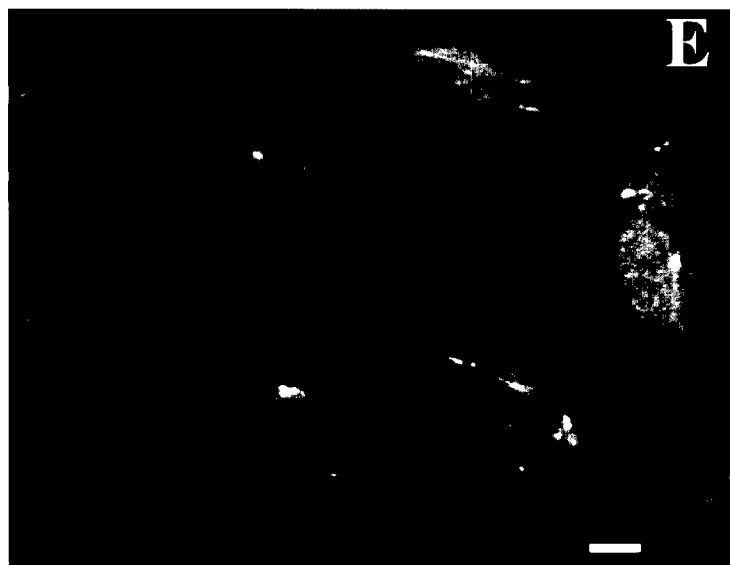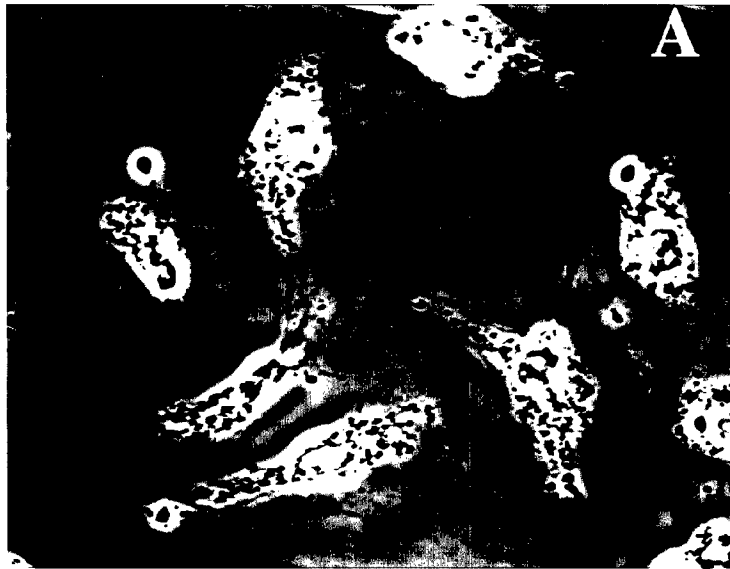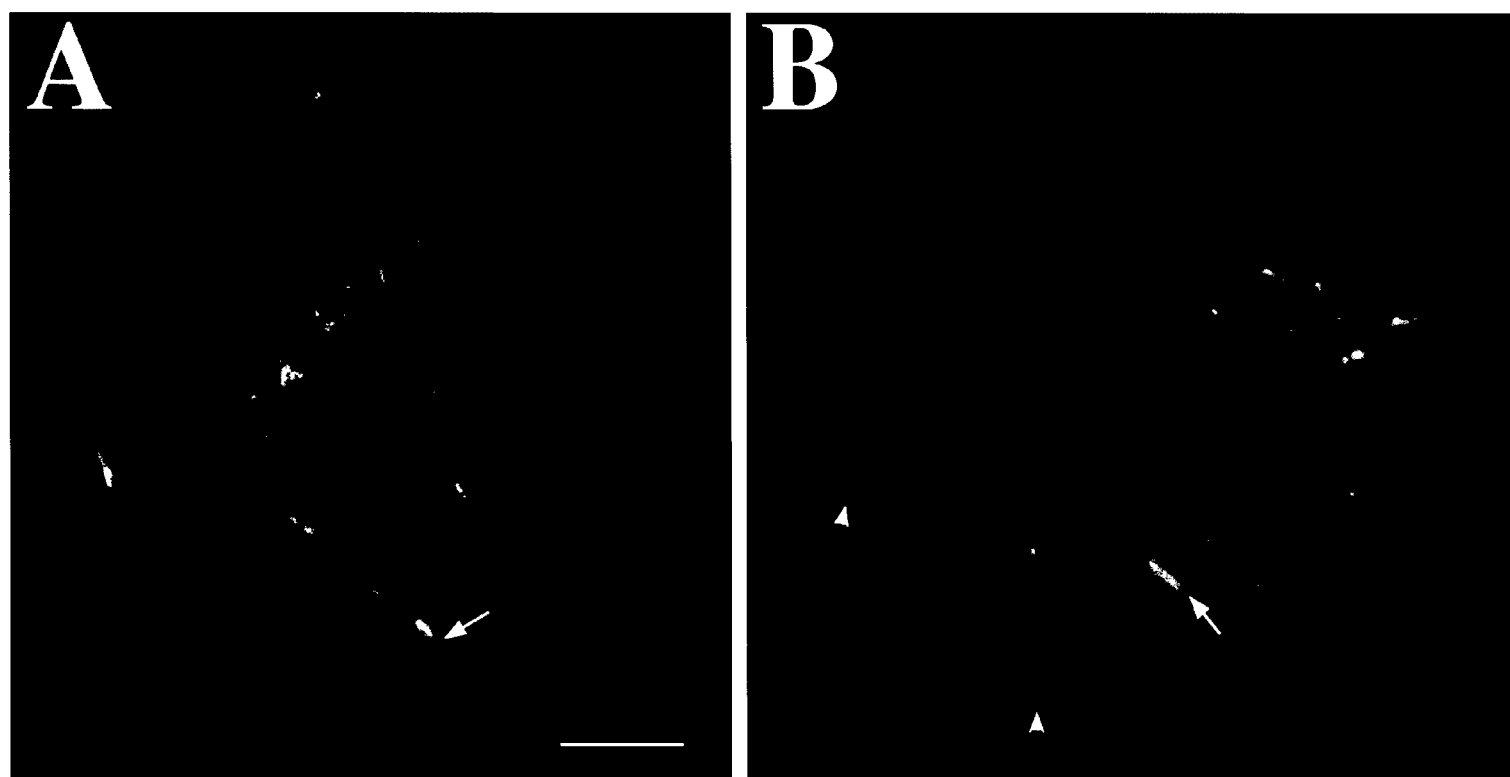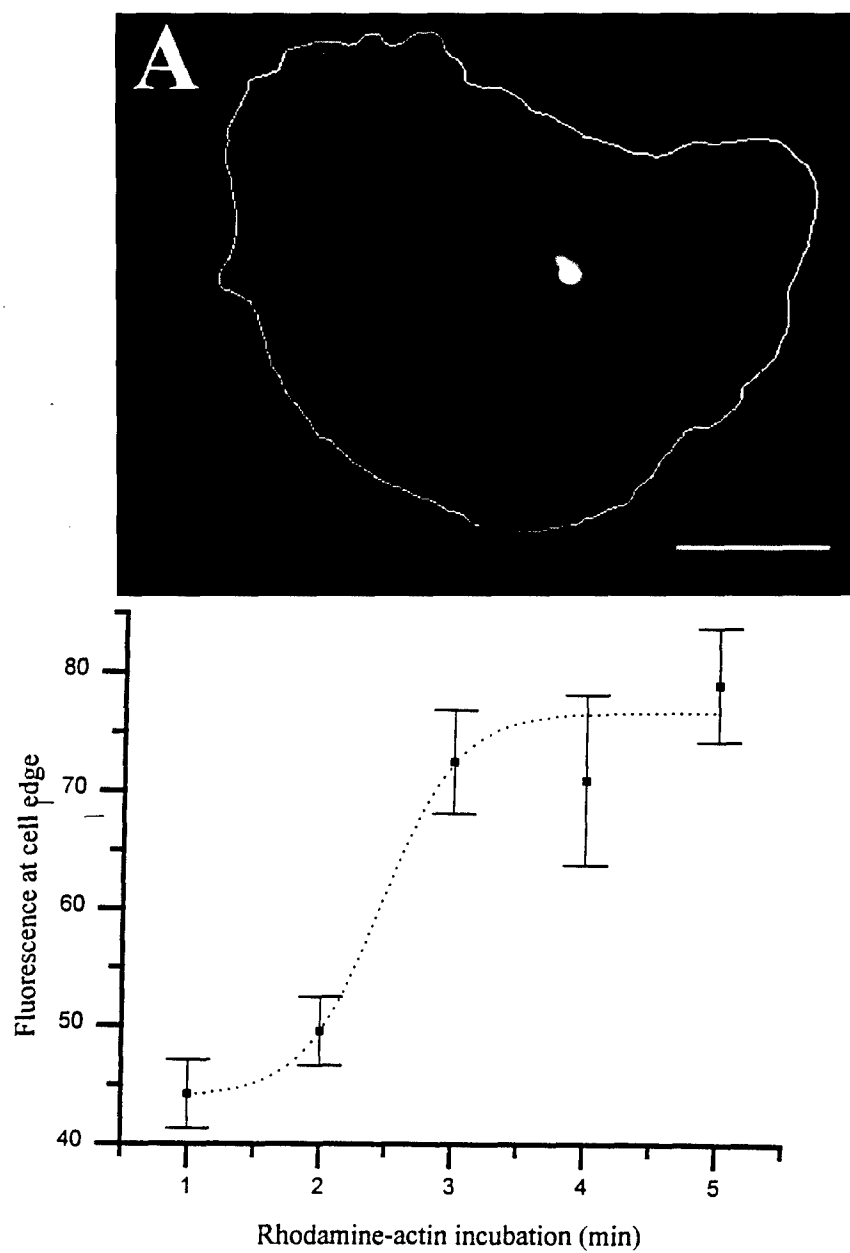
A

B

Figure 2

Figure 3

Figure 4A

Figure 4B
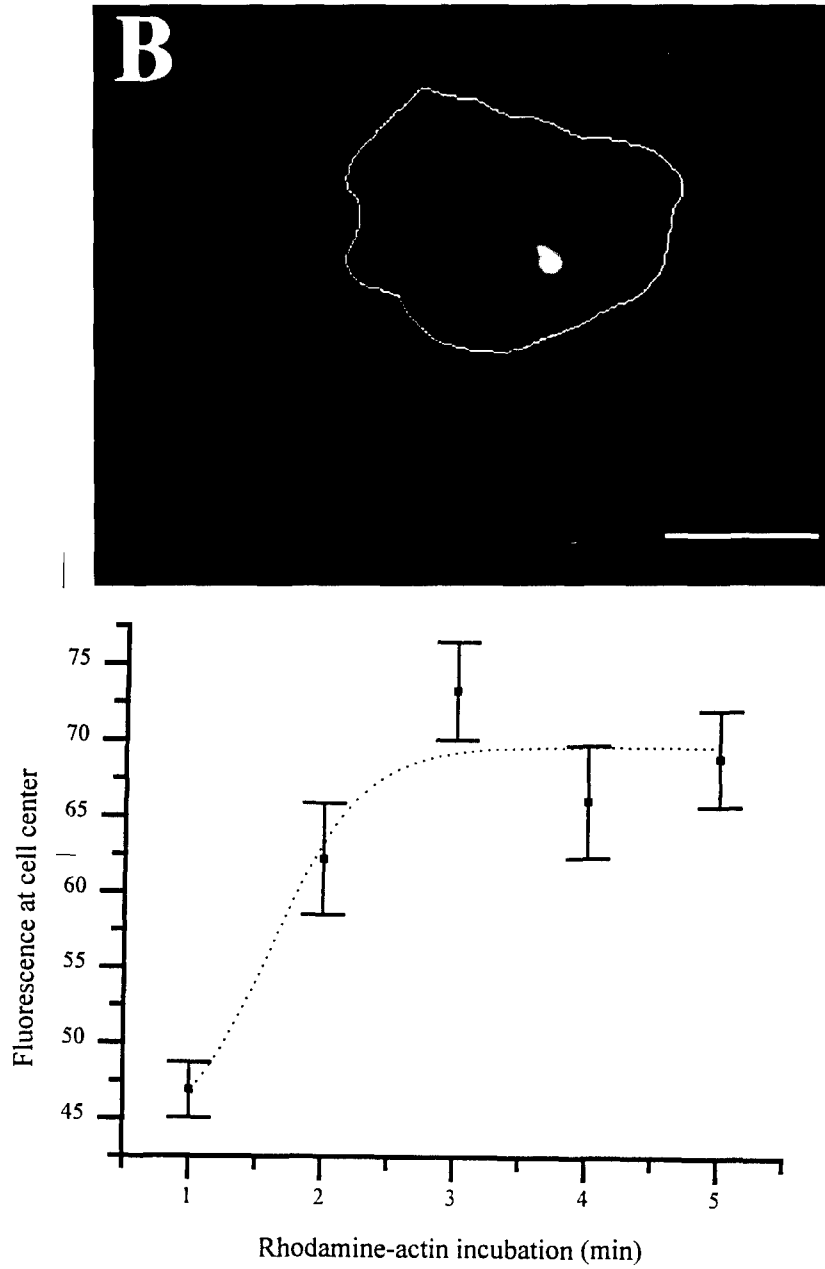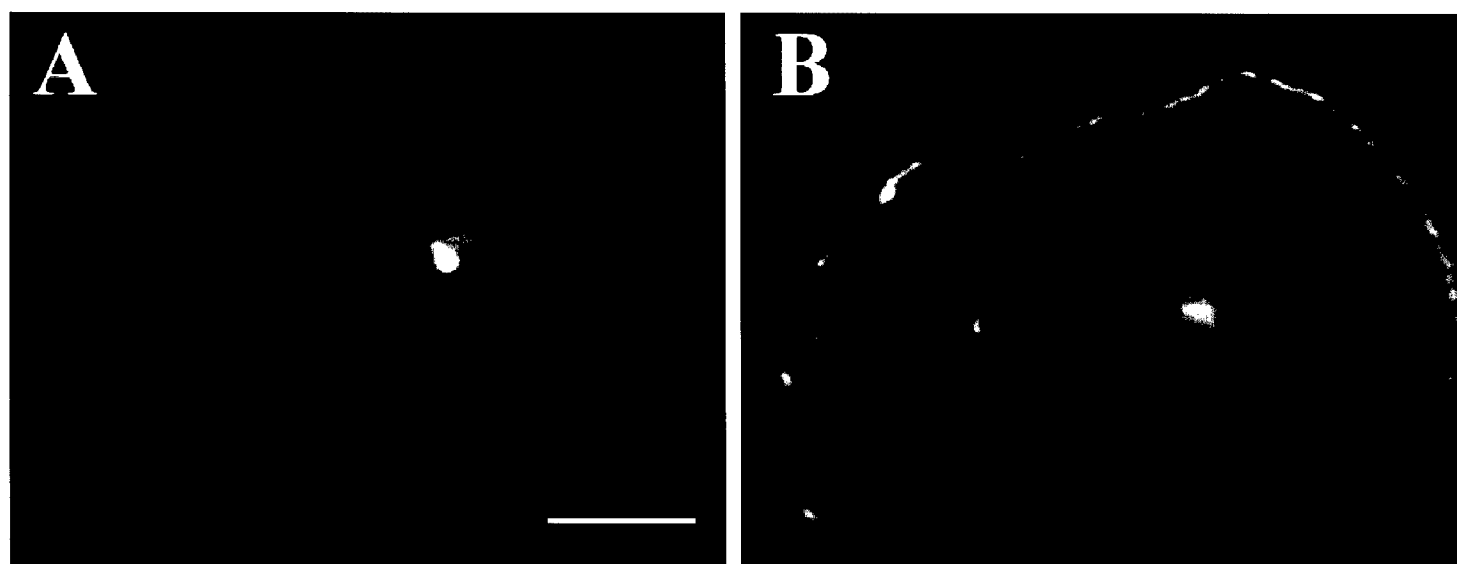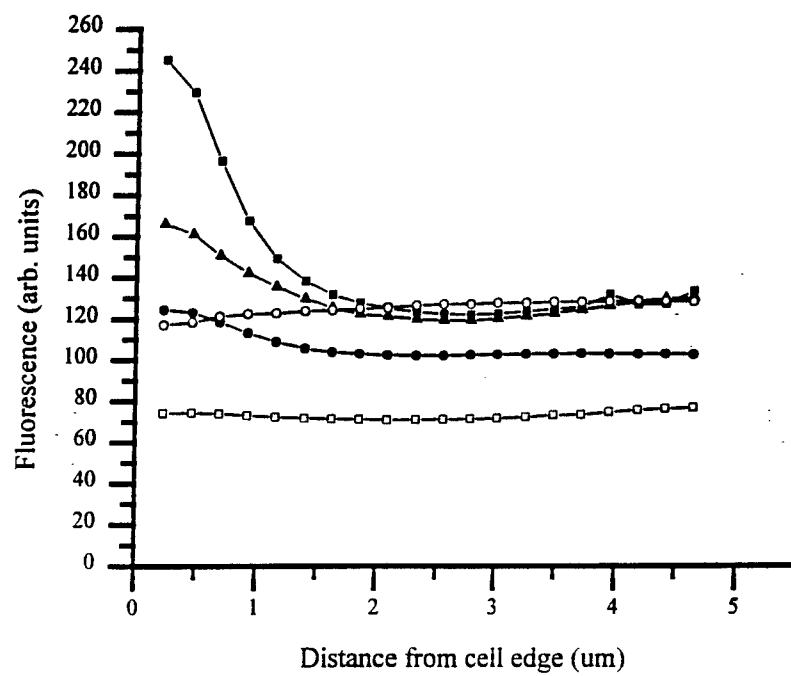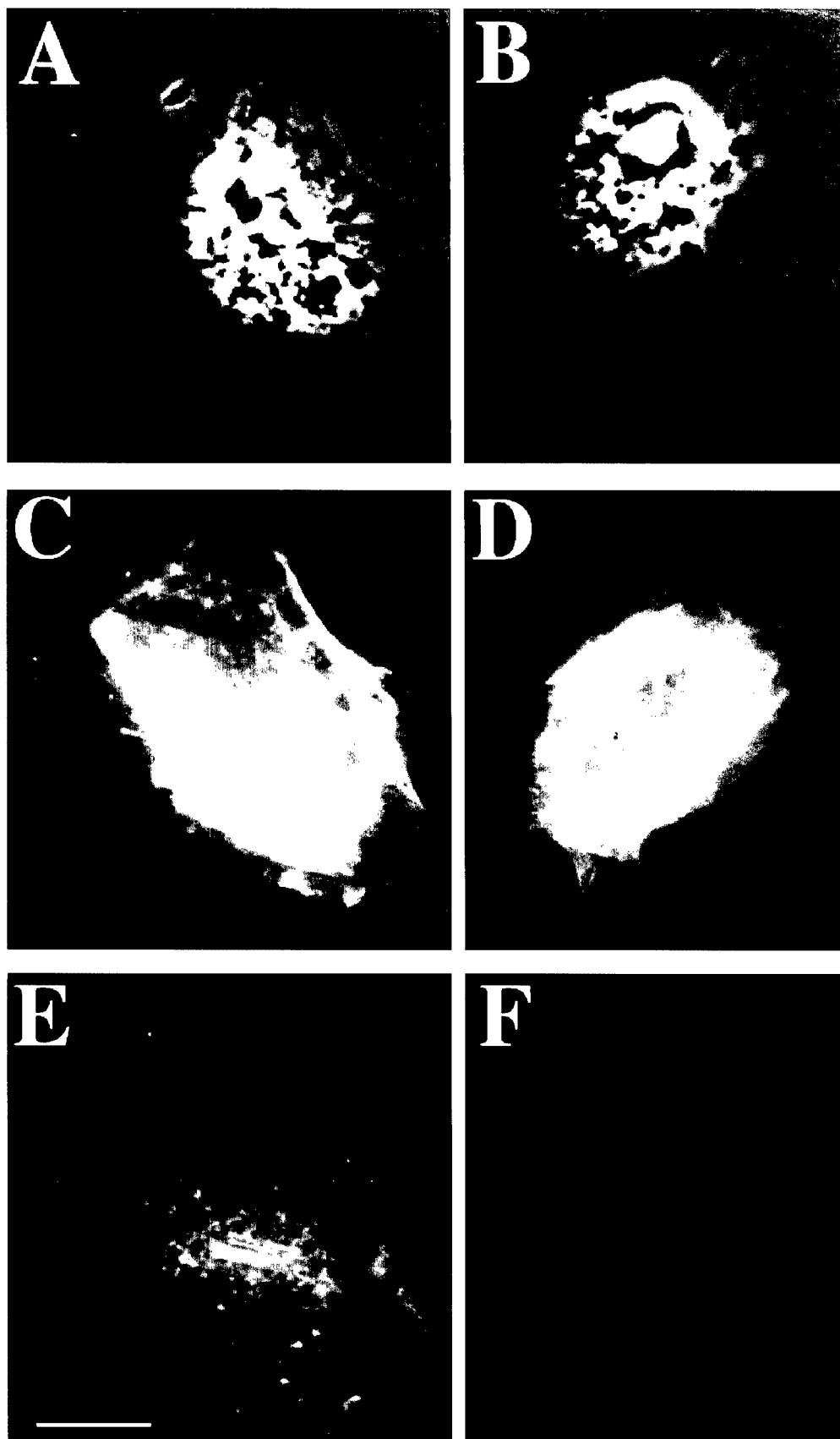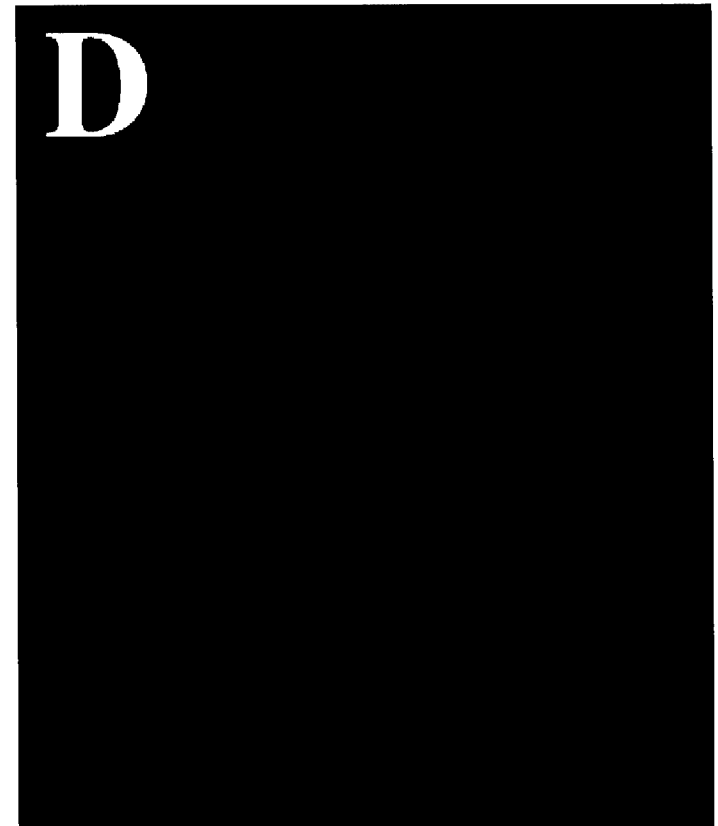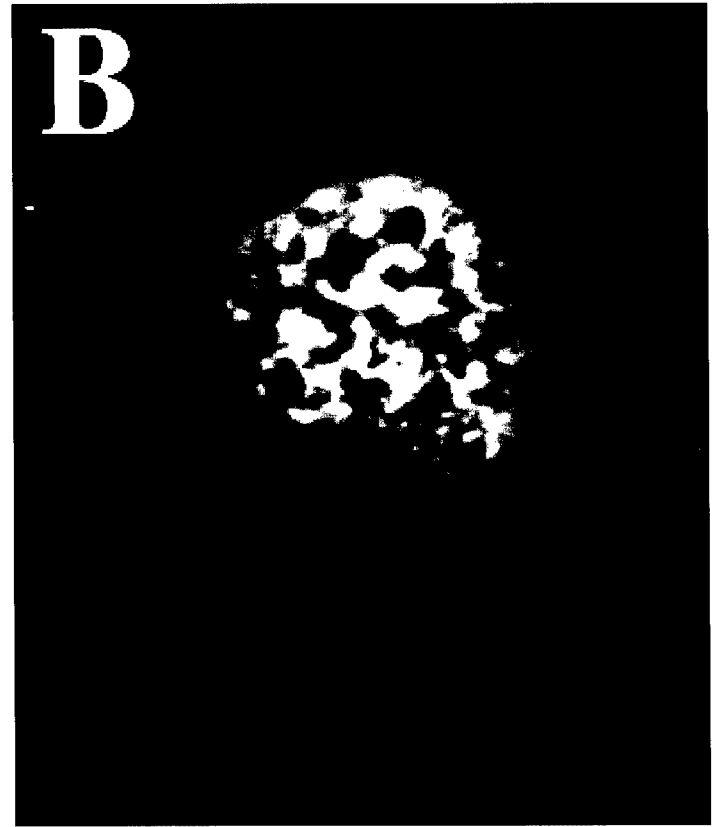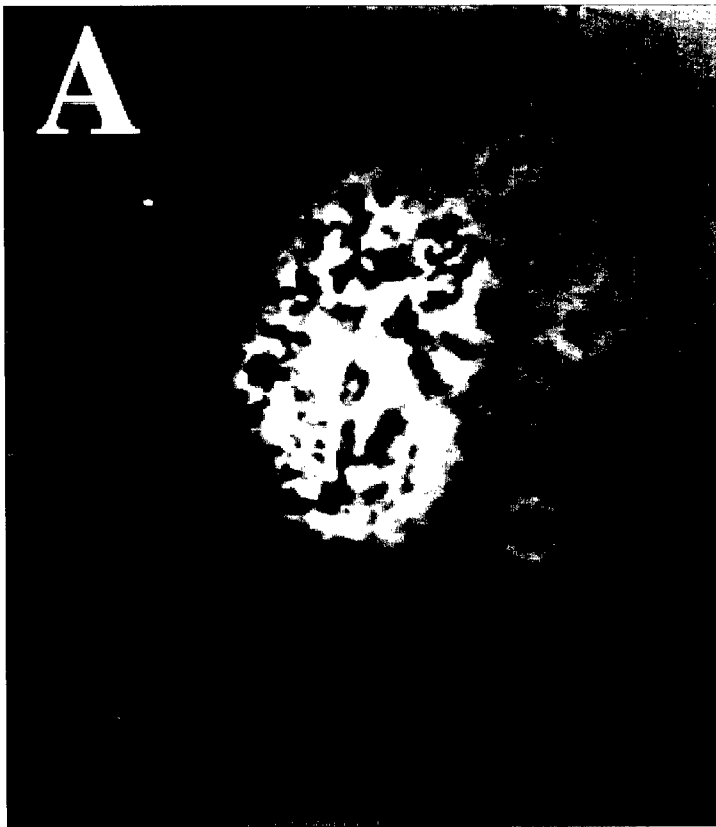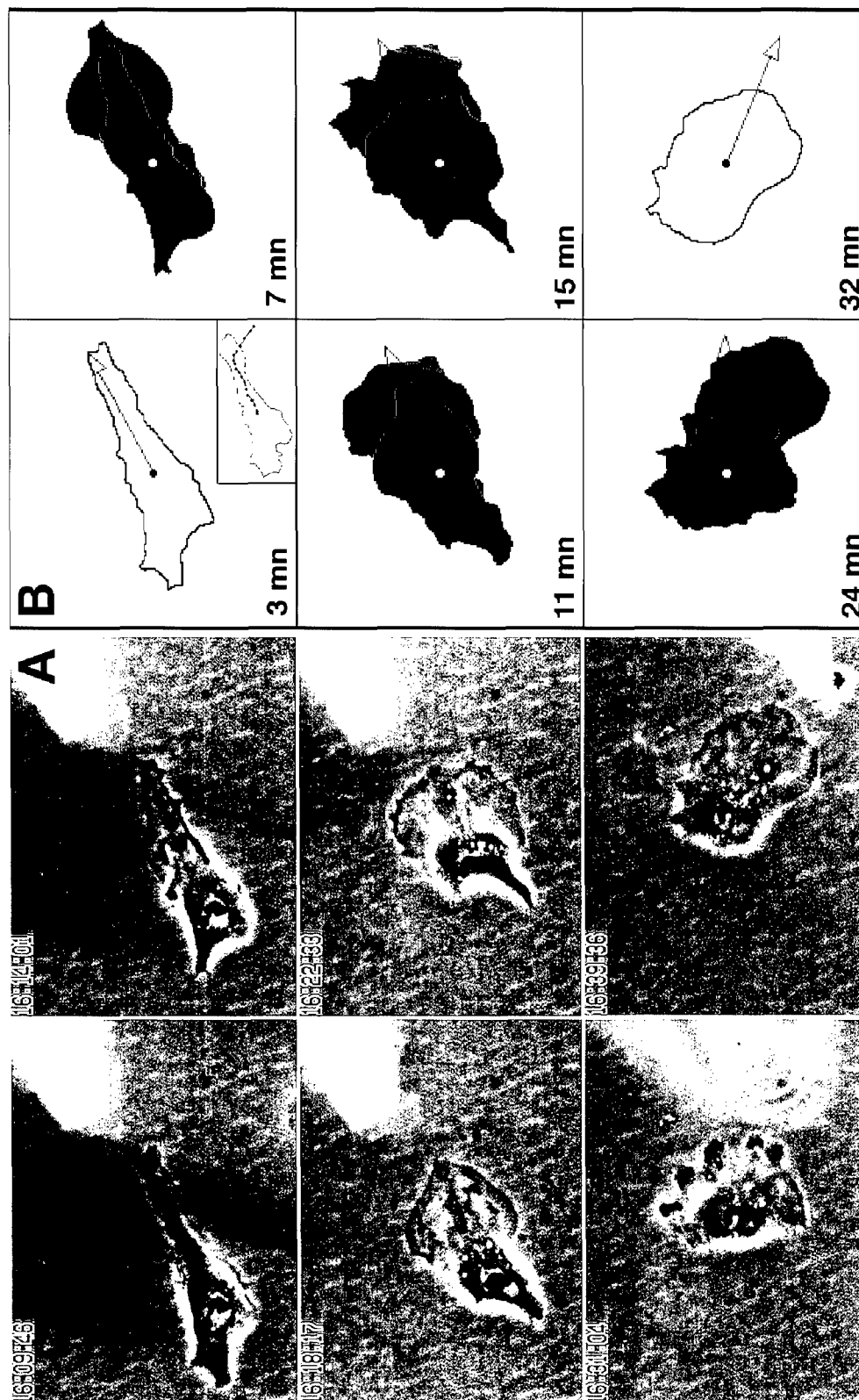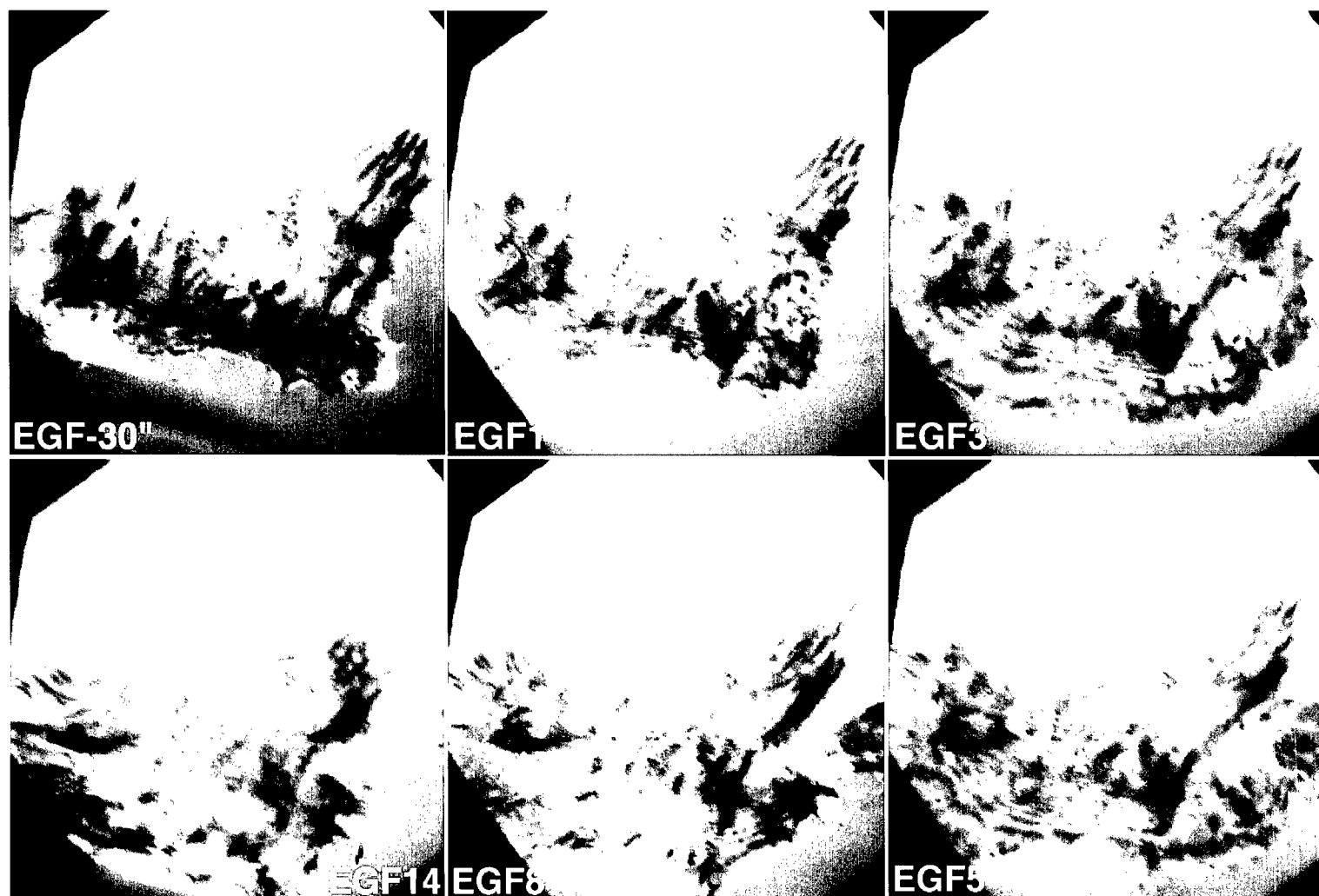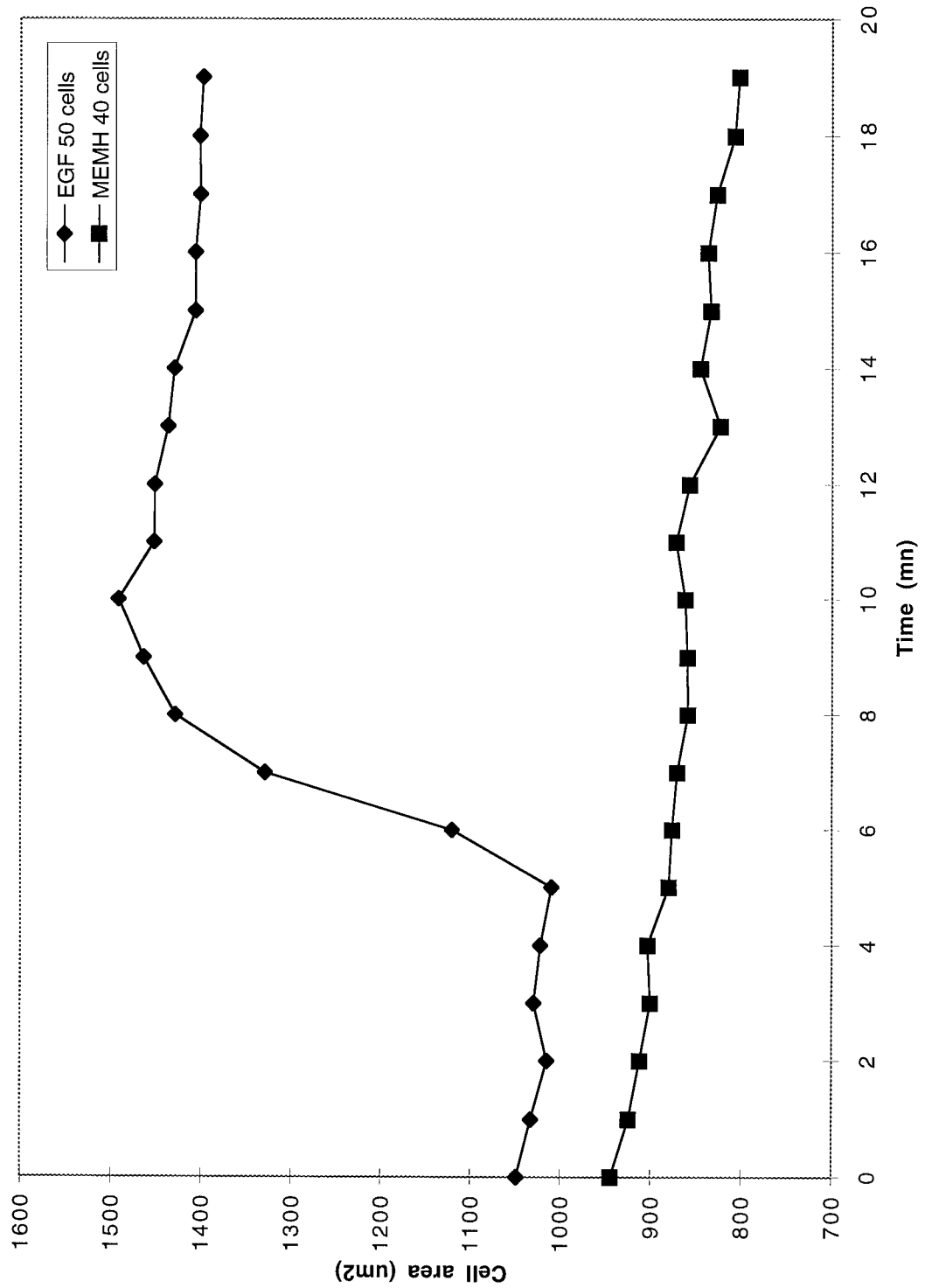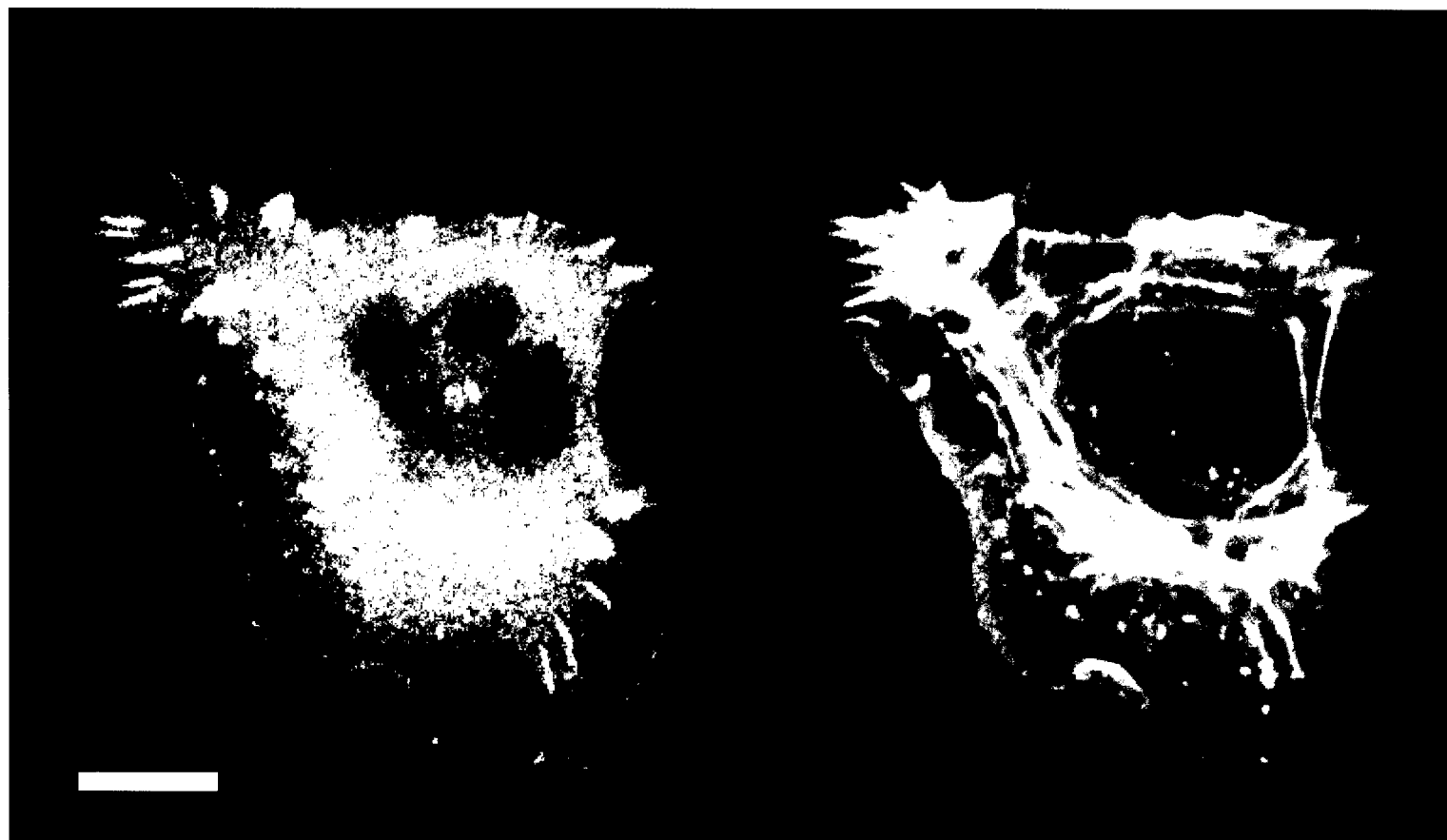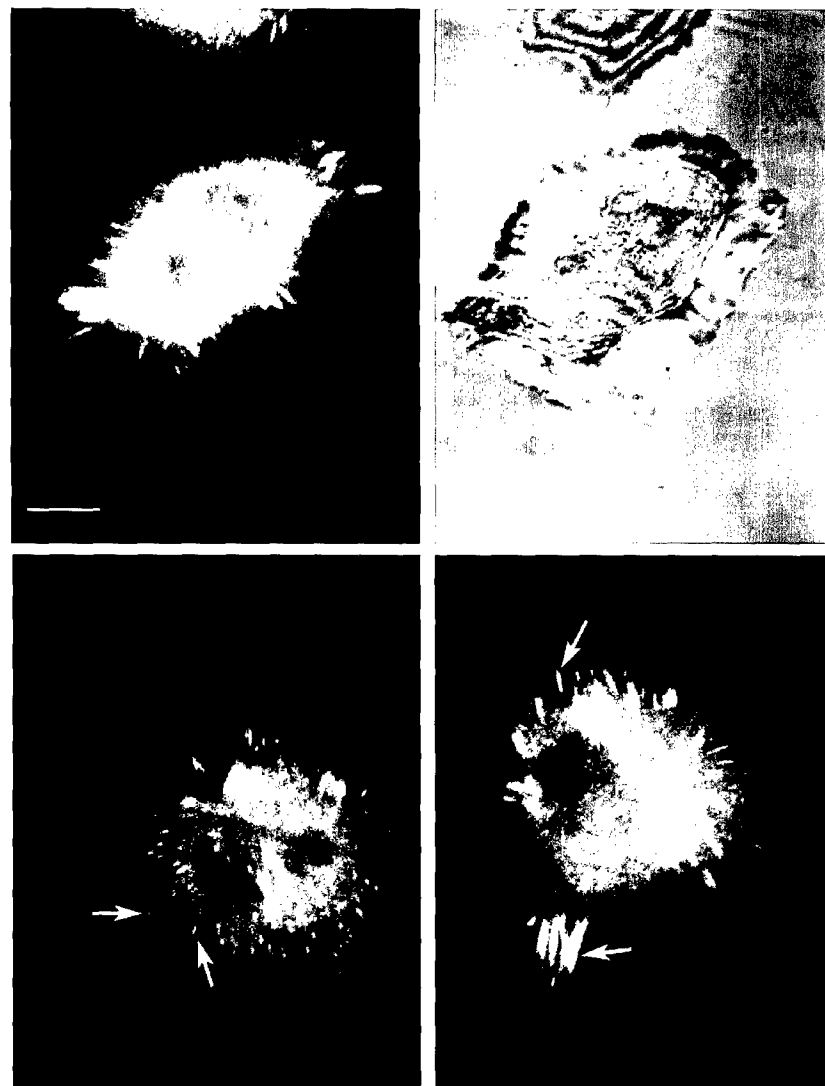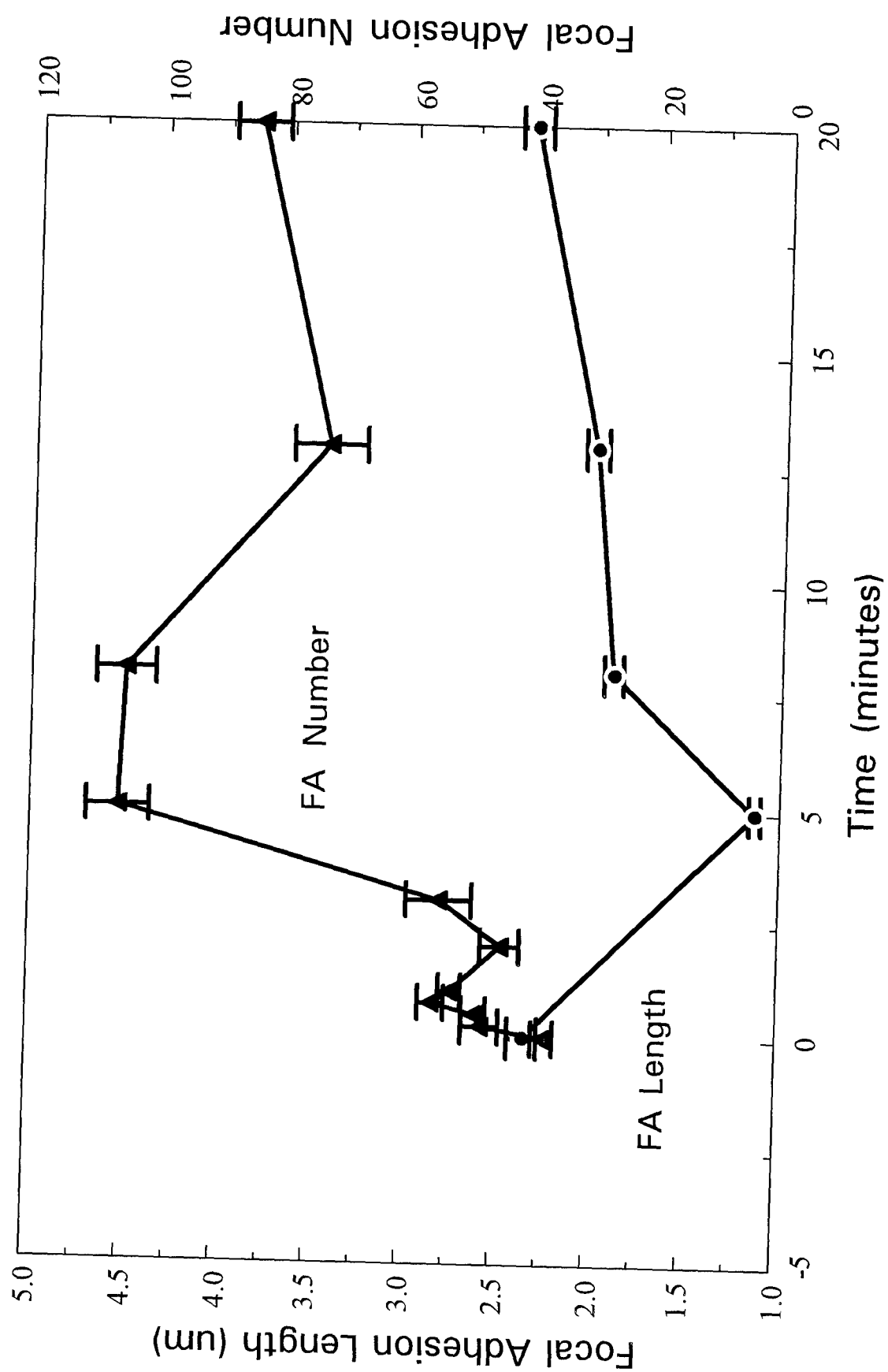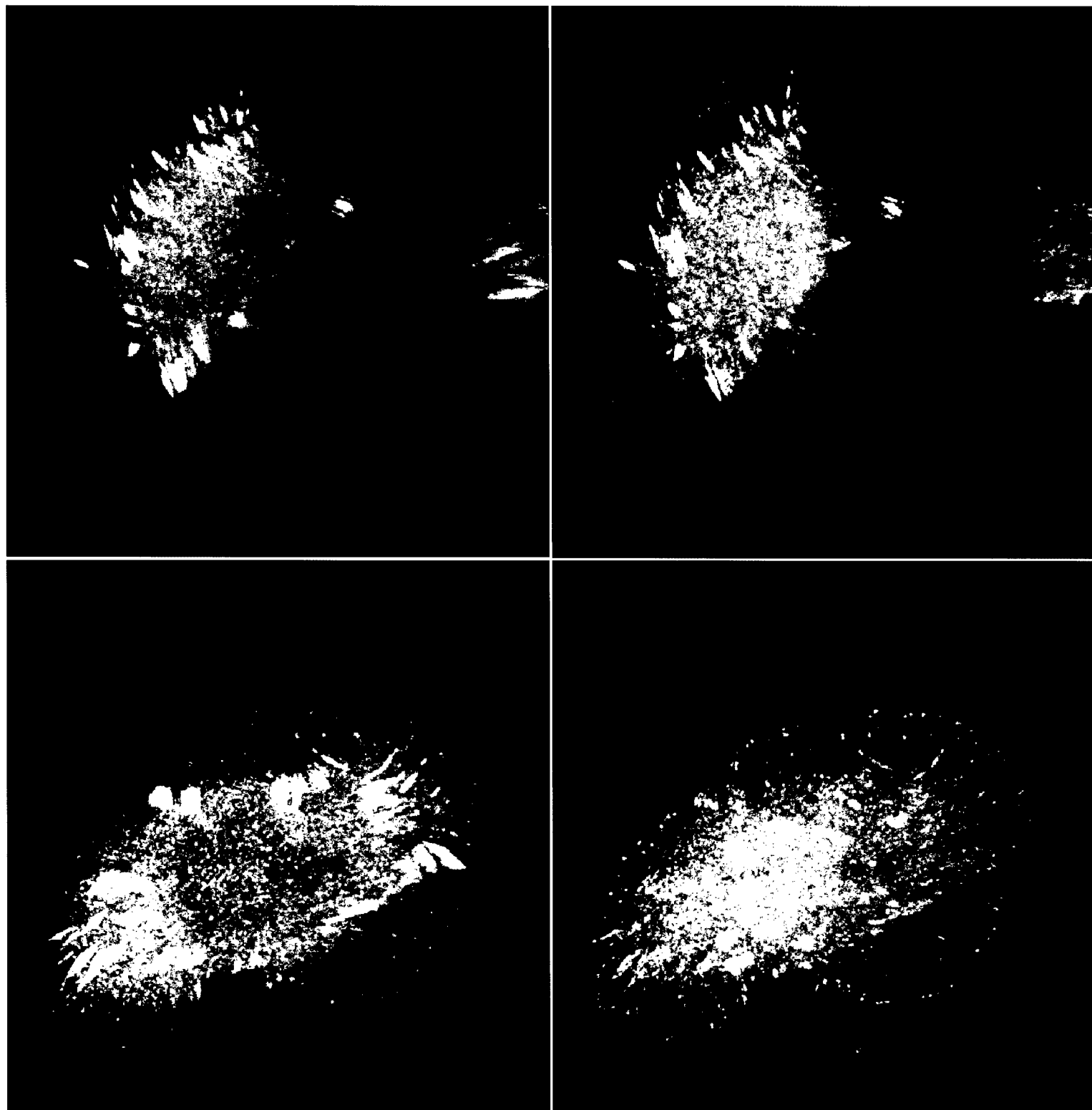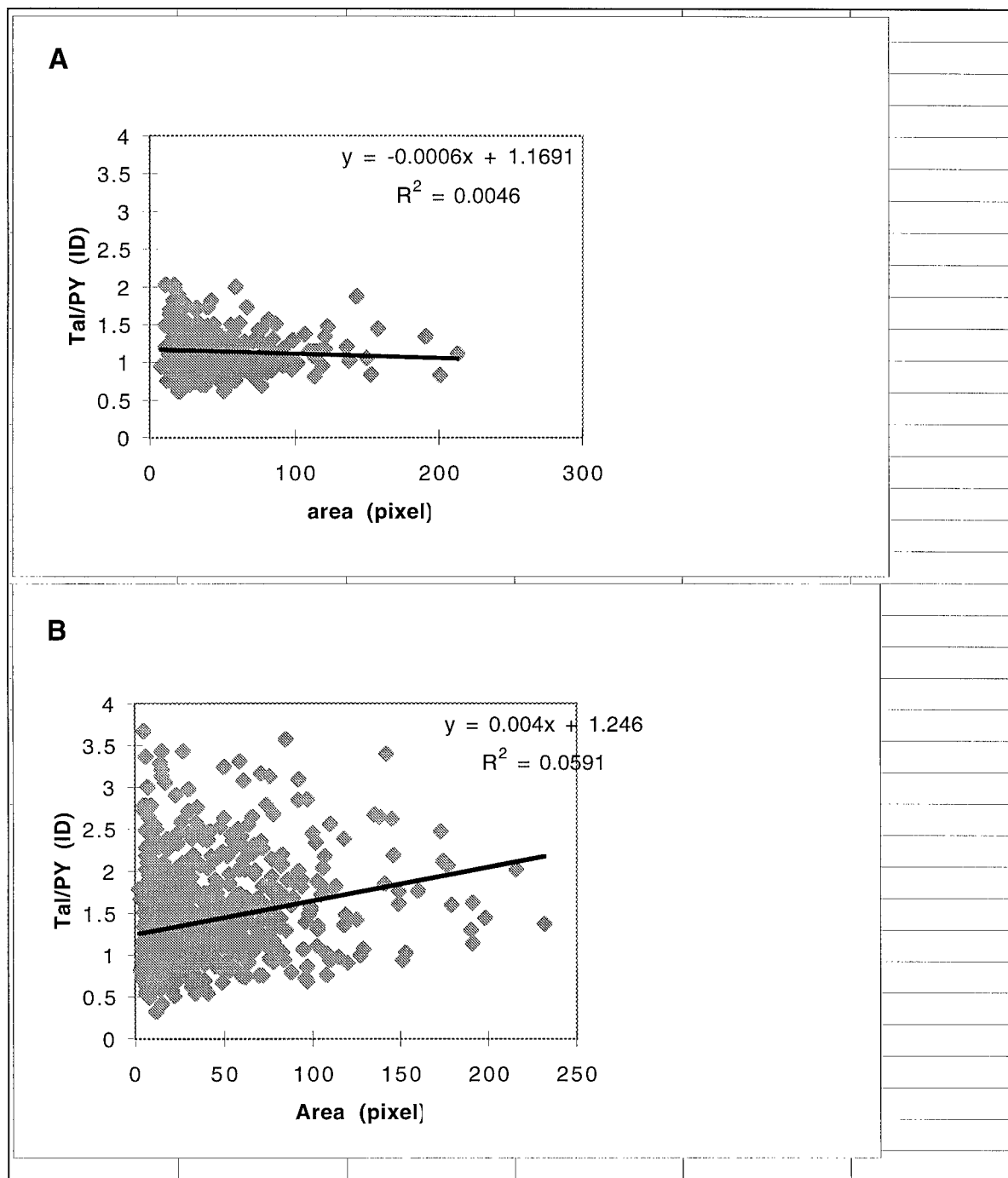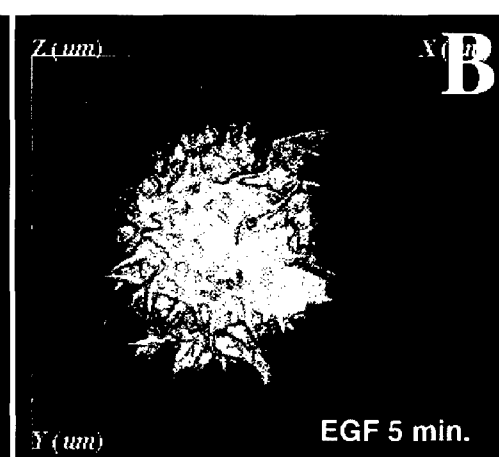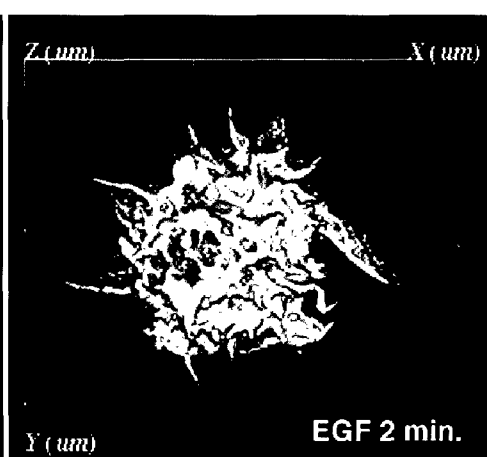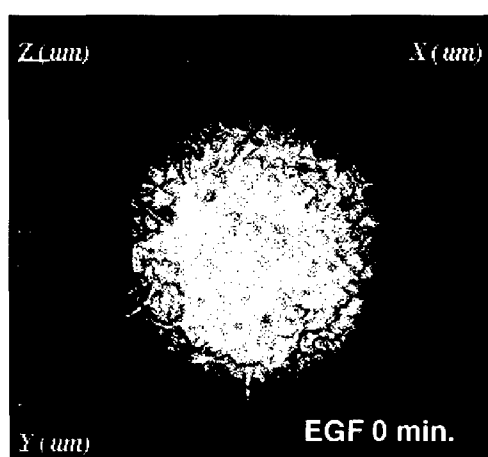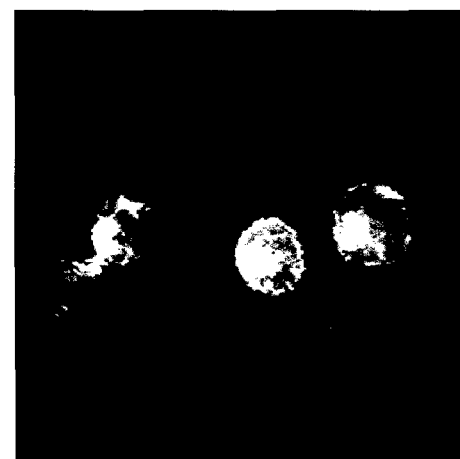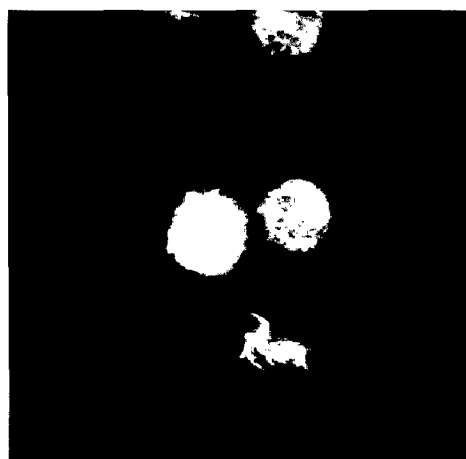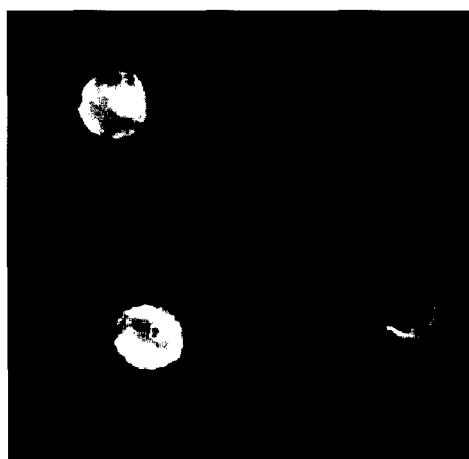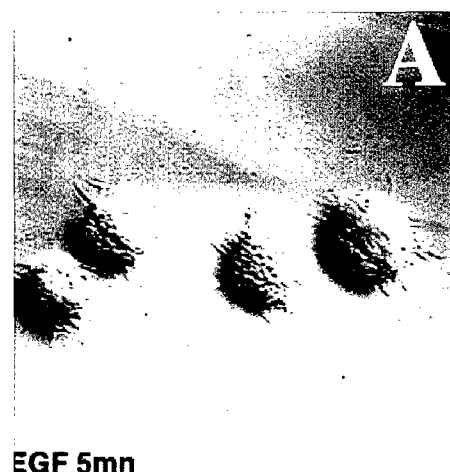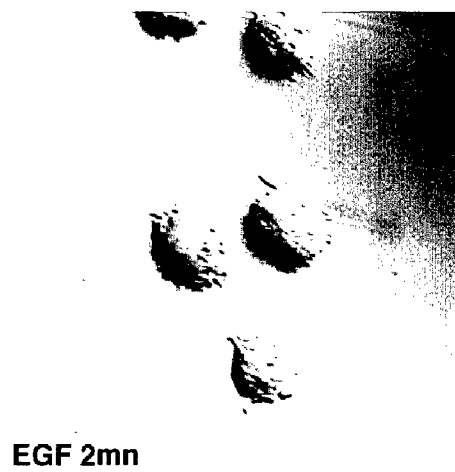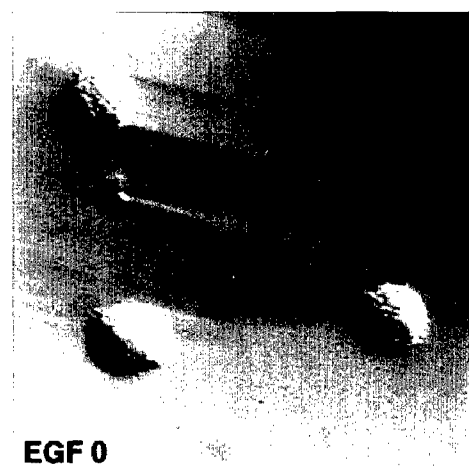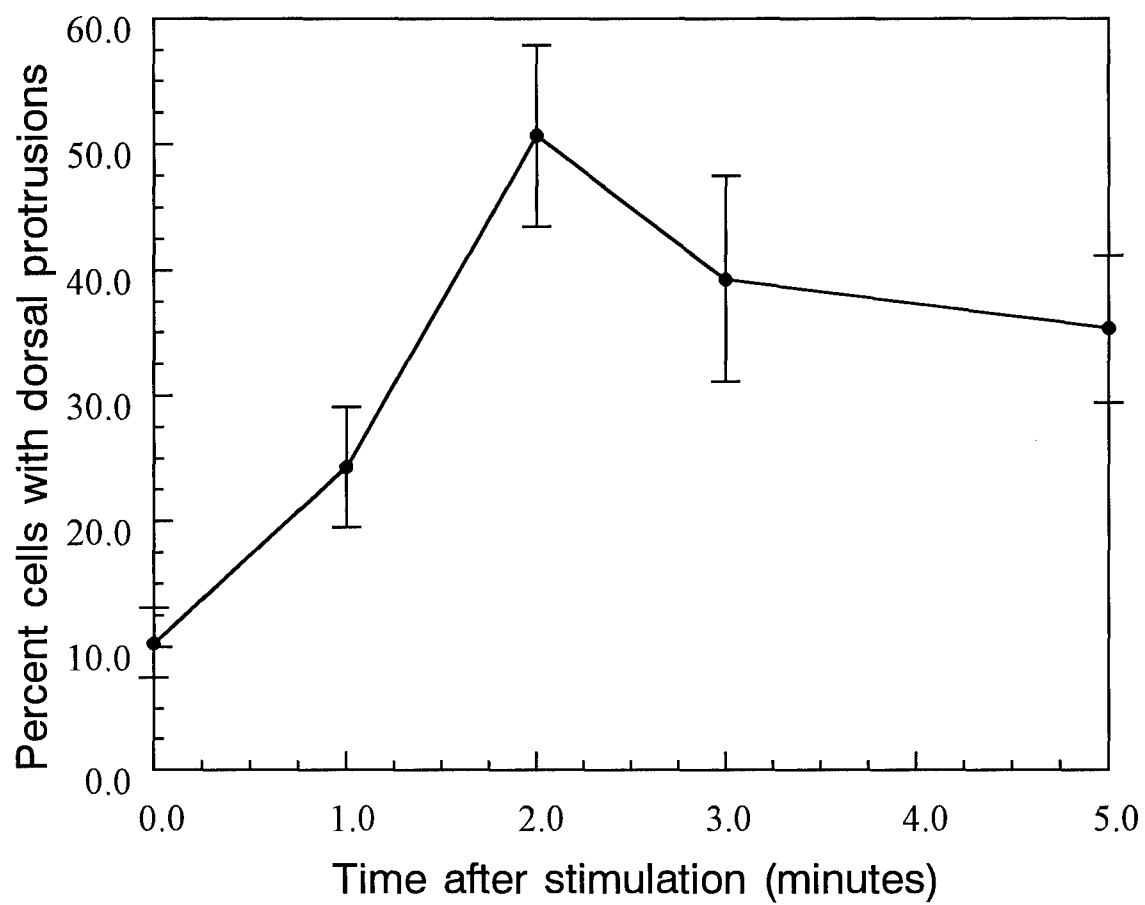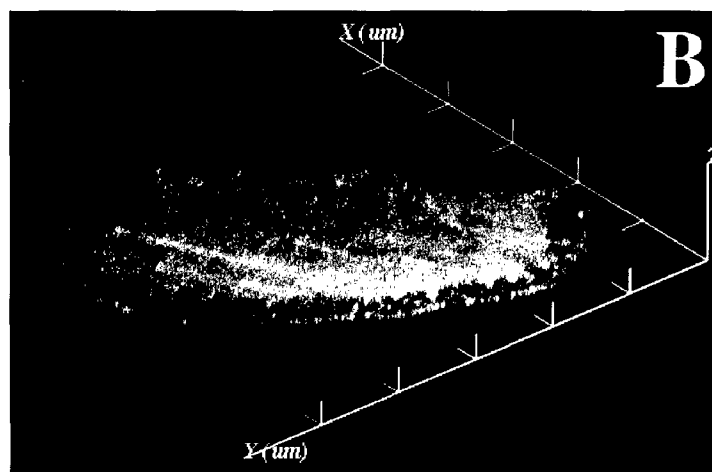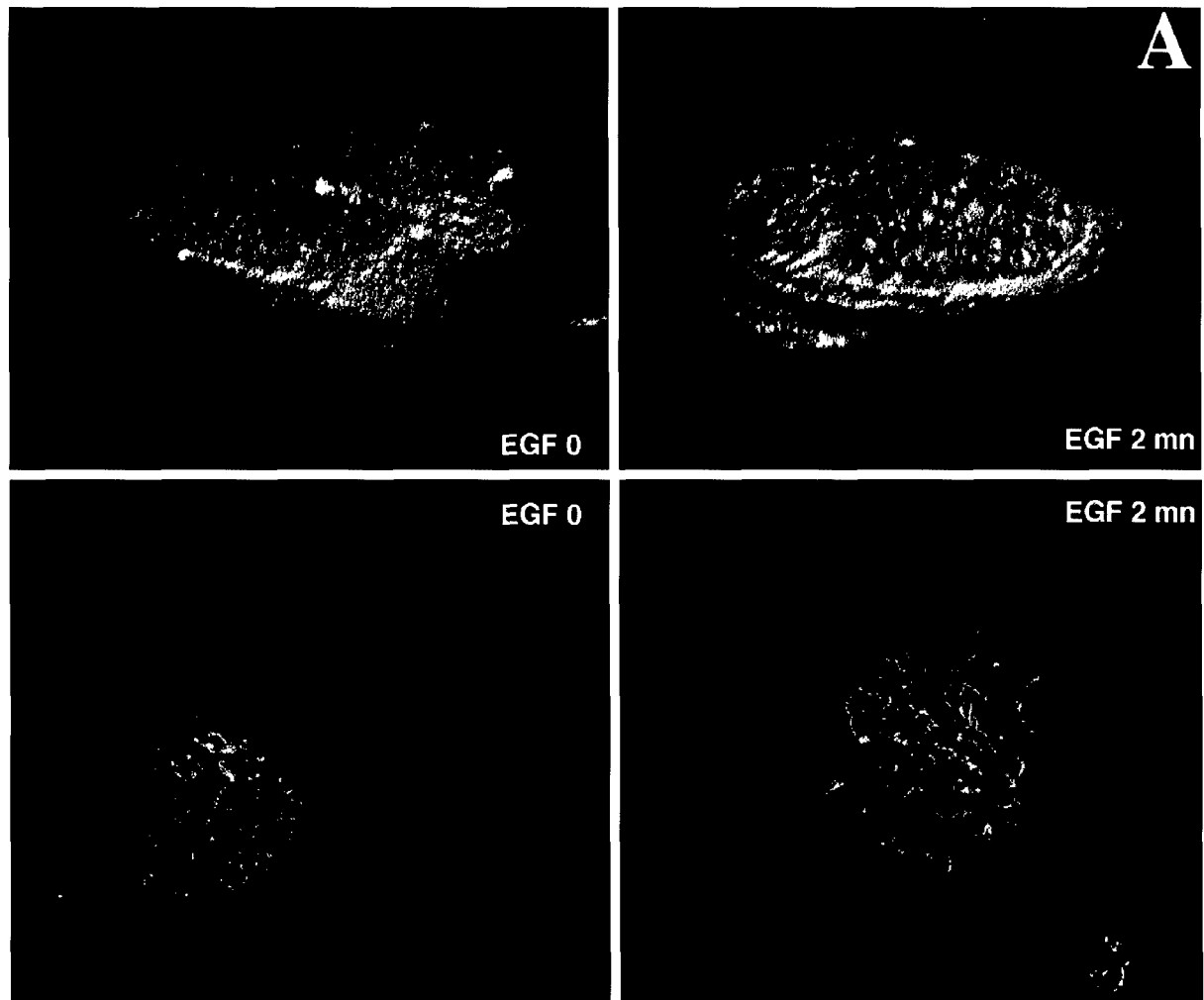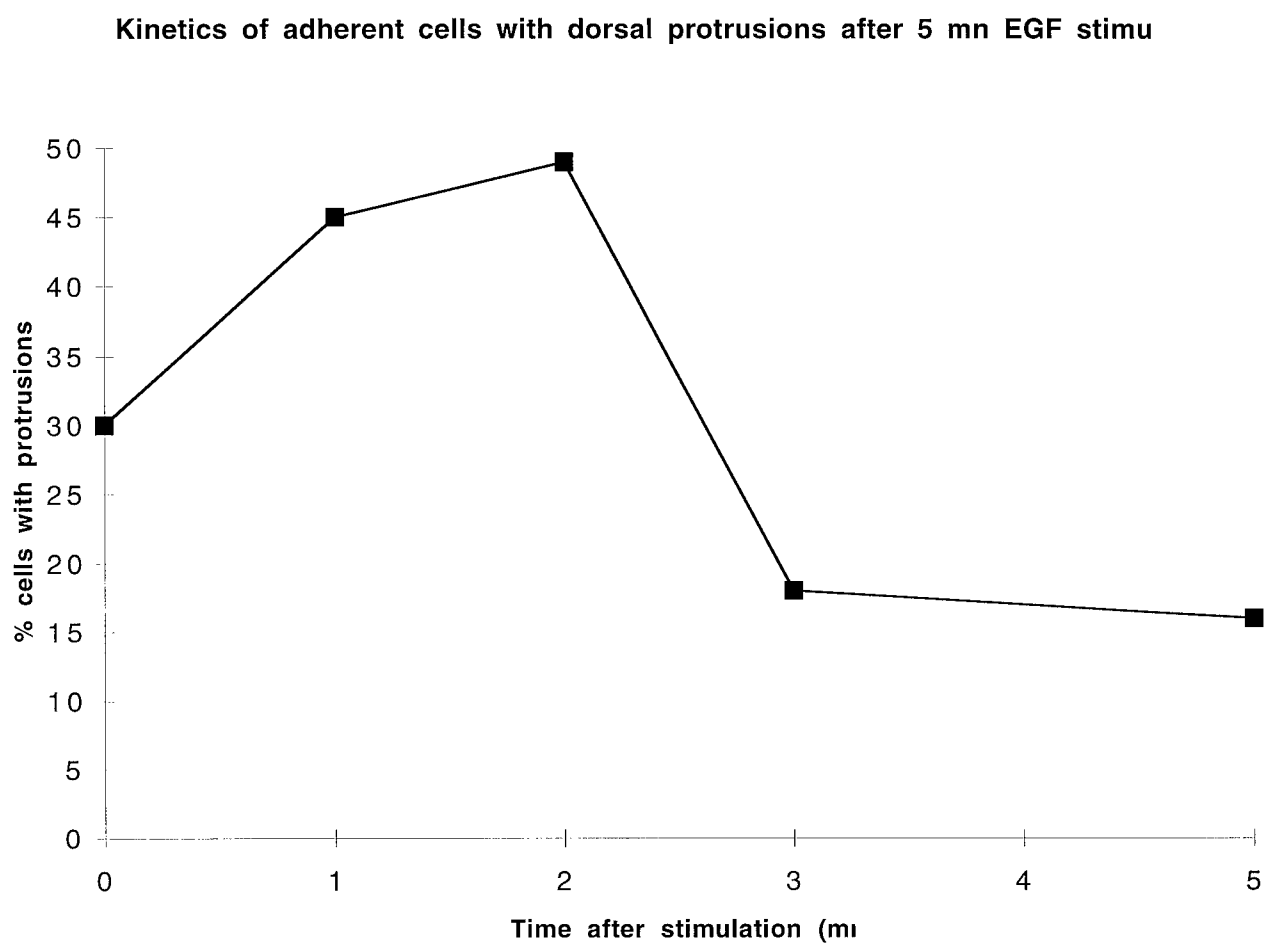
Rhodamine-actin incubation (min)

Figure 5

Figure 6 60

Figure 7

61

Figure 8   62

Figure 9 63

Figure 10

Sheet6 Chart 2

Figure 11

Page 1

Figure 12

Figure 13

Figure 14

Figure 15

69

A

$y = -0.0006x + 1.1691$

$R^2 = 0.0046$

B

$y = 0.004x + 1.246$

$R^2 = 0.0591$

Figure 17   71

EGF 0

EGF 2mn

EGF 5mn

EGF 0 min.

EGF 2 min.

EGF 5 min.

Figure 18

Figure 19 73

Figure 19B

Kinetics of adherent cells with dorsal protrusions after 5 mn EGF stimu

Figure 20

EGF 4 mn

EGF 8 mn

Figure 21B

Figure 22   78

Figure 23

79

Figure 23A

Figure 23B

A

B

Tumor   Liver

Tumor Liver

a   b   c   d

Figure 24

Figure 25

82
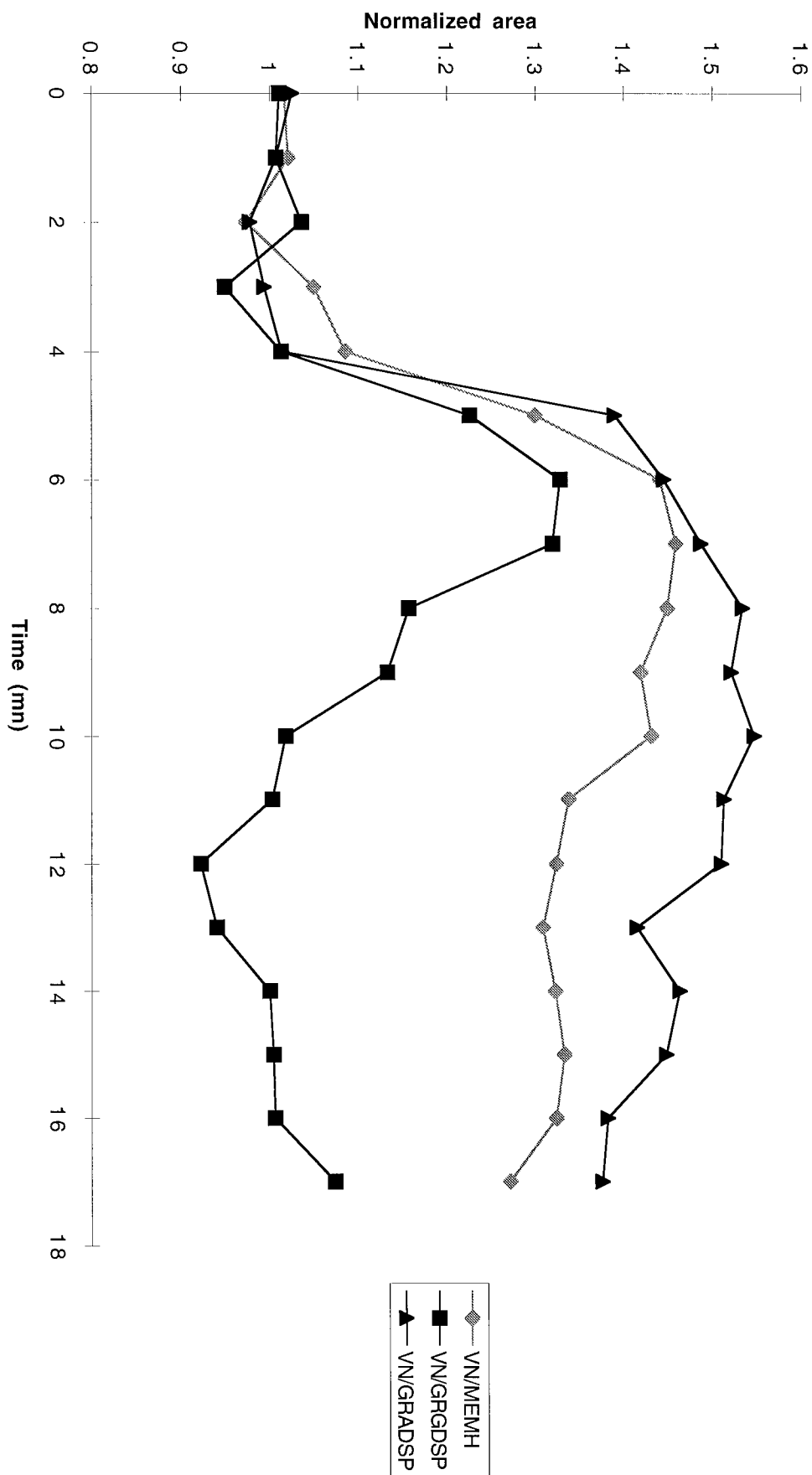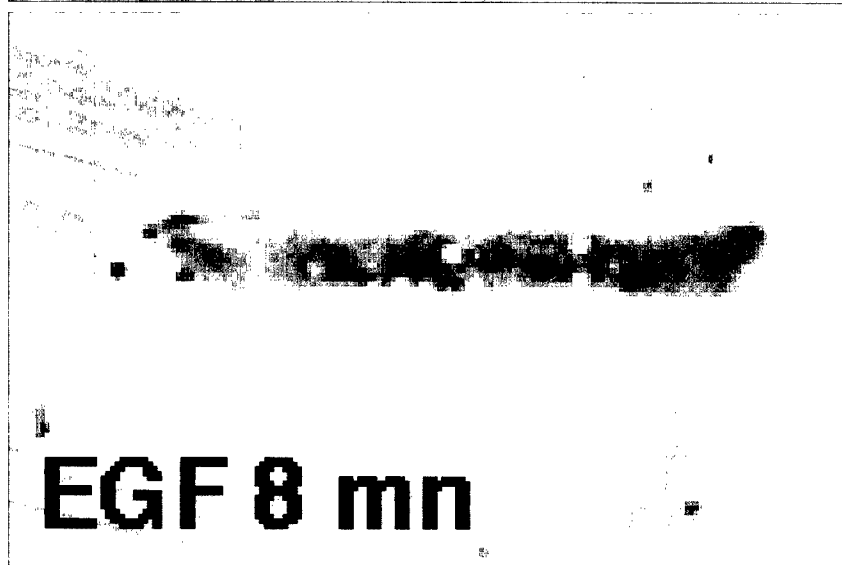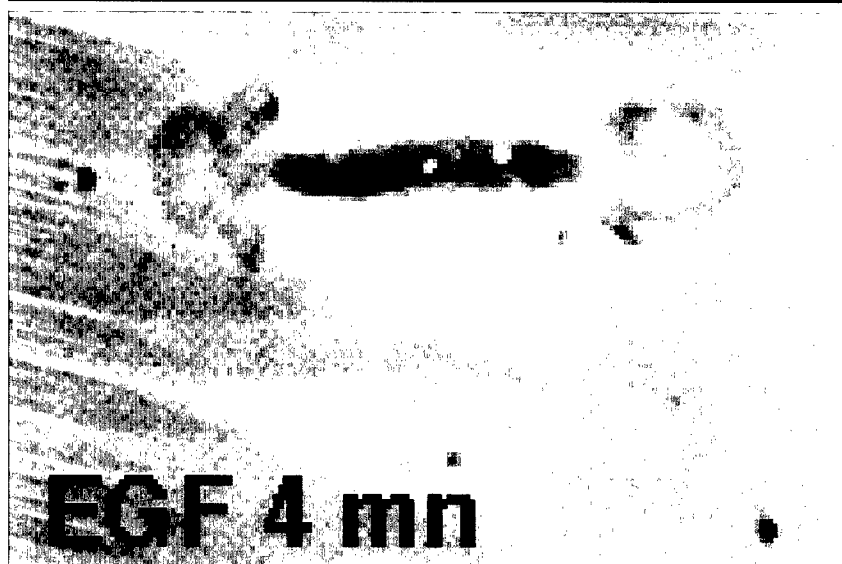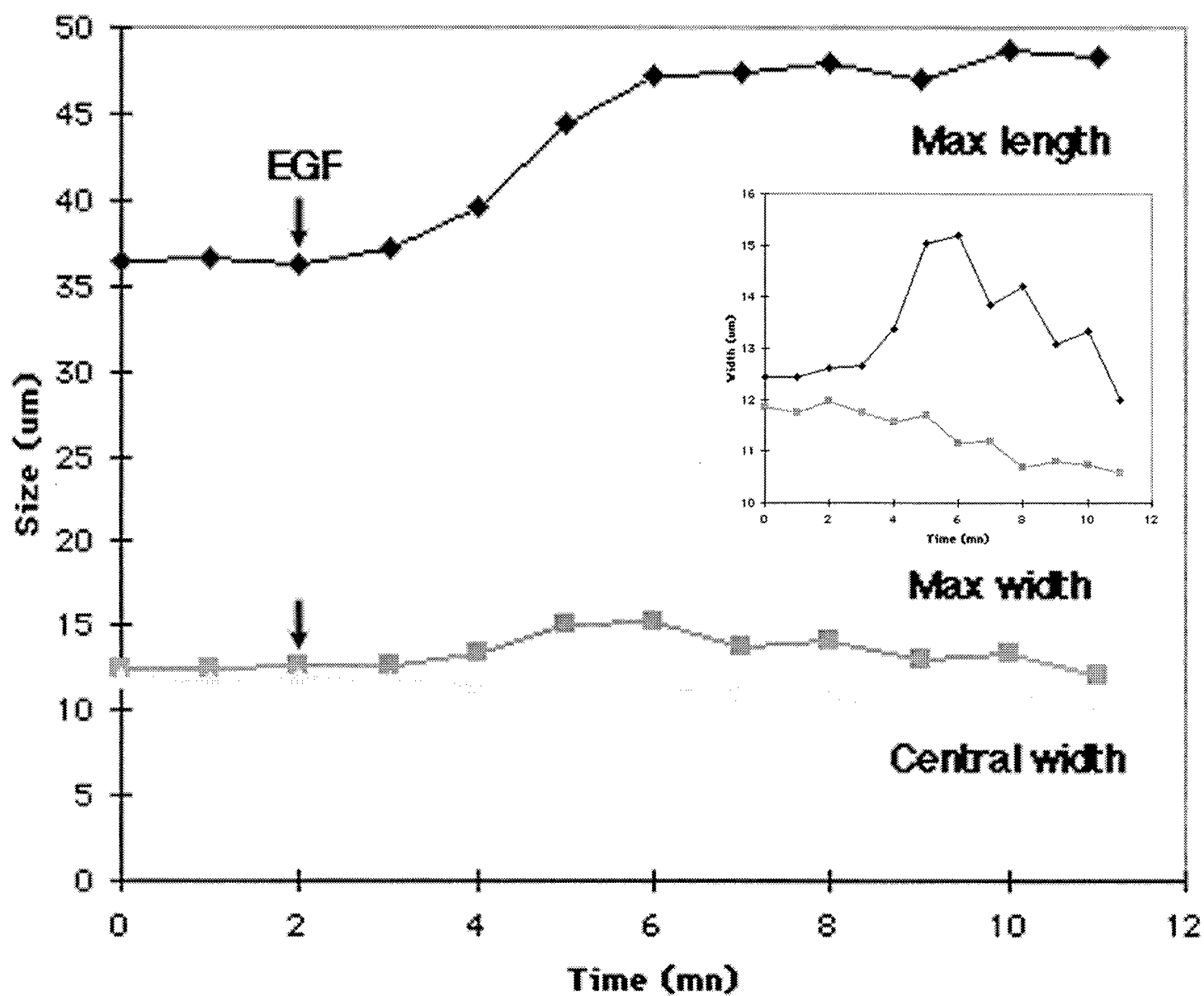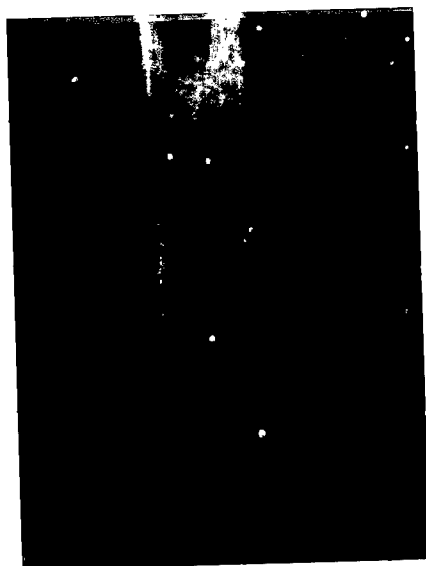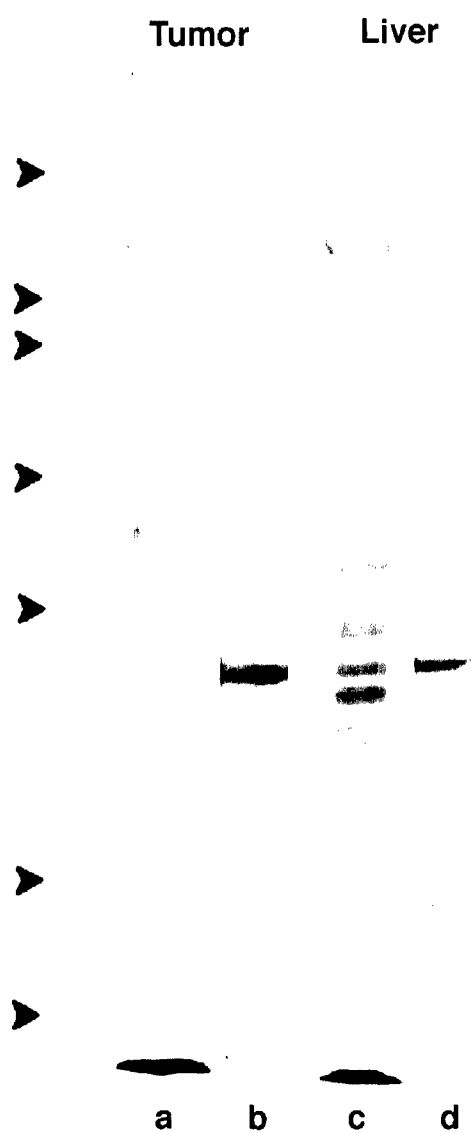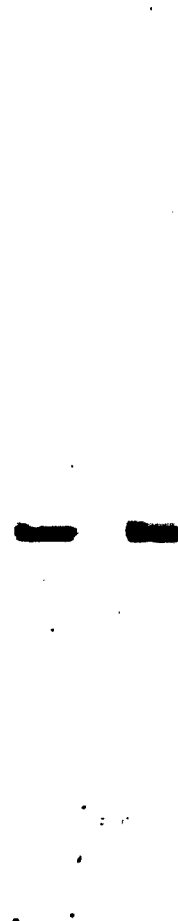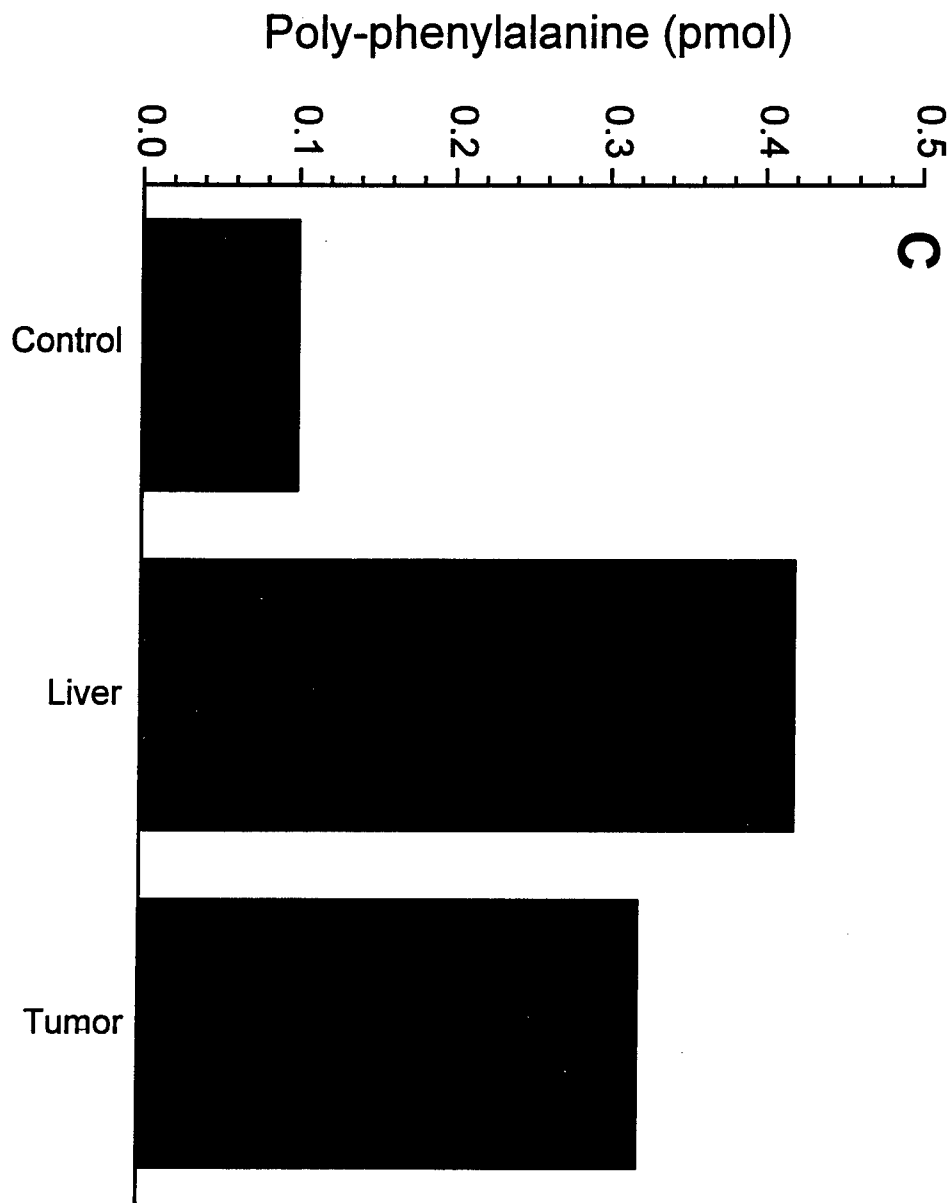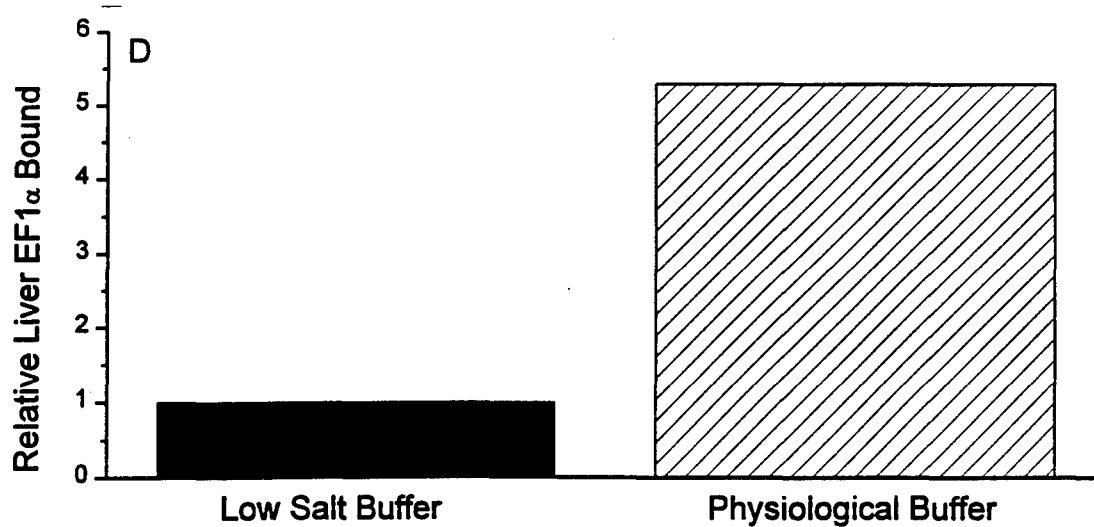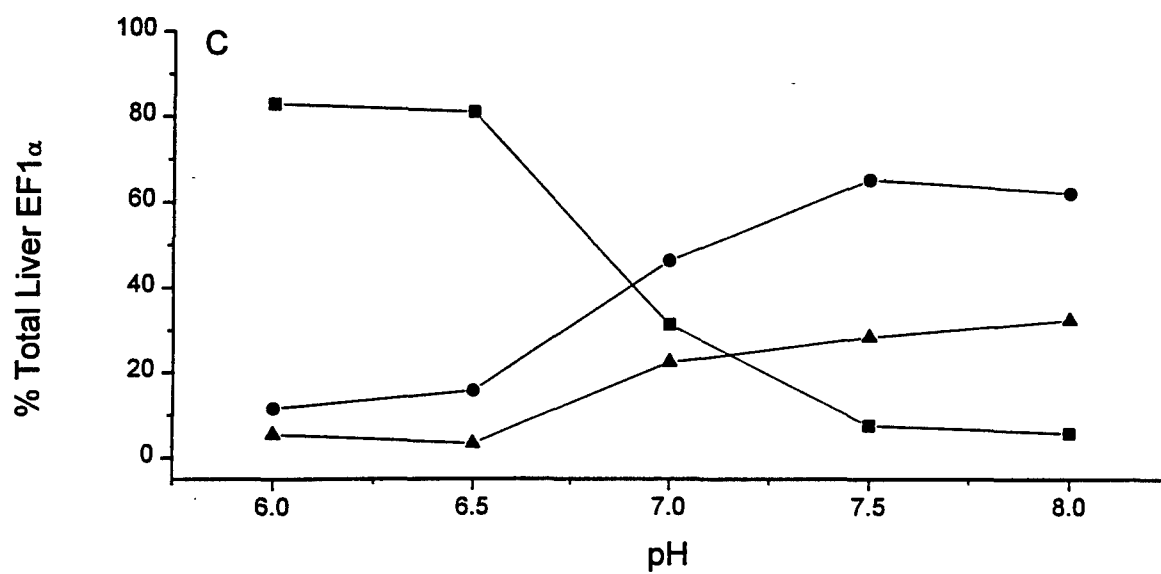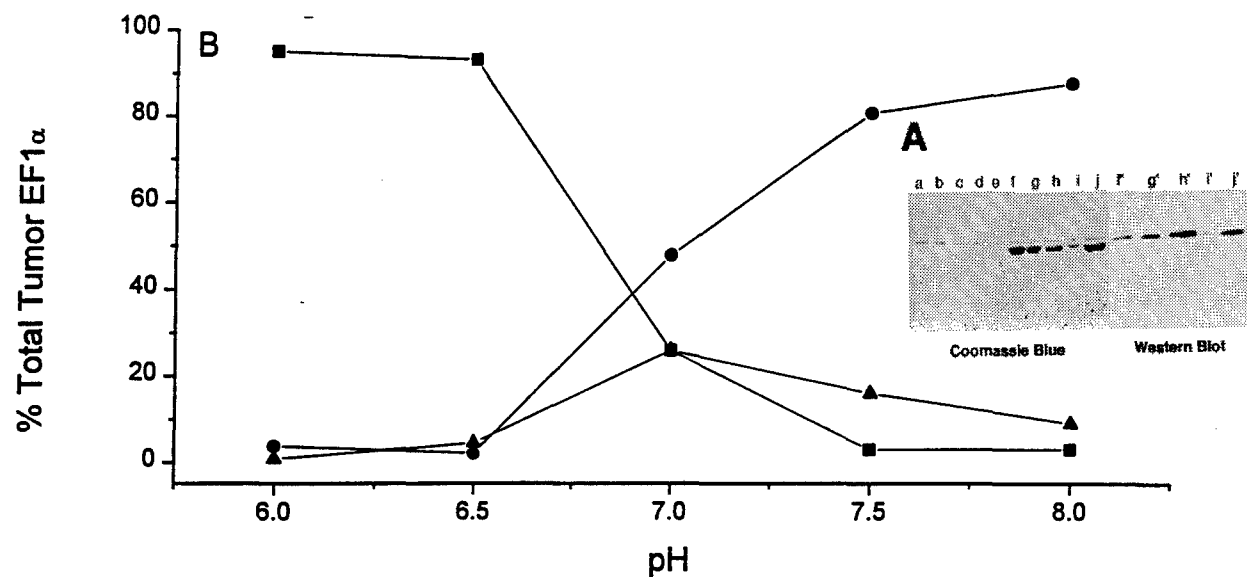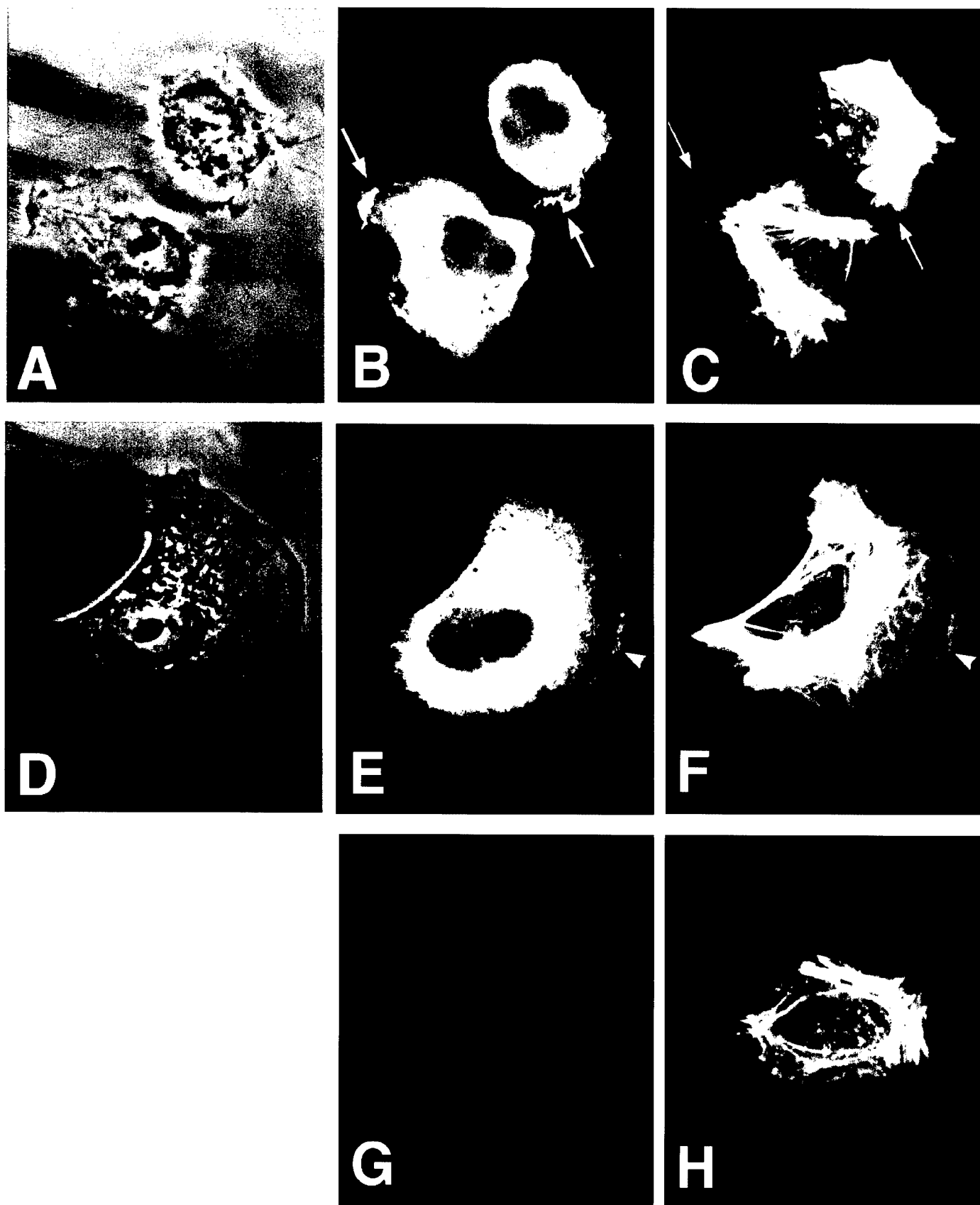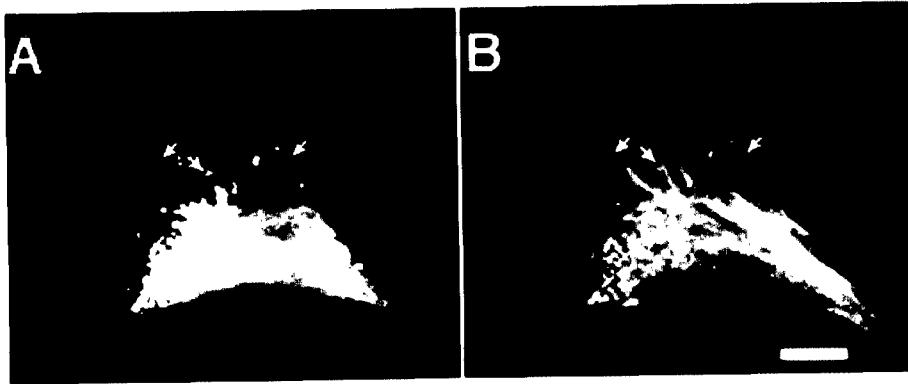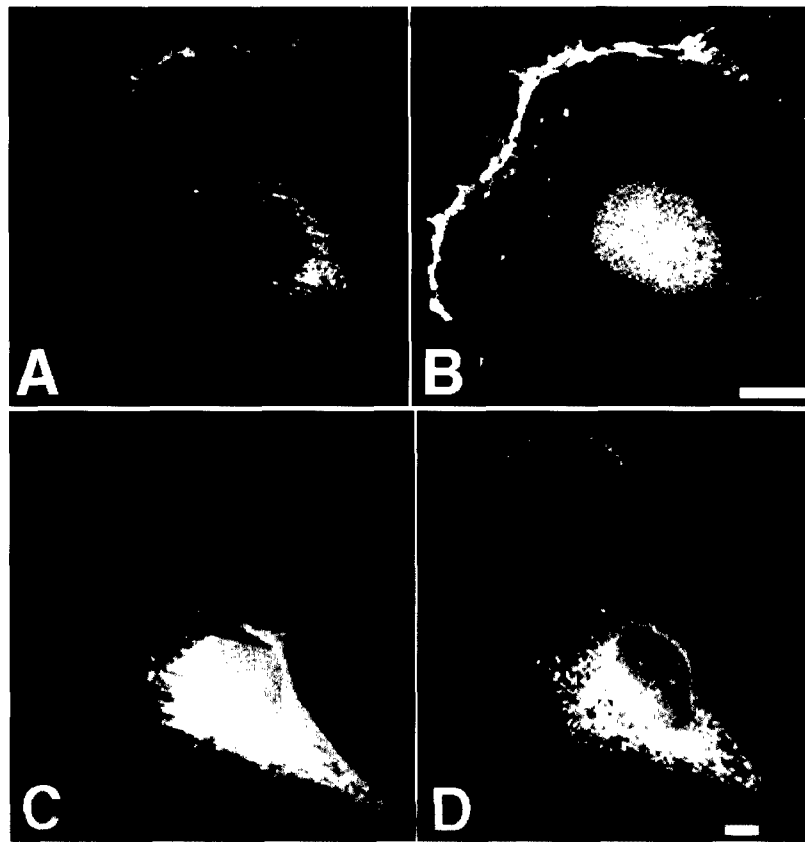
Figure 26

Figure 27

Figure 28   84
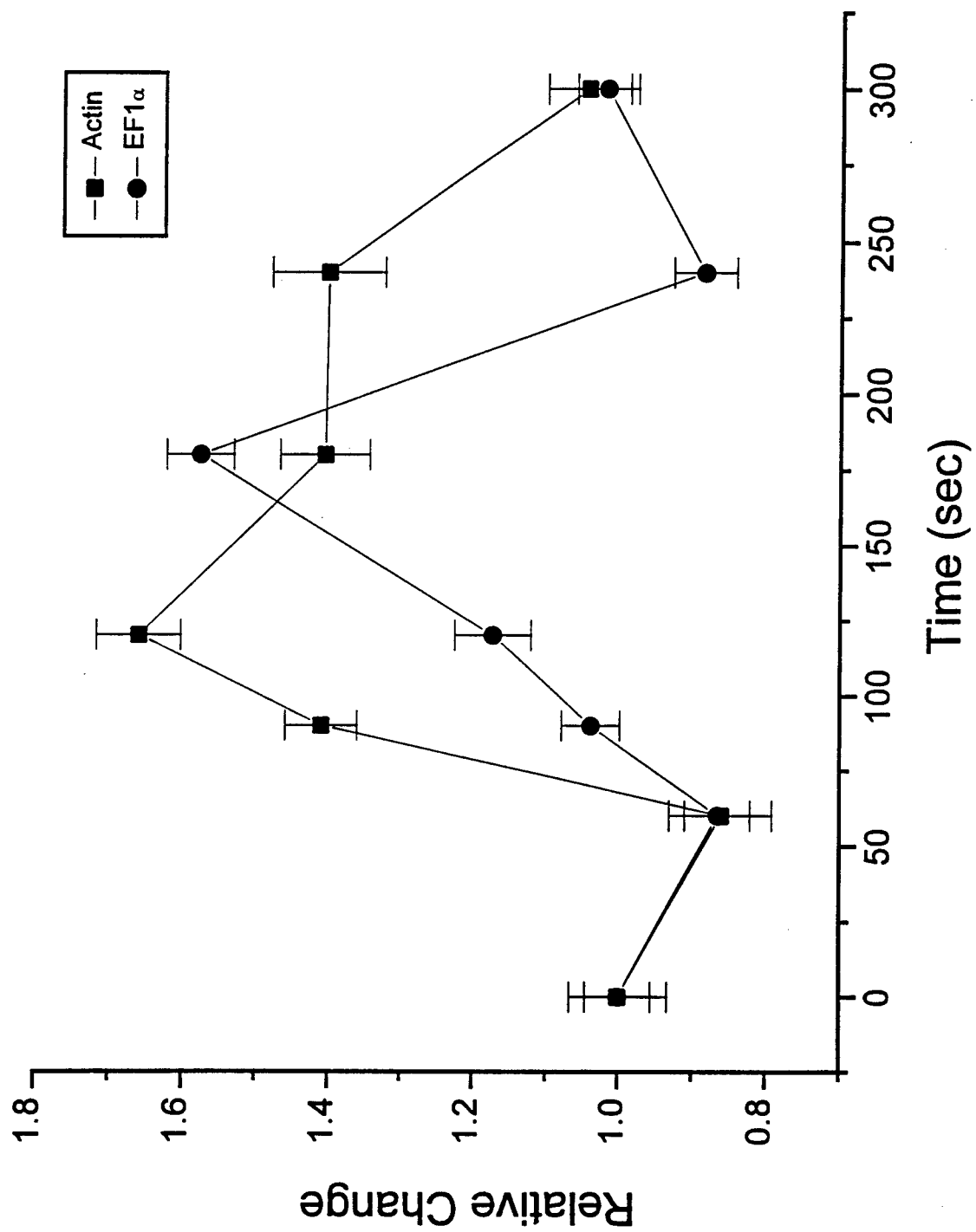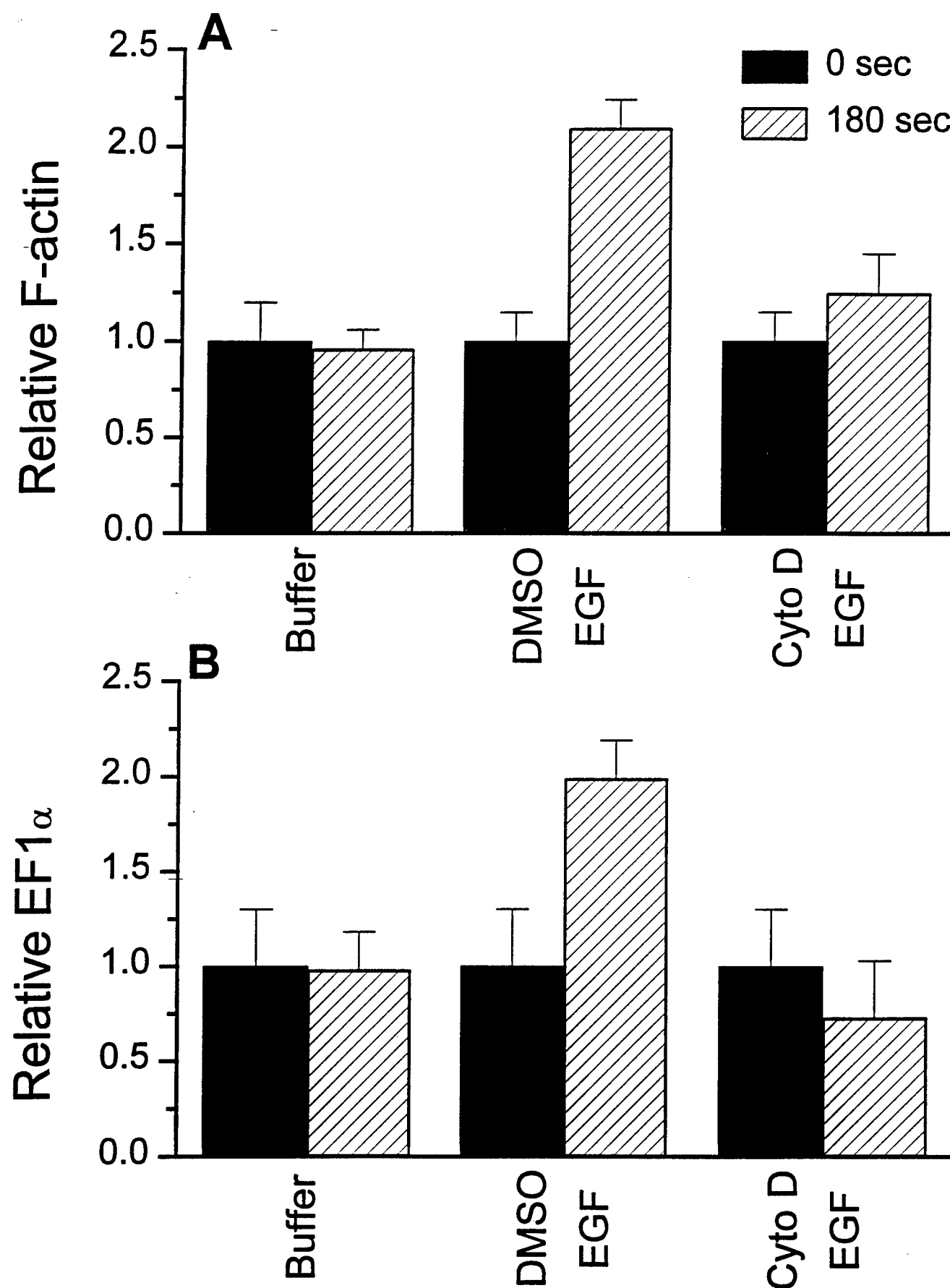
Figure 29

MCMR-RMI-S (70-1y)   14 Oct 99

MEMORANDUM FOR Administrator, Defense Technical Information
            Center, ATTN: DTIC-OCA, 8725 John J. Kingman
            Road, Fort Belvoir, VA 22060-6218

SUBJECT: Request Change in Distribution Statement

1. The U.S. Army Medical Research and Materiel Command has
reexamined the need for the limitation assigned to technical
reports written for Grant DAMD17-94-J-4314. Request the limited
distribution statement for Accession Document Number ADB219006 be
changed to "Approved for public release; distribution unlimited."
This report should be released to the National Technical
Information Service.

2. Point of contact for this request is Ms. Judy Pawlus at
DSN 343-7322 or by email at Judy.Pawlus@amedd.army.mil.

FOR THE COMMANDER:

                              PHYLIS M. RINEHART
                              Deputy Chief of Staff for
                                Information Management

Completed
2-8-2000
BW